

Evaluation of the Interactions Between Supercritical Carbon Dioxide and Polymeric Materials

Samuel P. Sawan, Yeong-Tarnng Shieh, and Jan-Hon Su
Polymer Science Plastics Engineering Program
Department of Chemistry
University of Massachusetts, Lowell
Lowell, Massachusetts 01854

This report resulted from direct collaboration and funding from the following sources:

Los Alamos National Laboratory
Toxics Use Reduction Institute, University of Massachusetts, Lowell
International Business Machines

Los Alamos
NATIONAL LABORATORY

*Los Alamos National Laboratory is operated by the University of California
for the United States Department of Energy under contract W-7405-ENG-36.*

An Affirmative Action/Equal Opportunity Employer

This report was prepared as an account of work sponsored by an agency of the United States Government. Neither The Regents of the University of California, the United States Government nor any agency thereof, nor any of their employees, makes any warranty, express or implied, or assumes any legal liability or responsibility for the accuracy, completeness, or usefulness of any information, apparatus, product, or process disclosed, or represents that its use would not infringe privately owned rights. Reference herein to any specific commercial product, process, or service by trade name, trademark, manufacturer, or otherwise, does not necessarily constitute or imply its endorsement, recommendation, or favoring by The Regents of the University of California, the United States Government, or any agency thereof. The views and opinions of authors expressed herein do not necessarily state or reflect those of The Regents of the University of California, the United States Government, or any agency thereof.

Evaluation of the Interactions Between Supercritical Carbon Dioxide and Polymeric Materials

Samuel P. Sawan, Yeong-Tarng Shieh, and Jan-Hon Su
Polymer Science Plastics Engineering Program
Department of Chemistry
University of Massachusetts, Lowell
Lowell, Massachusetts 01854

This report resulted from direct collaboration and funding from the following sources:

Los Alamos National Laboratory
Toxics Use Reduction Institute, University of Massachusetts, Lowell
International Business Machines

Los Alamos
NATIONAL LABORATORY
Los Alamos, New Mexico 87545

CONTENTS

BACKGROUND	3
I. Absorption, Swelling, and Dissolution of Carbon Dioxide in Polymers at Elevated Pressures	7
1.0 INTRODUCTION	9
2.0 EXPERIMENTAL PROCEDURE	10
3.0 RESULTS AND DISCUSSION	12
3.1 Changes in Appearance	13
3.2 Weight Changes of Polymers	14
3.3 Effects of the Treatment Conditions on the Weight Changes of Polymers	17
3.4 Effects of the Dimensions of Samples on the Weight Changes of Polymers	17
3.5 Desorption of Carbon Dioxide	17
3.6 Solubility of Polymers in Carbon Dioxide	20
3.7 Solubility Parameters of Polymers and Carbon Dioxide	24
3.7.1 Definition of Solubility Parameter	24
3.7.2 Solubility Parameter of CO ₂	25
3.7.3 Solubility Parameters of Polymers	27
3.7.4 Solubility of Carbon Dioxide in Polymers	28
4.0 CONCLUSION	31
5.0 REFERENCES	32
II. Thermal Properties	33
1.0 INTRODUCTION	35
2.0 EXPERIMENTAL PROCEDURE	36
3.0 RESULTS AND DISCUSSION	36
4.0 CONCLUSION	43
III. Mechanical Properties	45
1.0 INTRODUCTION	47
2.0 EXPERIMENTAL PROCEDURE	49
3.0 RESULTS AND DISCUSSION	49
4.0 CONCLUSION	55
BIBLIOGRAPHY	57
APPENDIX	61

BACKGROUND

Supercritical fluid technology has been widely used in extraction and purification processes in foods and pharmaceuticals and for techniques such as supercritical fluid chromatography. Recently there has been interest in using super and subcritical fluids, such as carbon dioxide, as substitutes for chlorofluorocarbons (CFCs) for cleaning applications in which the choices of environmentally acceptable alternatives are very limited. Unfortunately, almost no information exists on the use of super and/or subcritical carbon dioxide for this purpose. Consequently, there exists a great need to develop information on the use of carbon dioxide for cleaning applications.

Cleaning considerations entail a wide variety of issues. A few of these issues include the definition of cleaning, i.e., how clean is clean; the removal or solubility of a wide variety of possible contaminants or agents, including particles; and the potential interaction of the cleaning material with the substance to be cleaned. In general, most metals and glasses would be expected to have little interaction with carbon dioxide because of their high crystallinities and their general imperviousness to gases. Polymeric materials, however, may be expected to show a wide diversity of interaction with carbon dioxide, varying from essentially no effect to very pronounced effects based upon dissolution or even chemical degradation of a polymeric substance.

To this end, we have been evaluating the interactions between super and subcritical carbon dioxide and polymeric materials to explore the applicability of using the CO₂ fluid for the precision cleaning of polymers.

Supercritical carbon dioxide has a critical temperature of 31°C and a critical pressure of 1,070 psi. Carbon dioxide has a number of advantages, including low human toxicity, no waste solvent, low cost, ready availability of the gas, complete recovery of extracted agents, environmental acceptability of the gas, and no ozone depletion. Replacement of CFCs has become a high national, indeed, international priority because of their implication in ozone depletion. Thus, a suitable alternative to CFCs is being widely sought to meet industrial and commercial needs. Super and subcritical carbon dioxide appear to have many similarities to CFCs (for example, a CO₂ fluid can solubilize the same range of compounds as CFCs); therefore, CO₂ fluid is an ideal candidate for further exploration. The major difficulty in the application of carbon dioxide is that it is inherently a nonatmospheric process as discussed above.

Another important characteristic of the supercritical phase is the viscosity of the phase itself. Supercritical cleaning fluids (SCFs) have viscosities similar to gases and extraction capabilities similar to liquids. Thus, SCFs possess the ability to clean under small cavities, such as beneath the package of surface-mounted electronic components. In addition, because SCFs are perfectly wetting, issues such as surface tension are not a concern (actually, in a single phase the concept of wetting is inap-

appropriate and is used here simply to illustrate the concept that surface tension is not a relevant variable). Thus, small cavities, for example, do not present a cleaning problem per se except in the consideration of mass transport and diffusional problems.

Many polymeric materials are known to undergo significant absorption of gases and vapors. The absorption of carbon dioxide in polymers can plasticize the material and cause a decrease in the glass transition temperature. This absorption also can induce crystallization of the material and cause an increase in the melting temperature and the melting enthalpy. Recently, several experiments have been reported that examined the effect of high-pressure carbon dioxide on polymeric materials, such as silicone rubber, polycarbonate, cellulose acetate, polyvinylidene fluoride, polymethyl methacrylate, polystyrene, polyvinyl benzoate, low density polyethylene, polysulfone, and polyvinyl chloride [1–10]. Investigations have focused on the solubility issue [2, 8], the swelling and absorption behaviors [1, 5–9], and the reduction in the glass transition temperatures of polymers [3, 4].

Also of note are experiments performed using high-pressure gases to cause blowing of conventional polymers to avoid the use of CFCs or other types of solvent-blowing aids for the formation of foams [11, 12]. These experiments suggest that gases such as carbon dioxide readily dissolve in a variety of polymers and may lead to bubble formation in such polymers when the pressure is reduced to an atmospheric level and/or the temperature is raised above the glass transition temperature of the polymer. This phenomenon may be the most troubling in noncross-linked or swellable/soluble polymer systems since this would lead to substantial changes in the physical and barrier properties of such polymers. In addition, it has been found that carbon dioxide remarkably accelerates the absorption of many low-molecular-weight additives in a number of glassy polymers [10]. This effect is the result of the high diffusivity, solubility, and plasticizing action of compressed carbon dioxide in polymers. Upon the release of the pressure, absorbed carbon dioxide rapidly diffuses from the polymer, while the other compounds desorb much more slowly. The amount of additive absorbed, therefore, can be determined from the plateau weight of the sample after most of the carbon dioxide has escaped. This phenomenon may be useful for the impregnation of glassy polymers with many additive compounds.

Such effects indicate that many polymers will be directly affected by high-pressure carbon dioxide and that care should be exercised in evaluating the short- and long-term effects of supercritical carbon dioxide on such polymers. Plasticization of polymers suggests that components of various polymers may be removed, allowing for the degradation or loss of chemical and/or physical properties. Further, plasticization suggests that the degree and amount of crystallinity may be changed in polymers that could also significantly affect the performance and mechanical properties of such materials. Thus, a significant need exists for the careful evaluation of the interactions between supercritical carbon dioxide with polymers.

In this report, we present (1) the results of testing a broad spectrum of polymers in carbon dioxide over a range of temperatures and pressures and (2) the evaluation of the effect of high-pressure carbon dioxide on the chemical/physical properties of the polymers. The carbon dioxide conditions included both super and subcritical points. The testing was performed, in a static manner, with four controlled variables: temperature, pressure, treatment time, and decompression time. The evaluation of the interactions between high-pressure carbon dioxide and polymers included absorption, swelling, solubility, plasticization, crystallization, and mechanical properties. The results of these evaluations are discussed in three sections: "I. Absorption, Swelling, and Dissolution of Carbon Dioxide in Polymers at Elevated Pressure," "II. Thermal Properties," and "III. Mechanical Properties."

Comprehensive data have been collected and are provided in the appendix in the section "Data Reference"; the data include polymer names, polymer structures, polymer ID, trade names, manufacturers, appearance and dimensions, weight change, thermal properties (i.e., glass transition temperature, melting temperature, and melting enthalpy), mechanical properties (i.e., tensile strength, elongation, and modulus of elasticity), and surface properties. It is hoped that these data will provide a useful reference for individuals interested in cleaning applications of super and subcritical carbon dioxide.

**I. Absorption, Swelling, and Dissolution of Carbon Dioxide
in Polymers at Elevated Pressures**

1.0 INTRODUCTION

Supercritical carbon dioxide has recently begun to be studied as a substitute for chlorofluorocarbons (CFCs) as a cleaning solvent for industrial processes. Common materials of construction in industry include all of the familiar materials, such as ceramics, glasses, metals, polymers, and adhesives. Of these materials, it is anticipated that polymers and adhesives will show the greatest variability of response to treatment with supercritical (or high-pressure) gases such as carbon dioxide. This expected variability occurs for many reasons, including the following: (1) the complex nature of polymer morphology, oftentimes including both crystalline and amorphous regions; (2) the extensive variability in polymer structure, leading to large differences in solubility characteristics (e.g., solubility parameter); and (3) the basic material characteristics, such as glass transition temperature and plasticization effects, of polymers. These characteristics can be more pronounced in polymeric materials than in ceramics or metals and often occur under conditions in which the supercritical fluid would be employed.

Because of this highly variable nature of potential interactions between polymers and a supercritical cleaning solvent, there is a considerable need to characterize any adverse interactions and to define suitable conditions under which a wide variety of materials may be reasonably processed with little or no damage. Therefore, an assessment of the interactions between pure polymeric materials and super and subcritical carbon dioxide is an absolutely essential first step in understanding such interactions. The results of an assessment would provide information on how to appropriately design and implement widely acceptable cleaning strategies.

Potential interactions between a supercritical fluid and a polymeric material may include the following: (1) absorption of carbon dioxide by polymers; (2) swelling of polymers by carbon dioxide; (3) dissolution of polymers in carbon dioxide; (4) dissolution of carbon dioxide in polymers; (5) plasticization and a decrease in the glass transition temperature; (6) crystallization and an increase in the melting temperature and the melting enthalpy; (7) changes in the mechanical properties of polymers; (8) changes in the surface properties of polymers; and (9) nucleation of voids within polymer structures.

Variations in the thermal properties (5 and 6 above) and the mechanical properties (7 above) of polymeric materials are discussed separately in this report. This section of our report will detail our results on the absorption and swelling of polymers when exposed to carbon dioxide and the dissolution characteristics of various polymeric materials under a variety of conditions.

It is well known that absorption and swelling occur when polymers are exposed to gases, vapors, liquids, and in some cases, solids. There have been several previous works discussing the phenomena of absorption and swelling of carbon dioxide in certain polymers, such as silicone rubber, polycarbonate [1, 5, 8], cellulose acetate [2], polyvinylidene fluoride, polymethyl methacrylate [3, 5, 9], polystyrene [4, 5], polyvi-

nyl benzoate [6], low-density polyethylene [7, 8], polysulfone [8], and polyvinyl chloride [10]. However, these polymers were studied separately over a wide pressure range. The phenomena of absorption and swelling have not been studied on a broad spectrum of polymers under conditions that approximate reasonable processing conditions for materials that may be used in manufacturing. A comparison of weight change data will be shown for 20 different polymers that were treated in both sub and supercritical carbon dioxide under 7 different conditions. These results will be discussed in general to isolate important factors which affect the weight change (and possibly the dimensions) of polymers.

The absorption of carbon dioxide can result in swelling and/or dissolution of a polymer. The extent of either or both swelling and dissolution depends on the solubility of carbon dioxide in the polymer and/or the solubility of the polymers in carbon dioxide. When the system pressure is reduced, absorbed carbon dioxide may nucleate into bubbles and cause either the formation of foam or small defects in the polymer structure that may significantly alter the mechanical properties of the material. In addition, carbon dioxide can extract the plasticizer, if present, in the polymer and thus cause embrittlement. In this report, we will also discuss the solubility issues. Our intention is to correlate the weight change data of carbon dioxide-treated polymers with the solubility parameters of carbon dioxide and polymers.

2.0 EXPERIMENTAL PROCEDURE

Twenty different polymers were collected from commercially available sources in sheets of two different thicknesses. Coupon-shaped samples of 1×4 cm were made for all carbon dioxide treatments. Five samples were used in every experiment. Thus, the reported weight change data was an average of 5 values. The carbon dioxide treatments included 3 subcritical and 4 supercritical points as indicated in Table 1. The treatments were performed in a 5-liter, high-pressure windowless extractor. Decompression was performed using a 1-liter windowed separator that was connected to the extractor (See Figure 1). The samples were uniformly distributed in the extractor to allow for uniform exposure to the fluid. Both the treatment time and the decompression time were controlled for 1 hour except condition C7 in which a 5-hour decompression time was used. After treatment, the samples were ready for weight change measurements in 20 minutes. In most cases, the weight changes were also monitored 6 more times on different days. Between measurements, the samples were stored in dust-free polyethylene bags at $23 \pm 2^\circ\text{C}$. All weights were measured to ten thousandth of a gram.

Table 1. Carbon dioxide conditions employed in polymer treatments.

Condition	Pressure (psi)	Temperature (°C)	Exposure Time (hours)	Decompression Time (hours)	CO ₂ Phase	No. of samples tested
C (control)	14.7	25				
C1	1,000	25	1	1	liq	13
C2	1,000	40	1	1	gas	20
C3	2,000	40	1	1	SCF	20
C4	3,000	25	1	1	liq	20
C5	3,000	40	1	1	SCF	20
C6	3,000	70	1	1	SCF	20
C7	3,000	70	1	5	SCF	13

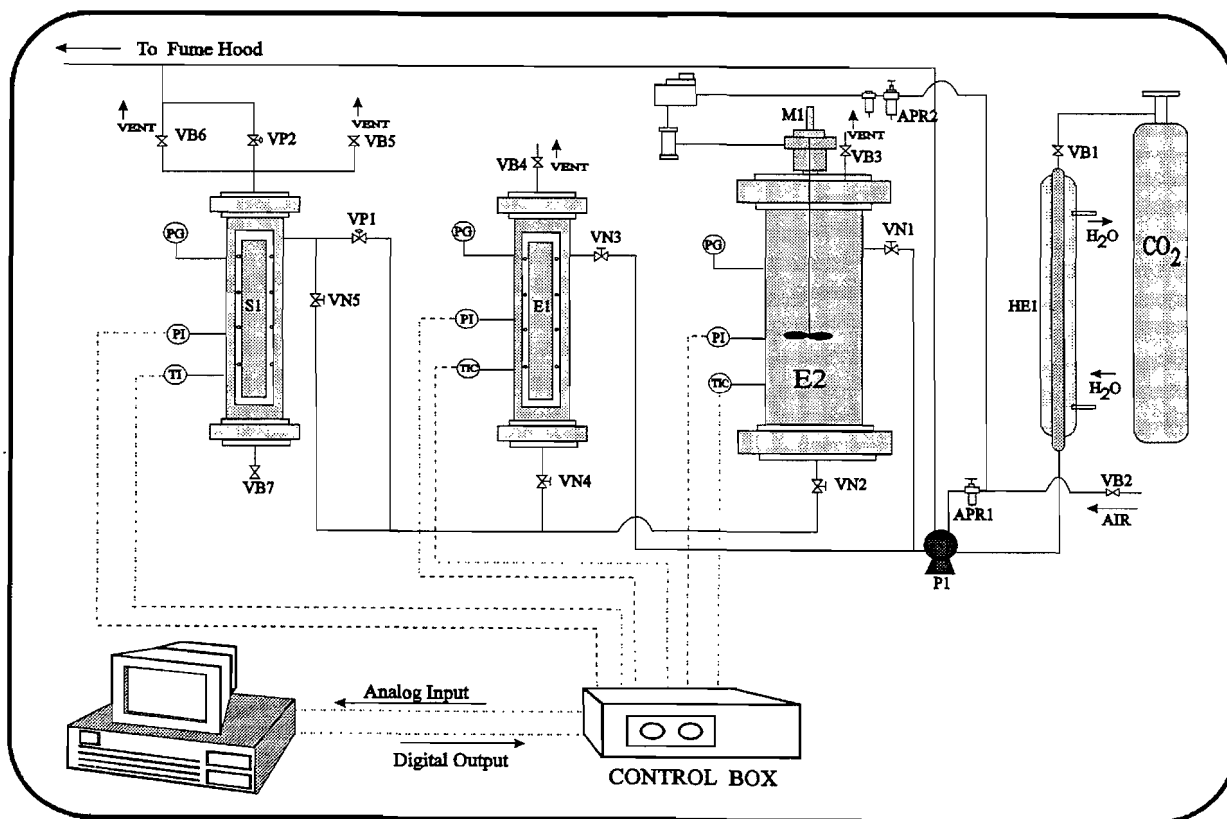


Figure 1. Supercritical carbon dioxide/polymer interactions testing system.

3.0 RESULTS AND DISCUSSION

The names and morphologies of the 20 polymers studied as well as their glass transition temperatures and melting temperatures are shown in Table 2. Five of the 7 conditions were performed on all polymers collected. The other 2 conditions were performed on only 13 polymers (See Table 1). A comprehensive data collection appears in the appendix, whereas this section of the report will be directed to general gravimetric findings and is not a complete discussion of the data (which will appear later under various formats). Furthermore, this discussion will address general similarities between materials that may be grouped together based upon similar response(s) to treatment with carbon dioxide.

Table 2. Morphologies, glass transition temperatures (T_g), and melting temperatures (T_m) of polymers treated with carbon dioxide.

Polymer ID	Polymer Name	Trade Name	Morphology	T _g (°C)	T _m (°C)
ABS	Acrylonitrile butadiene styrene	Royalite	Amorphous		
CAB	Cellulose acetate butyrate	Uvex	Amorphous	110	
HDPE	High-density polyethylene		Crystalline	-125*	140
HIPS	High-impact polystyrene		Amorphous	105*	
HMWPE	High-molecular-weight PE		Crystalline	-130*	142
LDPE	Low-density polyethylene		Crystalline	-21*	116
Nylon 66	Nylon 66	Nylon 66	Crystalline	50*	210
PC	Polycarbonate	Lexan	Amorphous	153	
PEI	Polyetherimide	Ultem	Amorphous	215	
PET	Polyethylene terephthalate	Mylar	Crystalline	69*	260
PETG	PET glycol modified	Vivak	Amorphous	79	
PMMA	Polymethyl methacrylate	Plexiglas	Amorphous	102	
POM	Polyoxymethylene	Delrin	Crystalline	-82*	175
PP	Polypropylene		Crystalline	-8*	166
PPO	Poly(2,6-dimethylphenylene oxide)	Noryl	Amorphous	210	
PSF	Polysulfone	Thermalux	Amorphous	190	
PU	Polyurethane		Amorphous		
PVC	Polyvinyl chloride		Amorphous	82	
PVDF	Polyvinylidene fluoride	Kynar	Crystalline	-40*	167
Teflon	Polytetrafluoroethylene	Teflon	Crystalline	-127*	335

*These values were obtained from *Polymer Handbook*, 2nd Edition, J. Brandrup and E. Immergut, Eds. (Wiley Interscience, 1975). (See section III in this report).

3.1 Changes in Appearance

Severe distortion and/or foam formation was visually apparent for PMMA, PETG, CAB, ABS, and HIPS, which are all amorphous materials, as a result of carbon dioxide treatment at pressures higher than 2,000 psi. This distortion and/or foam formation is readily apparent upon examination of the photographs of the various test specimens found in the appendix. Of these materials, PMMA was the most vulnerable to distortive effects caused by treatment with carbon dioxide. The other materials showed little or no gross deformation, although some had bubbles visible in them after decompression. For example, PC and PVC were found to have light dissolution on their edges after treatment at 3,000 psi and 70°C. PP turned to a light yellow from its initial white color under the same treatment condition (C6). LDPE and even Teflon were observed to have bubbles under the same treatment condition (C6).

The presence of such defects as pronounced bubble formation or changes in color may be obvious upon inspection of the samples or may require more-careful inspection of the samples to note the presence of voids or defects in the polymer contiguity caused by such bubbles. For example, the presence of color in the polypropylene sample suggests the formation of scattering domains (bubbles) leading to Rayleigh/Mie (particle) type scattering, which imparts the yellowish color to the samples (bubble dimensions which may roughly be on the order of the wavelength of visible light or smaller) [13].

The effect of the decompression time, that is, the time over which the pressure was released in the treatment vessel, was evaluated at two different points: (1) a one-hour decompression and (2) a five-hour decompression. Not surprisingly, the longest decompression times showed the least effect on any polymer that showed significant carbon dioxide uptake. Thus, samples that were decompressed over one hour may show very significant structural changes, including extensive foaming and/or bubble development. Comparatively, the same materials that were decompressed over five hours showed significantly less or no effect. The pictures included in the appendix show how dramatic such changes may be.

The practical aspects of these studies suggest that the use of high pressures and short decompression times would be, without question, inappropriate for the cleaning of materials containing polymers prone to the adsorption of large amounts of carbon dioxide (e.g., the acrylates). Interestingly, this same effect may have decidedly useful applications in the disassembly of a material for eventual recycling or reuse. These data should provide additional insight that potential investigators can use to fully exploit these effects.

3.2 Weight Changes of Polymers

Weight change data for polymer specimens measured immediately after treatment in carbon dioxide at conditions C2, C3, C4, C5, and C6 are shown in Tables 3 and 4. The weight changes for amorphous materials, such as PMMA, PETG, ABS, CAB, HIPS, PU, and PSF, were found to be more significant than those for crystalline materials, such as Teflon, LDPE, HDPE, PP, Nylon 66, POM, HMWPE, and PET. Two fundamental mechanisms contribute to changes in the weights of polymeric materials; these mechanisms are (1) carbon dioxide is absorbed by or dissolved in the polymers, which leads to an increase in the weights of the samples (assuming that contaminants or other materials are not being transported into the polymers) and (2) either the polymers or some agents, such as monomers, oligomers, additives, or plasticizers, in the polymers are dissolved or extracted from the polymeric material, which leads to a decrease in the weights of the samples.

The absorption/dissolution of carbon dioxide into a material is readily noted either (1) by observing a large positive change in the weight of the sample proportional to factors such as total surface area and surface to volume ratios or (2) by the presence of extensive foam or bubble formation in the sample. These effects indicate that the material is also significantly plasticized by the carbon dioxide (See "II. Thermal Properties").

The second mechanism can be obviously evidenced by a decrease in weight for some polymers, such as Nylon 66 and CAB, in the course of weight change evaluation. Often, other obvious changes, such as the loss of precise or well-defined edges in the test specimens, accompany the change in weight.

Since both dissolution into and dissolution of a sample may occur, neither effect can be fully known from initial weight change data. These effects often occur simultaneously and, in essence, are in competition during treatment; the extent of the effects vary depending on materials and treatment conditions employed. For example, it has been noted that dissolution of a polymer is considerably more significant than dissolution of carbon dioxide into the polymer for those amorphous materials, such as PVC, which did not demonstrate large positive weight changes.

Table 3. Observed weight changes for polymers treated with carbon dioxide at 40°C for 1 hour.*

Polymer	Thickness	Weight Change		
		1,000 psi	2,000 psi	3,000 psi
ABS	1.60 mm	4.32	4.87	7.35
	2.40 mm	3.16	4.14	7.24
CAB	1.50 mm	1.90	-2.10	-1.03
	2.40 mm	6.61	0.19	7.92
HDPE	0.80 mm	0.21	0.10	0.12
	2.25 mm	0.57	0.38	1.22
HIPS	1.00 mm	1.83	1.09	2.17
	1.50 mm	1.99	2.04	4.48
HMWPE	3.02 mm	0.34	0.55	0.67
LDPE	0.75 mm	0.31	0.15	-0.14
	2.20 mm	1.19	0.23	1.36
Nylon 66	0.80 mm	-0.10	-0.04	-1.14
	3.20 mm	0.05	-0.04	0.00
PC	3.00 mm	0.87	0.93	1.88
PEI	1.74 mm	0.56	0.88	1.04
PET	0.26 mm	0.89	0.69	1.81
PETG	1.00 mm	2.99	5.22	5.14
	2.40 mm	1.47	2.35	4.18
PMMA	1.50 mm	5.85	8.45	12.96
	3.00 mm	4.10	7.86	11.27
POM	0.80 mm	1.38	1.06	1.54
	1.50 mm	0.95	1.17	2.07
PP	0.70 mm	0.42	0.00	-0.11
	2.25 mm	1.56	0.69	1.98
PPO	6.63 mm	0.72	1.33	1.32
PSF	1.46 mm	1.25	2.27	2.23
PU	3.05 mm	2.25	4.39	3.54
PVC	2.24 mm	0.52	0.83	1.55
PVDF	1.50 mm	1.00	2.73	3.02
Teflon	0.80 mm	0.11	0.05	0.07
	1.70 mm	0.58	0.03	0.51

*A decompression time of one hour was used in all experiments. Weight changes (wt %) were measured the same day as the treatments.

Table 4. Observed weight changes for polymers treated with carbon dioxide at 3,000 psi for 1 hour.*

Polymer	Thickness	Weight Change		
		25°C	40°C	70°C
ABS	1.60 mm	6.49	7.35	0.08**
	2.40 mm	4.57	7.24	
CAB	1.50 mm	-4.40	-1.03	-5.16**
	2.40 mm	15.29	7.92	
HDPE	0.80 mm	0.28	0.12	0.27**
	2.25 mm	0.65	1.22	
HIPS	1.00 mm	1.92	2.17	0.08**
	1.50 mm	3.51	4.48	
HMWPE	3.02 mm	0.26	0.67	1.24
LDPE	0.75 mm	-0.02	-0.14	0.81**
	2.20 mm	1.40	1.36	
Nylon 66	0.80 mm	-0.29	-1.14	-0.47**
	3.20 mm	0.01	0.00	
PC	3.00 mm	1.16	1.88	
PEI	1.74 mm	0.52	1.04	2.06
PET	0.26 mm	0.79	1.81	2.02
PETG	1.00 mm	5.36	5.14	0.28**
	2.40 mm	2.52	4.18	
PMMA	1.50 mm	11.30	12.96	7.70**
	3.00 mm	9.51	11.27	
POM	0.80 mm	1.79	1.54	0.29**
	1.50 mm	1.68	2.07	
PP	0.70 mm	0.28	-0.11	0.19**
	2.25 mm	1.84	1.98	
PPO	6.63 mm	0.63	1.32	3.43
PSF	1.46 mm	1.25	2.23	4.09
PU	3.05 mm	2.48	3.54	2.78
PVC	2.24 mm	0.84	1.55	
PVDF	1.50 mm	1.15	3.02	3.58
Teflon	0.80 mm	0.09	0.07	-0.01**
	1.70 mm	0.82	0.51	

*A decompression time of one hour was used in all experiments.

**Weight changes (wt %) were measured the same day as the treatments.

3.3 Effects of the Treatment Conditions on the Weight Changes of Polymers

From the data shown in Tables 3 and 4, the effects of treatment pressures and temperatures on observed weight changes of polymeric materials can be ascertained. At present, it is unclear whether there are any direct or simple relationships between the observed weight changes and the treatment conditions employed. This is not unexpected since many changes are occurring simultaneously that will affect the observed changes in weight. For example, as the pressure increases, both the density and solubility parameter of the carbon dioxide change although not linearly. In addition, pressure changes can also be expected to directly affect polymer morphology although probably not to a very significant extent at such low pressures as employed in these experiments.

However, for PMMA and ABS, which both had large weight changes under all conditions, the weight changes appear to be directly proportional to the treatment pressures and temperature. For other materials with relatively small weight changes, the effects of pressures and temperatures were not obvious. Although the two mechanisms described in the previous section determined the resulting weight changes, there are many additional factors, such as structures, morphologies, values of T_g and T_m of materials, and dimensions of samples, that also may affect variations in the data.

3.4 Effects of the Dimensions of Samples on the Weight Changes of Polymers

As shown in Tables 3 and 4, two different thicknesses for 11 of the 20 polymer specimens were measured to ascertain the effects of dimensions on weight changes. Different thicknesses of the test specimens in the range tested led to different values of weight change at the same treatment conditions. However, for reasons described previously, no general relationship between the dimensions of samples and weight change data could be made.

3.5 Desorption of Carbon Dioxide

Weight increases of polymers after treatment in carbon dioxide indicate the absorption/dissolution of carbon dioxide in polymers. In most cases, the loss of carbon dioxide from polymers, as determined by the change in mass with time, showed a linear dependence on the logarithm of time. That is, the desorption (loss) of carbon dioxide was greatest immediately after removal from the treatment chamber and slowed exponentially with time. If these same data are treated in a diffusion consistent manner, that is, by plotting the weight change as a function of the square root of time ($t^{1/2}$), highly nonlinear behavior is noted, indicating that these systems show non-Fickian behavior. However, these nearly linear logarithmic plots may be

useful in predicting the general weight-loss behavior in polymers that absorb significant quantities of carbon dioxide.

Examples of such weight-loss behavior can be seen in Figures 2, 3, and 4. In these figures, the weight changes of PMMA, PVDF, and PPO are plotted as a function of the logarithm of time after removal from the carbon dioxide treatment chamber. The desorption rates, i.e., the slopes of the lines in Figures 2, 3, and 4, were not found to be dependent on treatment condition.

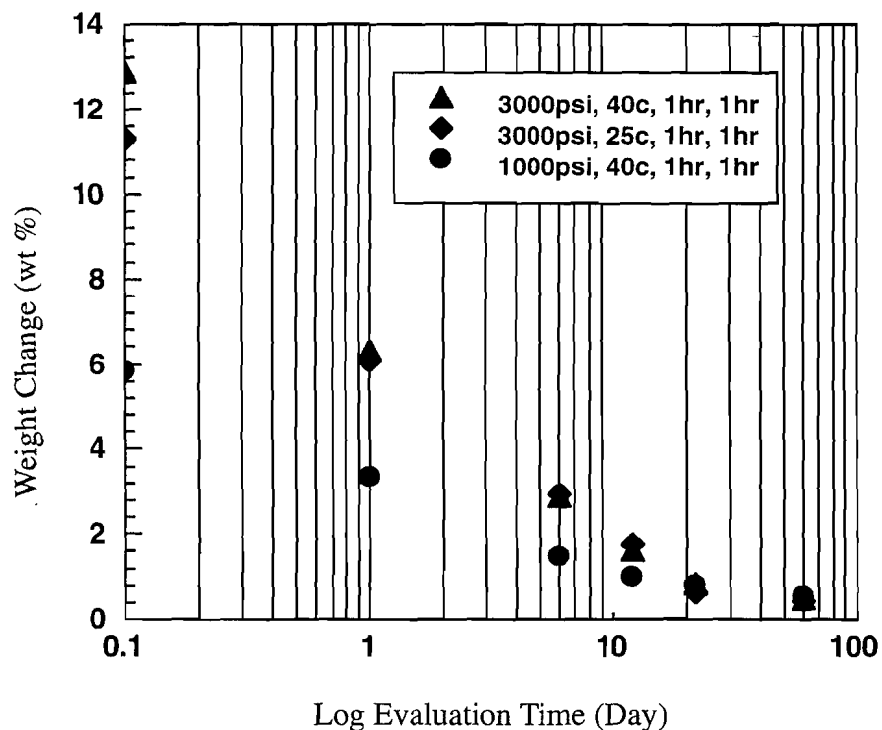


Figure 2. Weight changes for PMMA as a function of evaluation time. PMMA has been treated in carbon dioxide at three conditions.

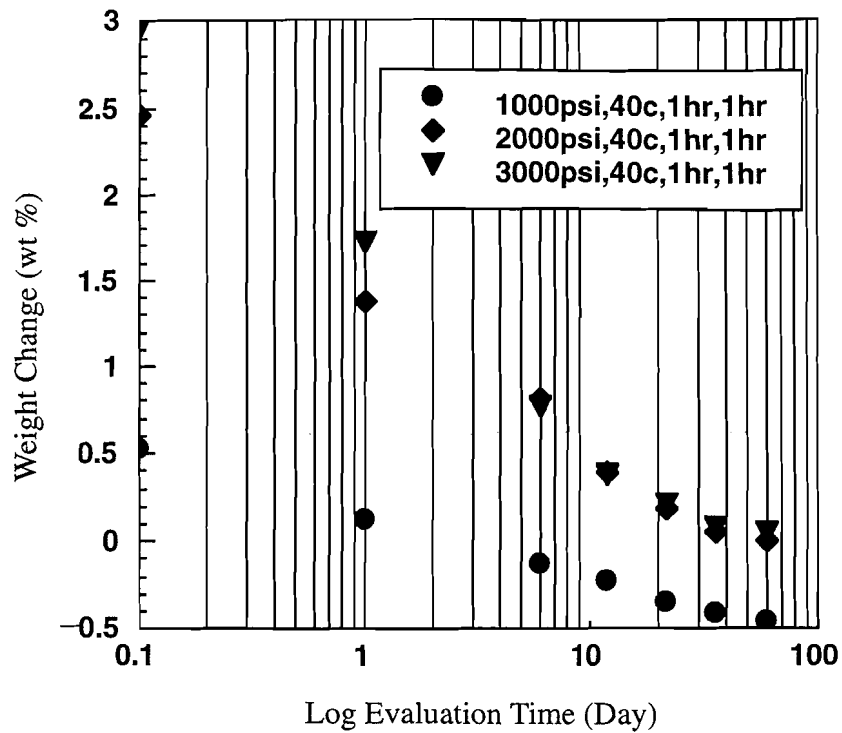


Figure 3. Weight changes for polyvinylidene fluoride as a function of evaluation time. Polyvinylidene fluoride has been treated in carbon dioxide at three conditions.

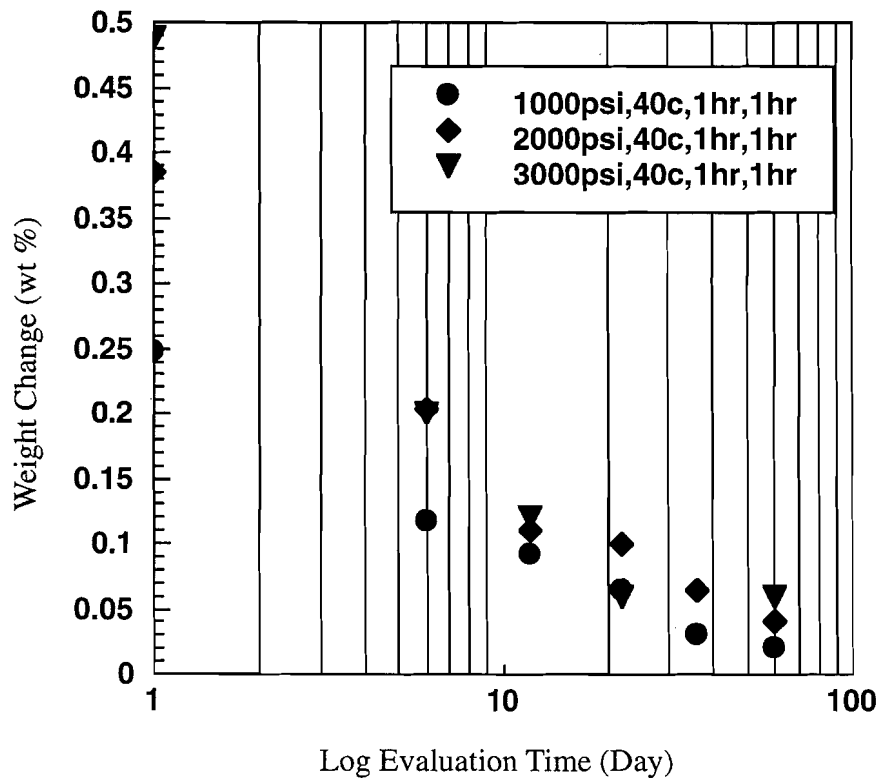


Figure 4. Weight changes for poly(2,6-dimethylphenylene oxide) as a function of evaluation time. Poly(2,6-dimethylphenylene oxide) has been treated in carbon dioxide at three conditions.

3.6 Solubility of Polymers in Carbon Dioxide

Figures 5 through 9 show weight change data for conditions C1, C3, C6, and C7, respectively, from two separate evaluations: (1) the same day as treatment and (2) 8 months (or 5 months as in Figure 8) after treatment. It is clear that some dissolution of some polymers in carbon dioxide does take place as evidenced from the differences in weight of the original sample and the weight 8 months after treatment, which allowed for the complete loss of any dissolved carbon dioxide. Weight loss for some polymers is evident even under the most mild conditions explored (for example, C1) as shown in Figure 5. Dissolution under these conditions was found to be significant for PMMA, Nylon 66, and CAB. As previously stated, changes in the weights of the polymer specimens may be caused by dissolution/extraction of either monomers, oligomers, polymers, additives, stabilizers, processing aids, plasticizers, etc.

Based on the assumption that such solubility does occur, Table 5 shows a comparison between the total solubility of carbon dioxide in polymers and the one-dimensional solubility parameter for polymers. The data in Table 5 clearly shows that the solubility of carbon dioxide was more significant in amorphous materials, such as PMMA, ABS, CAB, PSF and PPO, than in crystalline materials, such as HDPE, LDPE, PP, POM and Teflon. Although PVDF is a crystalline material, it has a significant amount of dissolved carbon dioxide, which is likely the result of the interaction between carbon dioxide and fluorine. This is not unexpected since fluorinated compounds have high solubilities in carbon dioxide, and indeed, high-molecular-weight fluorinated polymers can be synthesized and dissolve in supercritical carbon dioxide [14]. Although ABS had an unexpectedly low uptake of carbon dioxide under condition C6, this polymer showed extensive foam formation, which lead to nearly complete desorption of carbon dioxide during decompression. Thus, it is believed that much of the absorbed carbon dioxide, consistent with the weight changes seen for the other conditions tested, was lost in the foaming of the polymer.

In our investigation of the structures of the amorphous materials which have significant solubility of carbon dioxide, we found that these materials have polar groups such as COOR, -CN, S=O, and Ph-O. Thus, in addition to the morphology factor, the polarity of a polymer is crucial in determining the solubility of carbon dioxide. The solubility parameters of polymers and carbon dioxide are discussed in the next section.

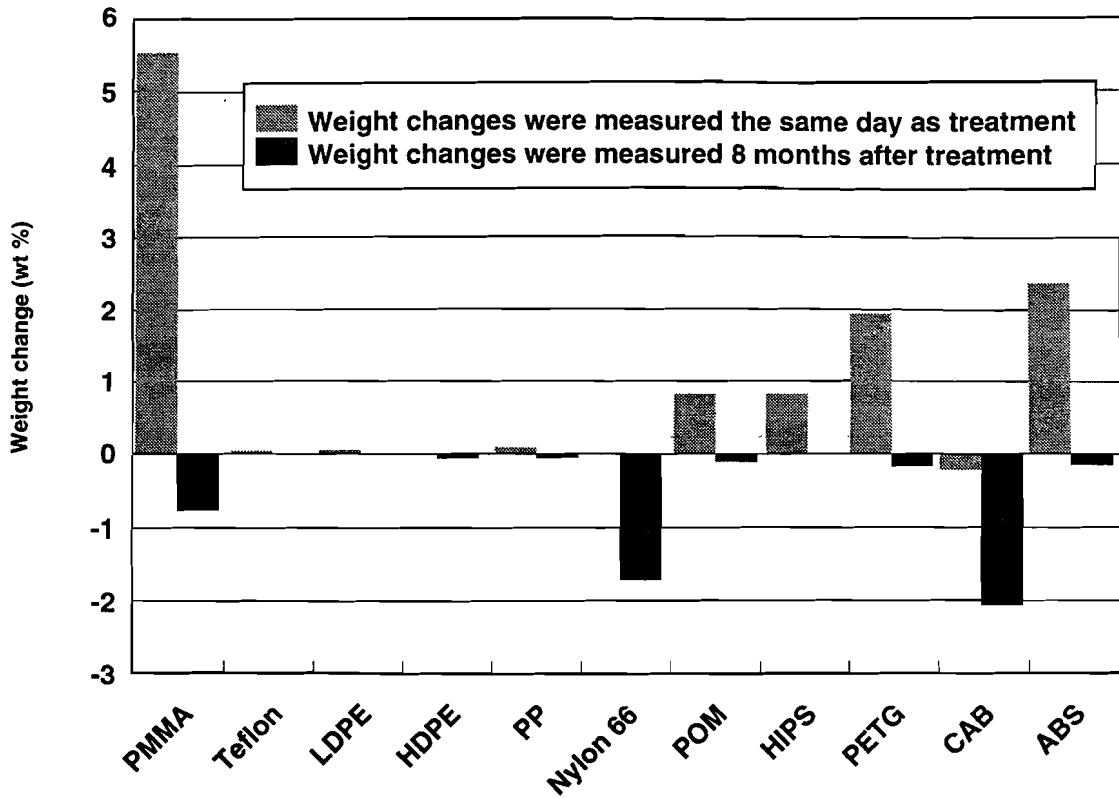


Figure 5. Weight changes for polymers treated in carbon dioxide at 1,000 psi and 25°C for 1 hour. The decompression time was 1 hour.

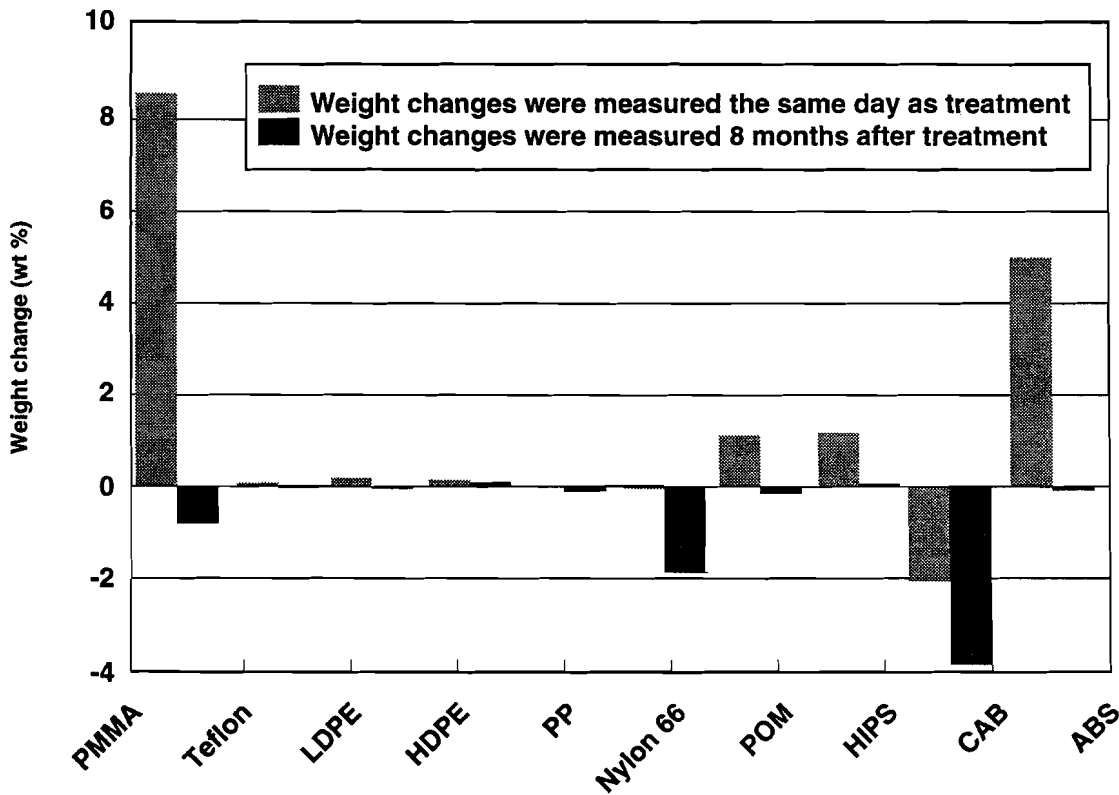


Figure 6. Weight changes for polymers treated in carbon dioxide at 2,000 psi and 40°C for 1 hour. The decompression time was 1 hour.

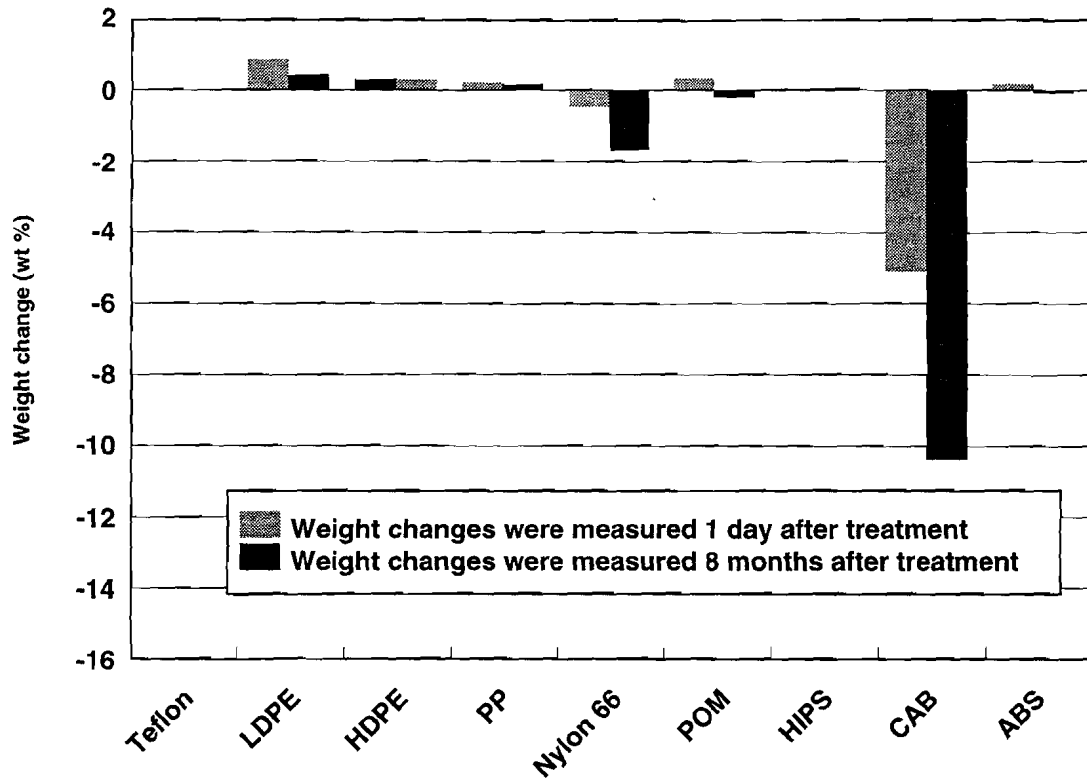


Figure 7. Weight changes for polymers treated in carbon dioxide at 3,000 psi and 70°C for 1 hour. The decompression time was 1 hour.

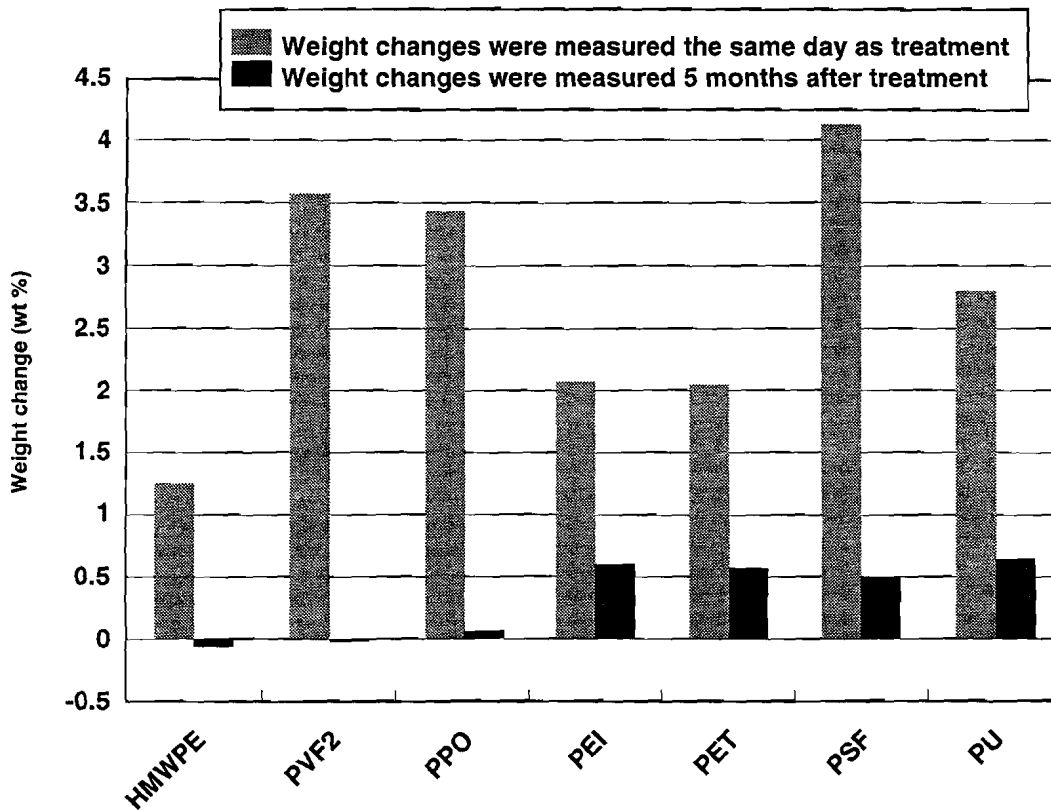


Figure 8. Weight changes for polymers treated in carbon dioxide at 3,000 psi and 70°C for 1 hour. The decompression time was 1 hour.

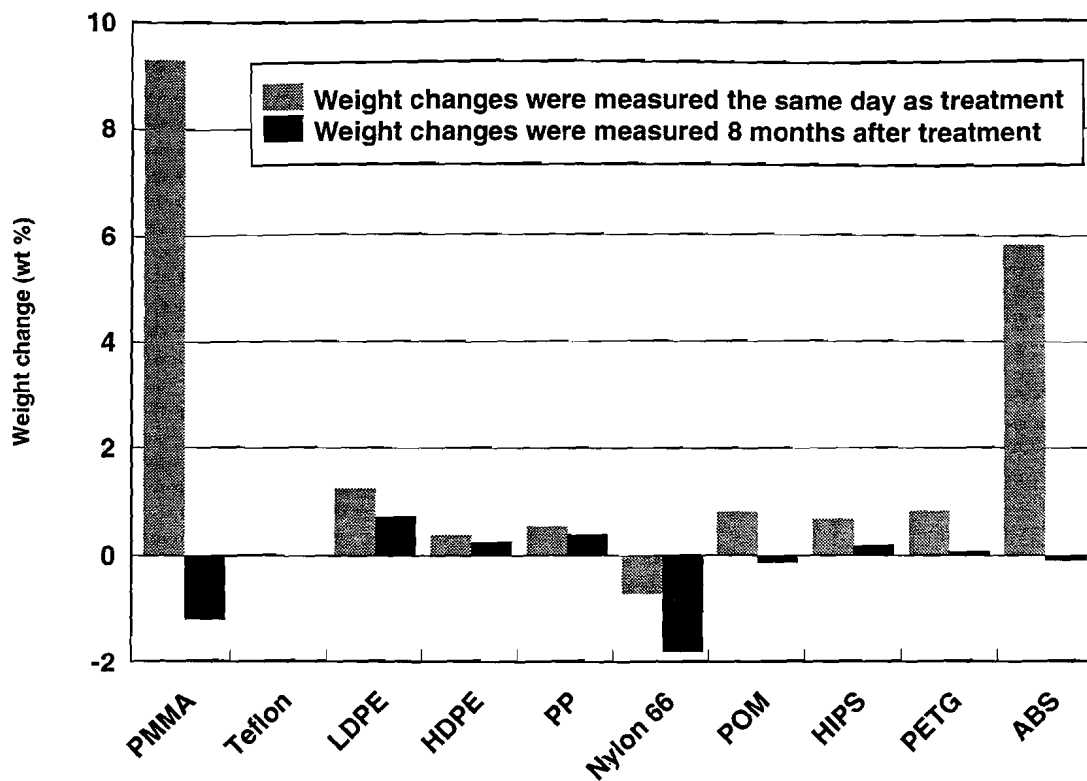


Figure 9. Weight changes for polymers treated in carbon dioxide at 3,000 psi and 70°C for 1 hour. The decompression time was 5 hours.

Table 5. Total solubility of carbon dioxide as determined gravimetrically 8 months after treatment.

Polymer	Solubility Parameter	Solubility of CO ₂ (wt %)			
		C1	C3	C6	C7
ABS	9.8	2.5	5.0	0.2	5.9
CAB	12.0	1.9	1.8	5.3	
HDPE	8.3	0.1	0.1	0.0	0.1
HIPS	8.8	0.8	1.1	0.0	0.5
HMWPE	8.3			1.3*	
LDPE	8.3	0.0	0.2	0.4	0.5
Nylon 66	13.7	1.8	1.8	1.3	1.1
PC	10.0				
PEI				1.5*	
PET	10.6			1.5*	
PETG	10.6	2.1			0.8
PMMA	9.3	6.3	9.3		10.5
POM	10.5	1.0	1.3	0.5	0.9
PP	8.1	0.1	0.2	0.1	0.1
PPO	8.9			3.4*	
PSF	10.5			3.6*	
PU	10.0			2.2*	
PVC	9.5		0.1		
PVDF				3.6*	
Teflon	6.4	0.0	0.1	0.0	0.0

*Evaluation time was 5 months after treatment.

3.7 Solubility Parameters of Polymers and Carbon Dioxide

3.7.1 Definition of Solubility Parameter

Solubility occurs when the free energy of mixing is negative. The equation for calculating the change in free energy is

$$\Delta G = \Delta H - T\Delta S , \quad (1)$$

where ΔG is the change in the Gibb's free energy, ΔH is the heating of mixing, T is the absolute temperature, and ΔS is the entropy of mixing. Since the dissolution of a polymer is always connected with a large increase in entropy, the magnitude of the enthalpy term ΔH is the deciding factor in determining the sign of the free-energy change.

Hildebrand and Scott proposed that

$$\Delta H_m = V_m [(\Delta E_1/V_1)^{1/2} - (\Delta E_2/V_2)^{1/2}]^2 \phi_1 \phi_2 , \quad (2)$$

where ΔH_m is the overall heat of mixing, V_m is the total volume of the mixture, ΔE is the energy of vaporization of component 1 or 2, V is the molar volume of component

1 or 2, and ϕ is the volume fraction of component 1 or 2 in the mixture [15]. The expression $\Delta E/V$ is the energy of vaporization per cubic centimeter and is described as the cohesive energy density.

If Equation 2 is rearranged as

$$\Delta H_m/V_m \phi_1 \phi_2 = [(\Delta E_1/V_1)^{1/2} - (\Delta E_2/V_2)]^2 , \quad (3)$$

it may be seen that the heat of mixing per cubic centimeter at a given concentration is equal to the square of the difference between the square roots of the cohesive energy densities of the components. It is therefore convenient to assign to this latter quantity the symbol δ . Thus,

$$\Delta H_m/V_m \phi_1 \phi_2 = (\delta_1 - \delta_2)^2 . \quad (4)$$

The quantity δ is known as the solubility parameter. It may thus be seen that the unit heat of mixing of two substances is dependent on $(\delta_1 - \delta_2)^2$. If the heat of mixing is not so large as to prevent mixing, then $(\delta_1 - \delta_2)^2$ has to be relatively small. In fact, if $(\delta_1 - \delta_2)^2 = 0$, mixing and dissolution is assured by the entropy factor. As the value approaches zero, $\delta_1 \rightarrow \delta_2$. This is mathematically equivalent to saying that if the δ values of two substances are nearly equal, the substances will be miscible.

3.7.2 Solubility Parameter of CO₂

The density of a fluid is extremely sensitive to pressure and temperature near the critical point ($P_r = 1$ and $T_r = 1$) as shown for pure carbon dioxide in Figure 10. Figure 11 shows the relationship between pressure and density for CO₂ at 37°C. It is clear that there is not a linear relationship between pressure and density at this temperature. Therefore, care needs to be exercised when doing experiments in this regime because of the possibility of large changes in density. In the experiments reported herein, pressures were chosen to maximize the variation of density of the gas during the static treatment of samples, i.e., pressures between 1,000 and 3,000 psi show a rather large overall change in the density of the carbon dioxide.

Consider the simple case of the solubility of a solid in pure CO₂. At ambient pressure, the density is 0.002 g/cm³; thus, the solubility of a solid in the gas is low. At the critical point, the density is 0.468 g/cm³, which is much closer to that of a typical organic liquid at ambient pressure leading to similar solubility. The solubility parameter as a function of supercritical density can be represented by the relationship

$$\delta = 1.25 P_c^{1/2} \rho_r / \rho_r(\text{liq}) , \quad (5)$$

where P_c is the critical pressure, ρ_r is the reduced density of the supercritical fluid, and $\rho_r(\text{liq})$ is the reduced density of the liquid, which is normally about 2.7 [16]. If

the unit $(\text{cal}/\text{cm}^3)^{1/2}$ is used for δ , Equation 5 can be simplified as

$$\delta = 8.52 \rho \quad (6)$$

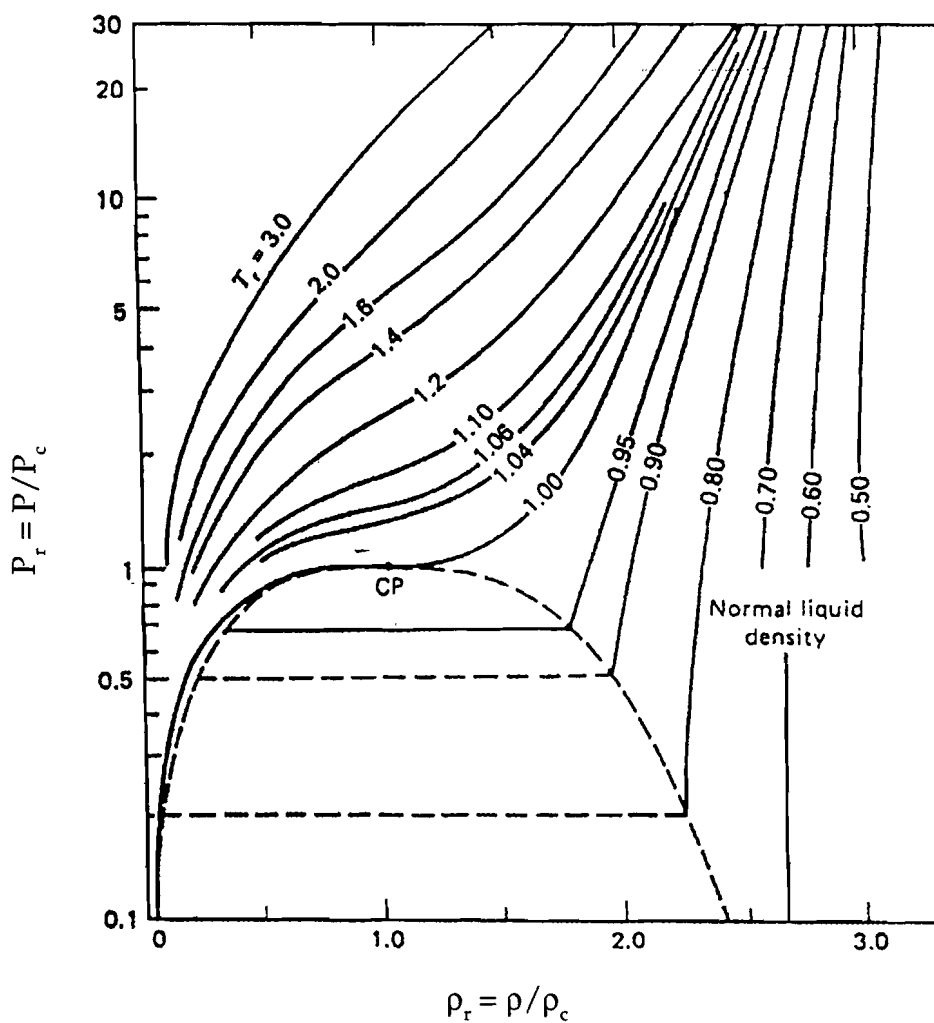


Figure 10. Pressure versus density isotherms for pure carbon dioxide ($T_c = 31^\circ\text{C}$, $P_c = 1,070$ psi, and $\rho_c = 0.468 \text{ g}/\text{cm}^3$).

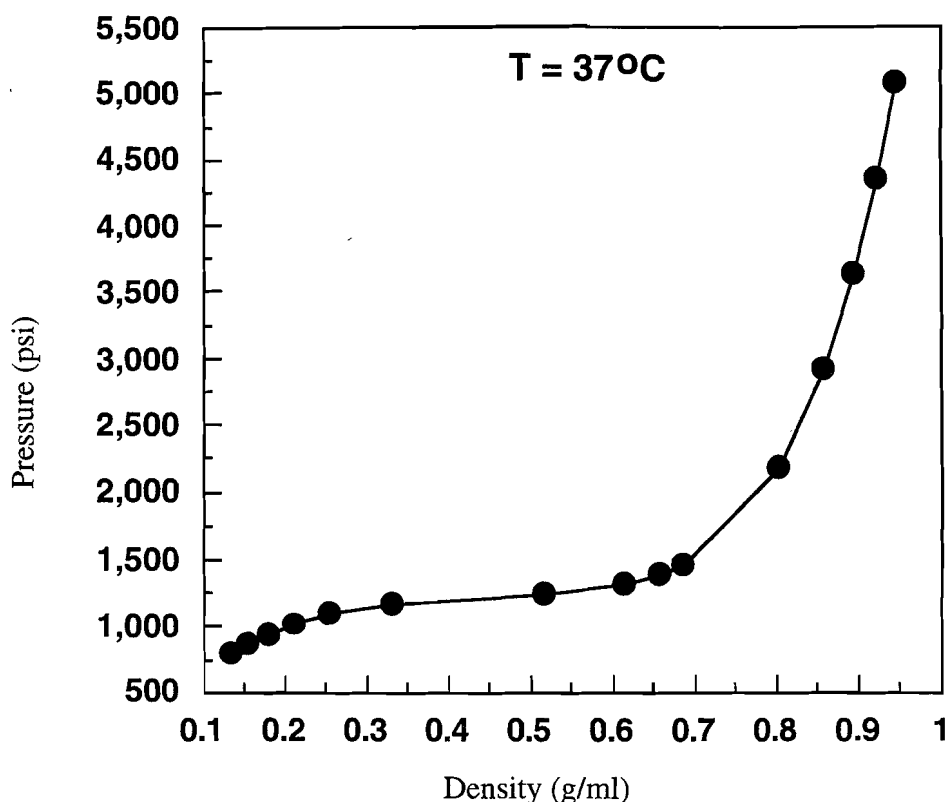


Figure 11. Pressure versus density at 37°C for pure carbon dioxide.

3.7.3 Solubility Parameters of Polymers

The solubility parameter of a solvent is a readily calculable quantity. The solubility parameter of a polymer (or for that matter, any nonvolatile substance) cannot be determined directly because most polymers cannot be vaporized without decomposing. There is a great variety of indirect methods for estimating polymer solubility parameters. For example, the solubility parameters of polymers may be (1) evaluated from polymer-liquid interaction parameters; (2) determined experimentally by observation of their dissolution behavior, degree of swelling, or other polymer property in a spectrum of liquids with a range of solubility parameters; (3) determined experimentally by turbidimetric titrations; (4) determined by Hansen parameters, i.e., three-component parameters; (5) determined by the viscosity of a dilute solution of a polymer; (6) calculated from the group contribution methods; or (7) determined by other methods. Table 5 shows the Hildebrand solubility parameters for some polymers, which were selected from the *Handbook of Polymer-Liquid Interaction Parameters and Solubility Parameter* [17]. In the handbook, the author has collected, from many sources, the solubility parameters for the most popular or widely used polymers; these parameters were determined using the various experiments and/or calculations as described above.

3.7.4 Solubility of Carbon Dioxide in Polymers

As described previously, if the solubility parameter of carbon dioxide equals that of a polymer, the two substances will be theoretically miscible (note, however, that most polymers can dissolve in a solvent due to additional factors other than just solubility parameter considerations). Based on this concept, the greatest miscibility between carbon dioxide and a polymer will occur when the solubility parameter of carbon dioxide equals that of the polymer, or conversely, the least absorption will occur when the solubility parameters differ by the greatest amount.

Figures 12 through 15 show plots of solubility of carbon dioxide in polymers as a function of solubility parameter differences between carbon dioxide and polymers. These figures indicate, however, that the solubilities of carbon dioxide in polymers are not solely dependent on the solubility parameter difference.

There are many reasons why the solubility parameter theory cannot be necessarily well applied to the polymer/carbon dioxide system. The first and most obvious reason is that no assumptions were made about the morphologies of polymers in deriving the solubility parameter. The solubility parameter governs only the heat of mixing of liquids or amorphous polymers. A crystalline polymer cannot dissolve in a solvent of similar solubility parameter without first destroying the crystallite. Secondly, the solubility parameters of polymers selected from the handbook were collected from many sources using different experiments and calculations. As a result, these solubility parameter values are better as references than as an absolute assessment of solubility/miscibility, although the differences in solubility parameter should reflect some trends with polymers.

Lastly, the concept of the solubility parameter may be extended from a one-dimensional analysis—as presented in section 3.7.1—in which all the molecular interactions are treated simply to a multidimensional approach in which individual aspects of solvent/solute miscibility are examined. Thus, we are extending the solubility approach to a three-dimensional one wherein the hydrogen bonding, dispersive, and dipolar interactions are individually assessed and summed as

$$\delta^2 = \delta_d^2 + \delta_p^2 + \delta_h^2,$$

where δ = total solubility parameter, δ_d = component due to dispersion forces, δ_p = component due to polar forces, and δ_h = component due to hydrogen bonding. We believe this approach will demonstrate a more satisfactory correlation for a wide variety of materials, especially those in which hydrogen-bonding interactions are important in the material. Combining this approach with corrections for morphological contents of the polymer should provide an accurate model for interactions between polymers and carbon dioxide.

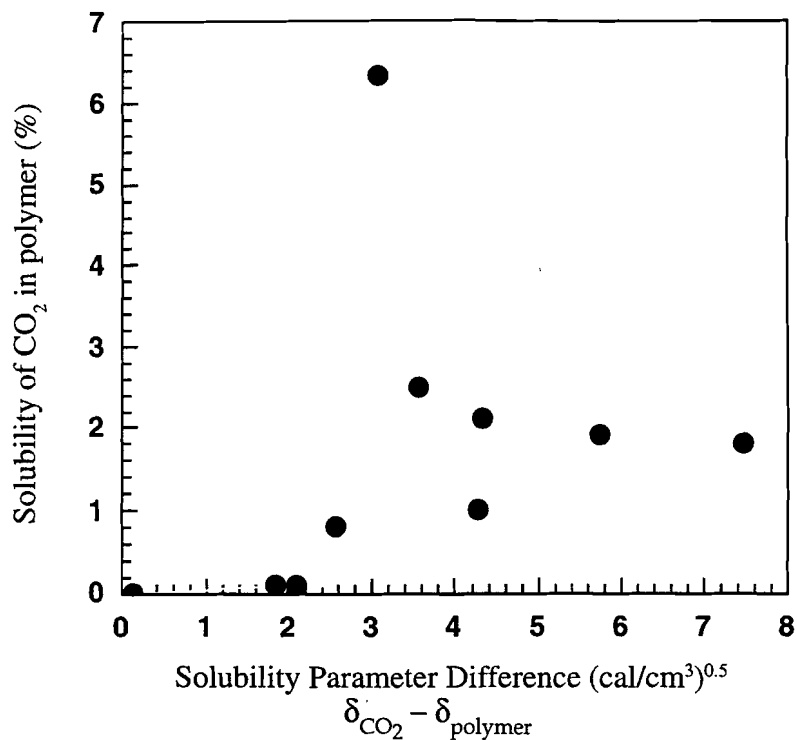


Figure 12. Solubilities of carbon dioxide in polymers evaluated 8 months after treatment at 1,000 psi, 25°C, 1 hour, 1 hour as a function of solubility parameter differences between polymers and carbon dioxide.

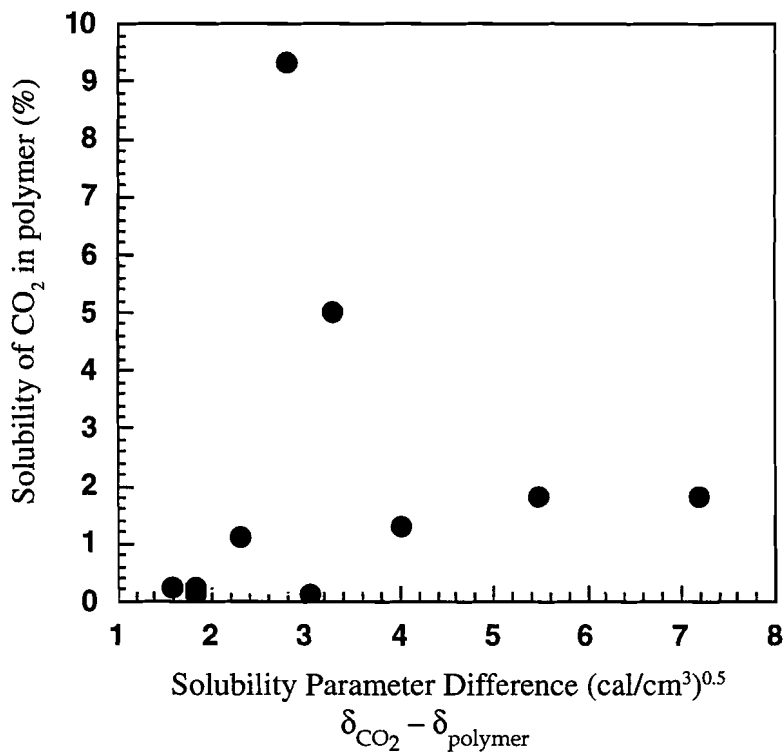


Figure 13. Solubilities of carbon dioxide in polymers evaluated 8 months after treatment at 2,000 psi, 40°C, 1 hour, 1 hour as a function of solubility parameter differences between polymers and carbon dioxide.

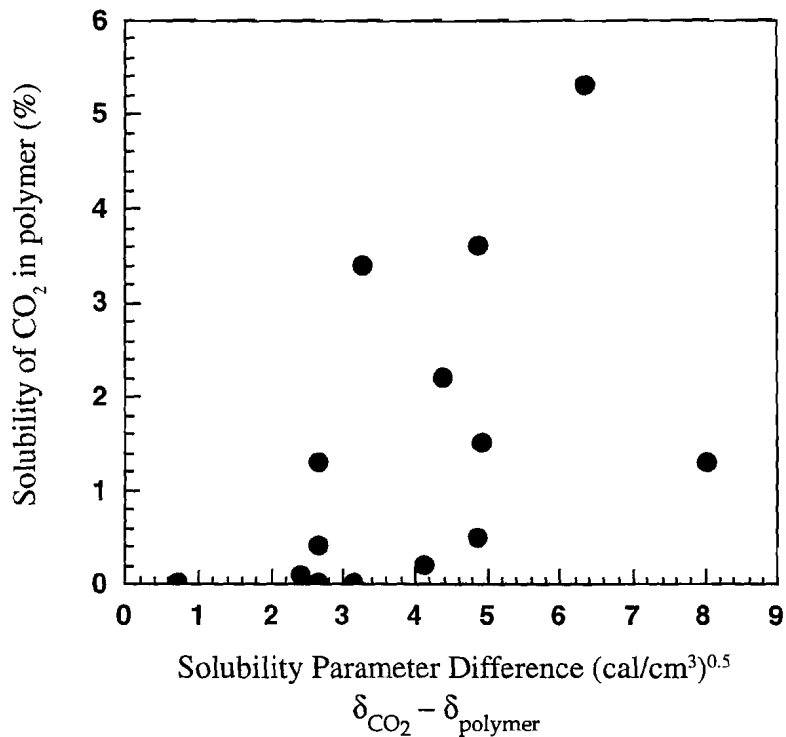


Figure 14. Solubilities of carbon dioxide in polymers evaluated 8 (or 5) months after treatment at 3,000 psi, 70°C, 1 hour, 1 hour as a function of solubility parameter differences between polymers and carbon dioxide.

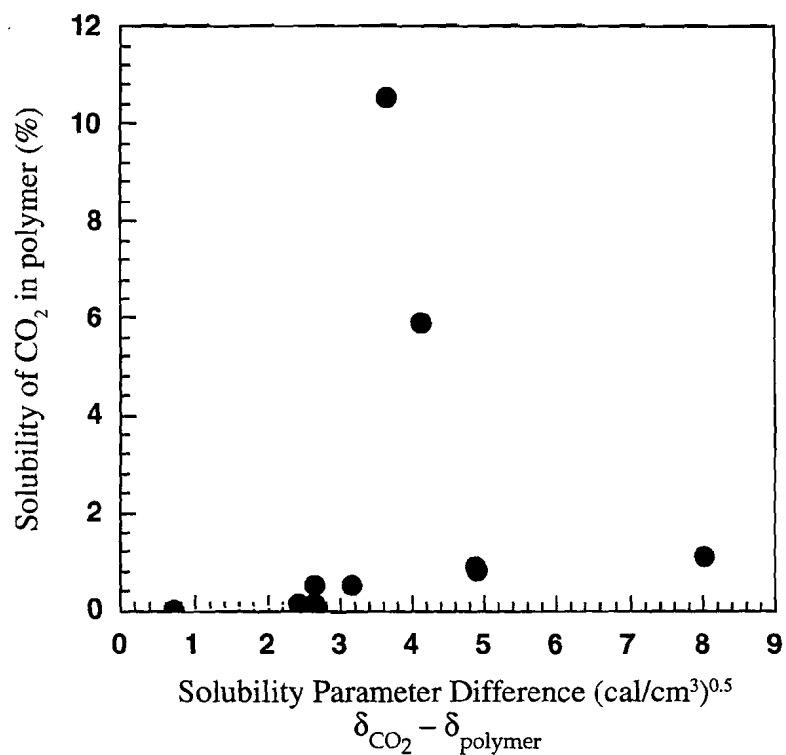


Figure 14. Solubilities of carbon dioxide in polymers evaluated 8 months after treatment at 3,000 psi, 70°C, 1 hour, 5 hours as a function of solubility parameter differences between polymers and carbon dioxide.

4.0 CONCLUSION

Carbon dioxide at high pressure can cause the absorption, swelling, and dissolution of some polymers as evidenced by the weight change data from treatments in carbon dioxide. Amorphous polymers have shown more significant absorption, swelling, and dissolution phenomena than crystalline polymers. Extensive foam formation has been found for some amorphous polymers, such as PMMA, PETG, ABS, CAB, and HIPS, when they are treated at pressures over 2,000 psi. These data indicate that polymer foams of various densities can readily be made from the above materials when they are heated above glass transition temperature in carbon dioxide at relatively low pressures.

The dissolution of polymers in carbon dioxide after treatment could be due to the extraction of monomers, oligomers, polymers, additives, plasticizers, etc. The extent of dissolution has been shown to be correlated with many factors of the polymer structure, including the morphology and chemical structure. Except in a few cases, a universal predictive approach for carbon dioxide-polymer interactions has not been found.

However, these data indicate a number of materials and real-life processing conditions for which either super or subcritical carbon dioxide may be employed as a cleaner with undue adverse effects on the materials or the final product.

5.0 REFERENCES

1. G. K. Fleming and W. J. Koros, "Dilation of Polymers by Sorption of Carbon Dioxide Elevated Pressures. 1. Silicone Rubber and Unconditioned Polycarbonate," *Macromolecules* **19**, 2285–91 (1986).
2. S. A. Stern, and A.H. DeMeringo, "Solubility of Carbon Dioxide in Cellulose Acetate at Elevated Pressures," *J. Polym. Sci.: Polym. Phys. Ed.* **16**, 735–51 (1978).
3. J. S. Chiou, J. W. Barlow, and D. R. Paul, "Plasticization of Glassy Polymers by CO₂," *J. Appl. Polym. Sci.* **30**, 2633–42 (1985).
4. W. C. V. Wang and E. J. Kramer, "Effects of High-Pressure CO₂ on the Glass Transition Temperature and Mechanical Properties of Polystyrene," *J. Polym. Sci.: Polym. Phys. Ed.* **20**, 1371–84 (1982).
5. R. G. Wissinger and M. E. Paulaitis, "Swelling and Sorption in Polymer–CO₂ Mixtures at Elevated Pressures," *J. Polym. Sci.: part B: Polym. Phys.* **25**, 2497–2510 (1987).
6. Y. Kamiya, K. Mizoguchi, Y. Naito, and T. Hirose, "Gas Sorption in Poly(vinyl benzoate)," *J. Polym. Sci.: part B: Polym. Phys.* **24**, 535–547 (1986).
7. T. Hirose, K. Mizoguchi, and Y. Kamiya, "Dilation of Polyethylene by Sorption of CO₂," *J. Polym. Sci.: part B: Polym. Phys.* **24**, 2107–15 (1986).
8. Y. Kamiya, T. Hirose, K. Mizoguchi, and Y. Naito, "Gravimetric Study of High-Pressure Sorption of Gases in Polymers," *J. Polym. Sci.: part B: Polym. Phys.* **24**, 1525–39 (1986).
9. W. J. Koros, G. N. Smith, and V. Stannett, "High-Pressure Sorption of CO₂ in Solvent-Cast PMMA and PET Films," *J. Appl. Polym. Sci.* **26**, 159–170 (1981).
10. A. R. Berens, G. S. Huvard, R. W. Korsmeyer, and F. W. Kunig, "Application of Compressed CO₂ in the Incorporation of Additives into Polymers," *J. Appl. Polym. Sci.* **46**, 231–242 (1992).
11. J. A. Martin, M.S. thesis, MIT (1981).
12. F. A. Waldman, M.S. thesis, MIT (1982).
13. K. Nassau, *The Physics and Chemistry of Color* (John Wiley and Sons, Inc., New York, New York, 1983), pp. 232–239.
14. J. M. De Simone, Z. Guan, and C. S. Eisbernd, "Synthesis of Fluoropolymers in Supercritical Carbon Dioxide," *Science* **257**, 945–947 (1992).
15. J. Hildebrand and R. Scott, *The Solubility of Nonelectrolytes*, 3rd ed. (Reinhold, New York, New York, 1950).
16. A. F. M. Barton, *Handbook of Solubility Parameters and other Cohesion Parameters*, 2nd ed. (CRC Press, Boca Raton, Florida, 1991).
17. A. F. M. Barton, *Handbook of Polymer-Liquid Interaction Parameters and Solubility Parameter* (CRC press, Boca Raton, Florida, 1990).

II. Thermal Properties

1.0 INTRODUCTION

The states of low-molecular-weight compounds are well known; the three states are crystalline, liquid, and gaseous. In contrast, no high-molecular-weight polymer vaporizes to a gaseous state; all polymers decompose before reaching the boiling point. In addition, no high-molecular-weight polymer attains a totally crystalline structure except in the single-crystal state. In fact, many important polymers do not crystallize at all but, rather, form glasses at low temperature. At higher temperatures, they form rubbers. The transition that separates the glassy state from the rubbery state is known as the glass–rubber transition or, simply, the glass transition. The glass transition temperature (T_g) is an indication of the glass-rubber transition.

Qualitatively, the glass transition region can be interpreted as the onset of long-range, coordinated molecular motion. While only 1–4 chain atoms are involved in motions below the glass transition temperature, about 10–50 chain atoms attain sufficient thermal energy to move in a coordinated manner in the glass transition region.

There are a number of structural features which determine the value of the glass transition temperature. Since the glass transition temperature is a temperature at which molecular rotation about single bonds becomes restricted, it is obvious that these structural features influence the ease of rotation. The features which affect the glass transition temperature are as follows:

- Groups attached to the backbone; these groups increase the energy required for rotation.
- Rigid structures (e.g., phenylene groups) incorporated in the backbone of the molecule.
- Secondary bonding (e.g., hydrogen bonding) between chains.
- Primary bonding (e.g., cross-linking) between chains.
- Length of side chains.
- Molecular weight.
- Copolymerization.
- Plasticization.

Plasticization is very important in polymer processing. For example, low-molecular-weight compounds are added to polyvinyl chloride during its processing to separate chains and increase their mobility. The effect of plasticization will cause a marked reduction in the glass transition temperature. The addition of about 40% of diethyl hexyl phthalate to polyvinyl chloride will reduce its glass transition temperature by about 100°C. As will be presented in this section, carbon dioxide can also plasticize polymers and cause a tremendous decrease in the glass transition temperature. On the other hand, the effect of plasticization may induce or increase crystallization during the outgas process of absorbed gases for those polymers which have the structural regularity.

In this section, we present an evaluation of the effect of high-pressure carbon dioxide on three polymers. The properties studied include the glass transition temperature (T_g), the melting temperature (T_m), and the melting enthalpy (ΔH). These polymers include two amorphous materials and one semicrystalline material.

2.0 EXPERIMENTAL PROCEDURE

Three polymer sheets of polymethyl methacrylate (PMMA), polyethylene terephthalate glycol modified (PETG), and polyethylene terephthalate (PET) were used as received from Rohm&Haas, Lustrо Plastics, and Du Pont; the trade names of the polymers are Plexiglas, Vivak, and Mylar, respectively. These polymers are all transparent and have thicknesses of 1.5, 1.0, and 0.26 mm, respectively. Coupon-shaped samples of 1×4 cm were made from all three polymers and subjected to carbon dioxide treatment at 3,000 psi and 25°C in a 5-liter, high pressure chamber. The treatment was held for 1 hour and then the high-pressure chamber was decompressed to atmospheric pressure for one additional hour. The carbon dioxide-treated samples were immediately subjected to differential scanning calorimetry (DSC) and thermogravimetric analysis (TGA) evaluations. These treated samples were stored in very clean polyethylene bags at $23 \pm 2^\circ\text{C}$ for more evaluations; for example, in addition to same-day treatment, treatments were performed the next day, the seventh day, and the sixteenth day. DSC evaluation was performed using Perkin Elmer DSC-2C to obtain the T_g , T_m , and ΔH ; a heating rate of 20°C per min was used for all three polymers. A Du Pont Model 2950 TGA was used to evaluate the total amount of carbon dioxide uptake in the polymers. A heating rate of 20°C per min was used for all thermogravimetric analyses.

3.0 RESULTS AND DISCUSSION

Both PMMA and PETG showed significant swelling as well as extensive bubble/foam formation in the bulk of the material when treated in carbon dioxide at 3,000 psi and 25°C for 1 hour and decompression for another hour. PET, however, showed no significant changes when treated under identical conditions. This is probably because of the completely amorphous character of both PMMA and PETG, whereas PET is a crystalline material.

Thermogravimetric analysis is an analytical technique for determining the weight change of a sample as a function of temperature. Figures 1 through 3 show representative thermogravimetric profiles for PMMA, PETG, and PET, respectively, that had been treated with carbon dioxide. The weight losses in the range of about 120 – 150°C has been assigned to the outgas of carbon dioxide from the polymers while weight losses occurring in the range of 290 – 400°C are due to the decomposi-

tion of the polymers. The outgas temperature of PMMA was higher than that of PETG since the glass transition temperature of PMMA is higher than that of PETG. From the figures, the amounts of CO₂ uptake in polymers can be obtained as a function of evaluation conditions employed. Data on the carbon dioxide dissolution for PMMA, PETG, and PET are shown in Tables 1, 2, and 3, respectively. It is immediately obvious that the carbon dioxide content decreased as a function of evaluation time. In other words, the carbon dioxide that is dissolved in these polymers continuously diminishes with time.

Of the samples reported here, PMMA showed the greatest uptake of carbon dioxide, while PETG and PET showed progressively lesser amounts when evaluated approximately 2 hours after treatment (See Tables 1, 2, and 3). PET showed a carbon dioxide uptake of less than 1 wt % because of the semicrystalline nature of the material. This uptake is due to the dissolution of the carbon dioxide in the amorphous regions of the sample. Compared with PETG, PMMA has a relatively high amount of CO₂ uptake in spite of a higher T_g for PMMA. Since both materials are amorphous, it is hypothesized that the presence of a side-chain ester functionality—as compared with the main-chain ester functionality of PETG—allows for the greater dissolution of carbon dioxide in PMMA. Hence, the side-chain ester functionality appears to interact more strongly with CO₂ than one in the main chain.

Figures 4 through 6 show semilog plots of the carbon dioxide uptake as a function of evaluation time. The plots for the amorphous polymers, PMMA and PETG, showed a linear correlation between the wt % of carbon dioxide and the log of time (See Section 3.5 in "I. Absorption, Swelling, and Dissolution of Carbon Dioxide in Polymers at Elevated Temperatures"). Carbon dioxide loss in the PET samples, however, did not demonstrate a similar linear behavior, which suggests a more-complex relationship between the outgassing of carbon dioxide and the morphology of the sample. It is speculated that the crystalline component in PET retarded carbon dioxide outgassing because of either greater mean free-paths of the gas through the more-complex lattice or through some specific adsorption with the crystallites in the sample. More detailed experiments are in progress to determine the exact nature of the nonlinear desorption characteristic for this material.

The T_g, T_m, and ΔH for PMMA, PETG, and PET are shown in Tables 1 through 3, respectively, as a function of time after treatment with carbon dioxide. Figures 7 and 8 show plots of T_g versus carbon dioxide content for PMMA and PETG, respectively. As expected, the glass transition temperatures of both polymers decrease as carbon dioxide contents in the polymers increase. This evidence suggests that plasticization by CO₂ occurs in the polymers. The most dramatic change in the T_g was noted immediately after treatment of the polymer samples and was, surprisingly, 22°C for PMMA and 42°C for PETG.

A significant increase in the degree of crystallinity for PET, a semicrystalline material, was not observed seven days after treatment in carbon dioxide (See Table 3). Interestingly, however, a significant increase in crystallinity for PET was noted 16

days after treatment. If absorbed by polymers, CO₂ is believed to be absorbed only in the amorphous regions of the material and not in the crystalline regions. Immediately following treatment, the absorbed CO₂ plasticizes the amorphous region of PET as was clearly evidenced in both PMMA and PETG. The plasticized PET chain segments may now adopt a crystalline form because of the increased chain mobility afforded by the carbon dioxide "solvent." Crystallinity was noted to increase only after sufficient "solvent" diffused out of the polymer to allow for the nucleation and crystallization of the polymer chains. Hence, the degree of crystallinity increased as a function of the evaluation time (See Table 3).

Table 1. Thermogravimetric data showing the amount of carbon dioxide uptake and glass transition temperature for PMMA.*

Evaluation Time (day)	% Weight Loss at 200°C	% of CO ₂ uptake	Tg (°C)
Untreated	-1.03		102
0.1	-8.99	7.96	80
1.0	-5.46	4.43	87
7.0	-3.69	2.66	100
16.0	-2.57	1.54	101

*Treated in carbon dioxide at 3,000 psi and 25°C for 1 hour.

Table 2. Thermogravimetric data showing the amount of carbon dioxide uptake and glass transition temperature for PETG.*

Evaluation Time (day)	% weight loss at 170°C	% of CO ₂ uptake	Tg (°C)
Untreated	-0.45		79
0.1	-5.43	4.98	37
1.0	-2.71	2.26	50
7.0	-1.23	0.78	69
16.0	-0.77	0.32	74

*Treated in carbon dioxide at 3,000 psi and 25°C for 1 hour.

Table 3. Thermogravimetric data showing the amount of carbon dioxide uptake, crystalline melting temperature, and enthalpy for PET.*

Evaluation Time (day)	Weight Loss at 170°C	% of CO ₂ uptake	T _m (°C)	ΔH (cal/g)
Untreated	-0.36		259	6.5
0.1	-1.08	0.72		
1.0	-0.67	0.31		
7.0	-0.52	0.16	261	6.9
16.0	-0.50	0.14	262	9.5

*Treated in carbon dioxide at 3,000 psi and 25°C for 1 hour.

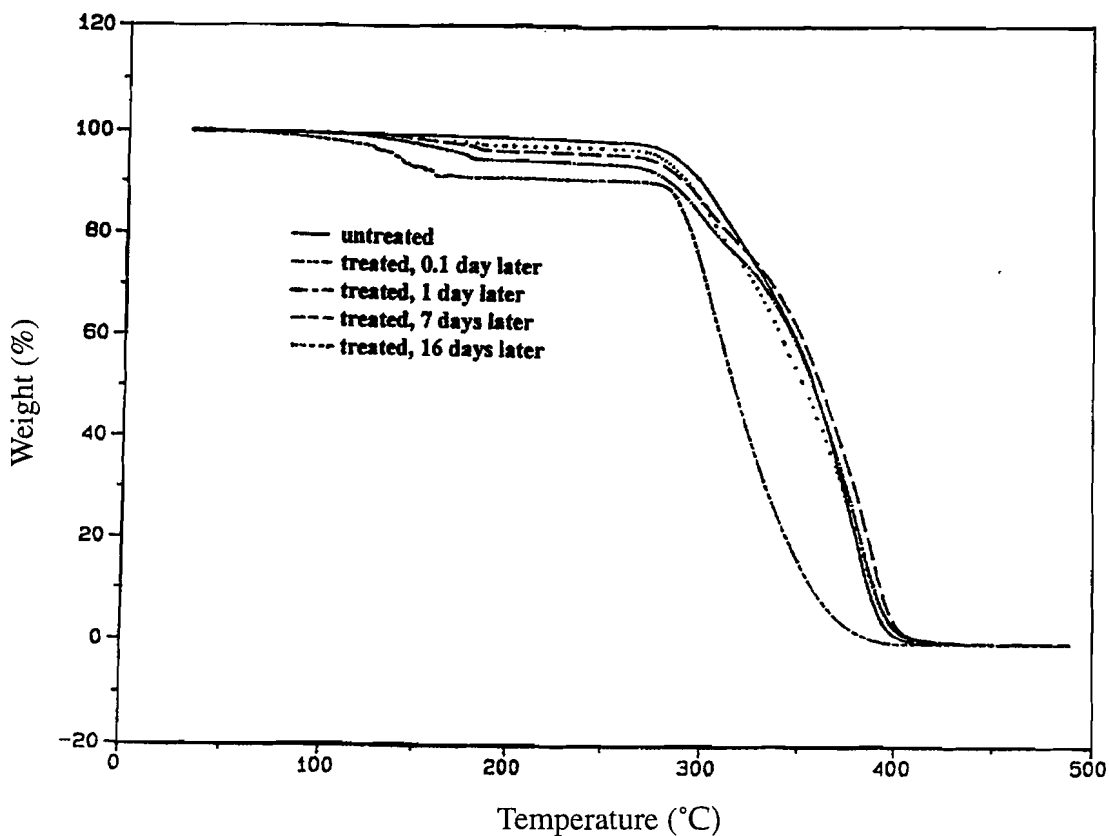


Figure 1. TGA traces for PMMA as a function of evaluation time. The treatment condition was in CO₂ at 3,000 psi, 25°C, 1 hour, 1 hour.

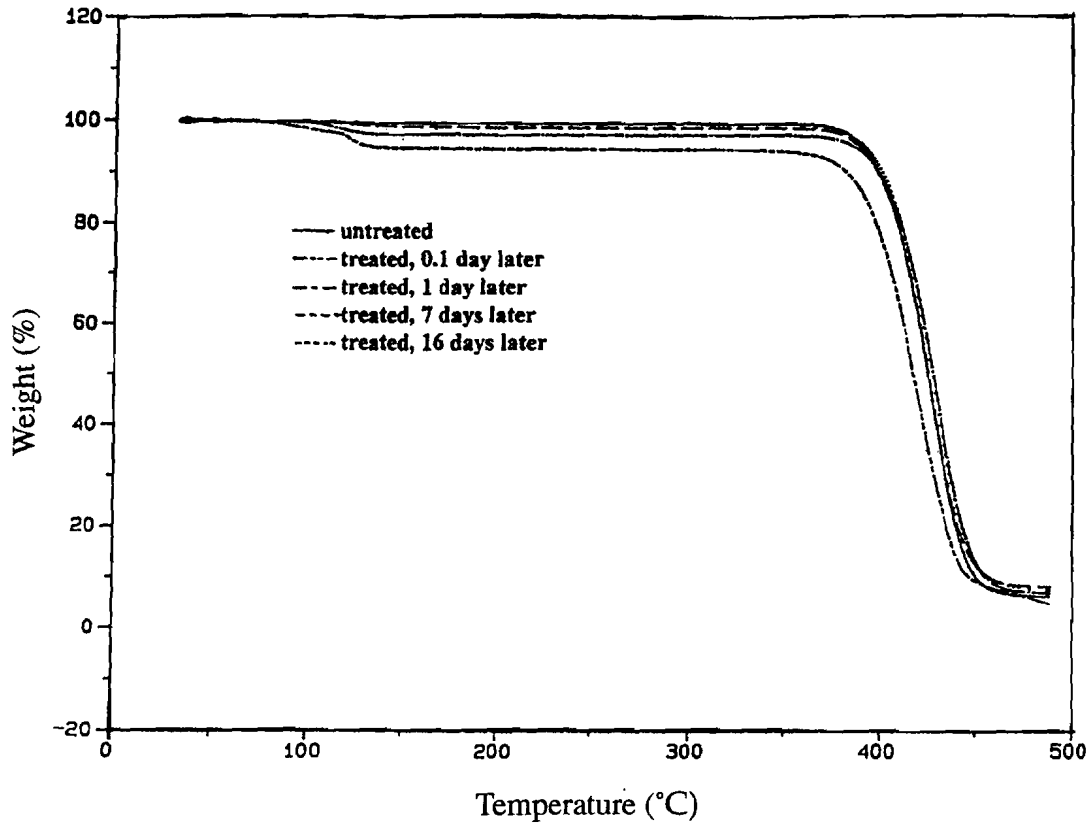


Figure 2. TGA traces for PETG as a function of evaluation time. The treatment condition was in CO₂ at 3,000 psi, 25°C, 1 hour, 1 hour.

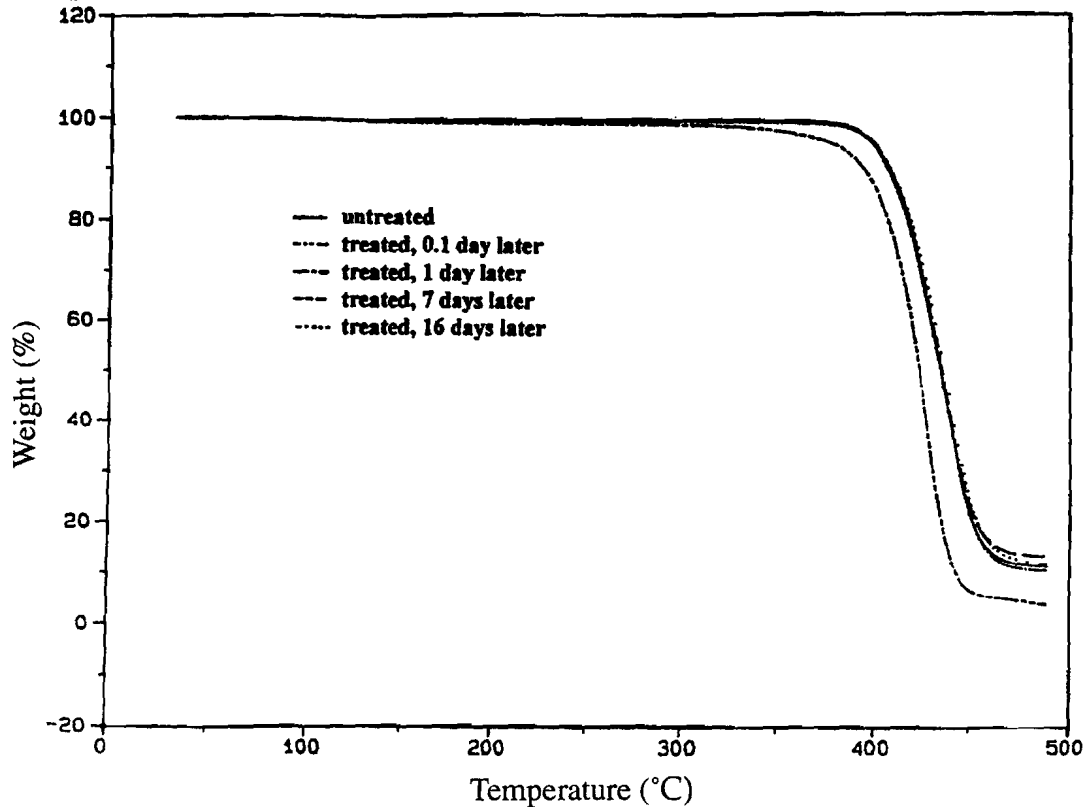


Figure 3. TGA traces for PET as a function of evaluation time. The treatment condition was in CO₂ at 3,000 psi, 25°C, 1 hour, 1 hour.

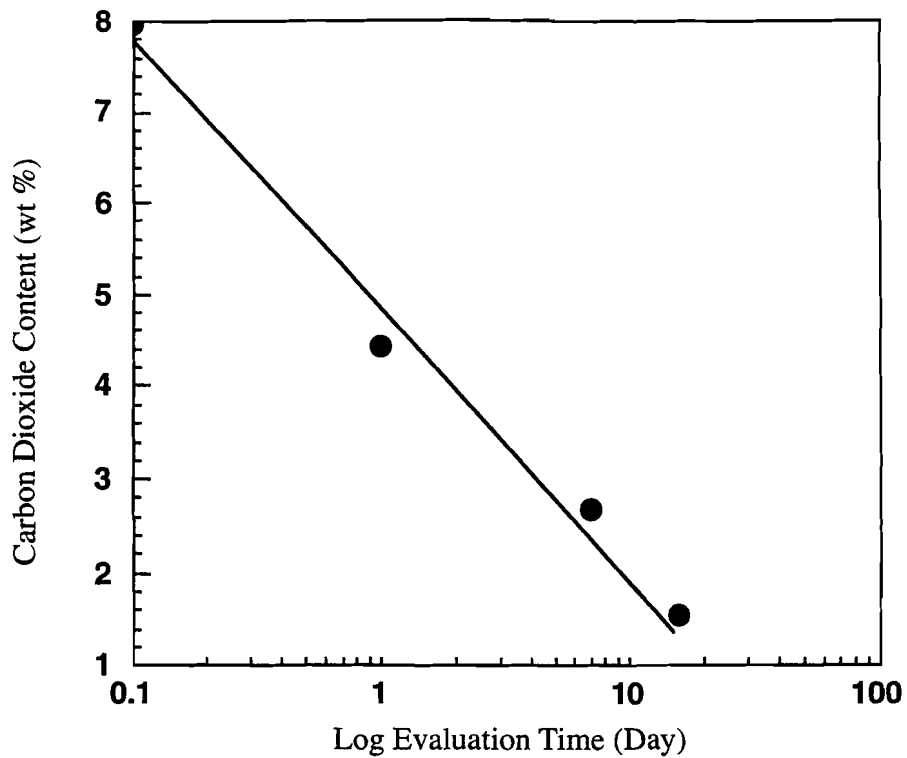


Figure 4. Carbon dioxide content (from TGA data) in PMMA as a function of evaluation time. PMMA has been treated in carbon dioxide at 3,000 psi and 25°C for 1 hour.

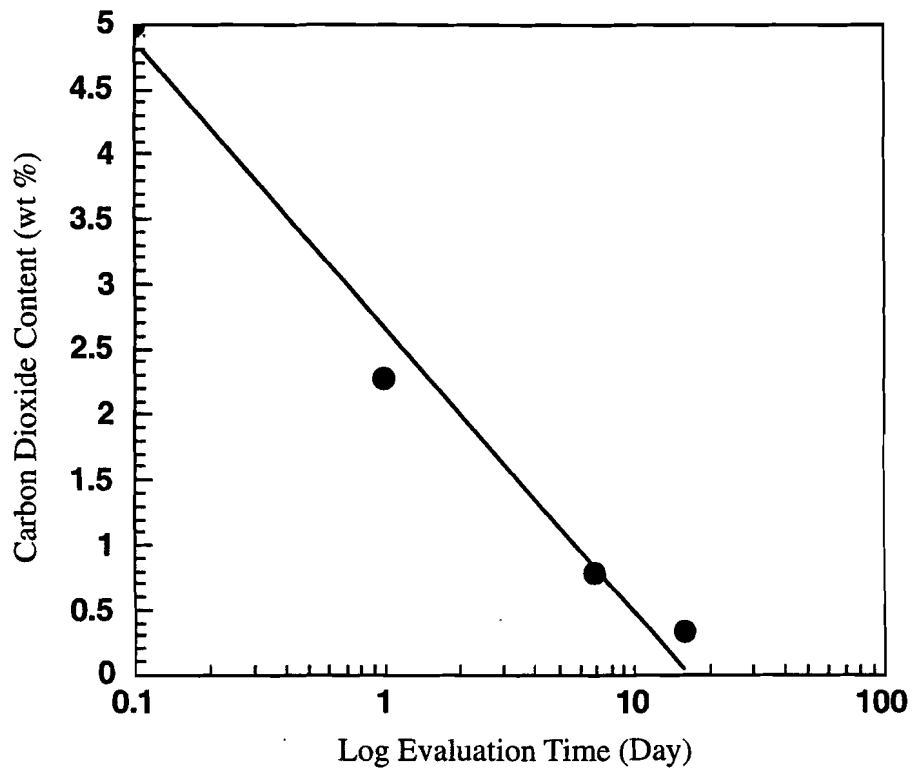


Figure 5. Carbon dioxide content (from TGA data) in PETG as a function of evaluation time. PETG has been treated in carbon dioxide at 3,000 psi and 25°C for 1 hour.

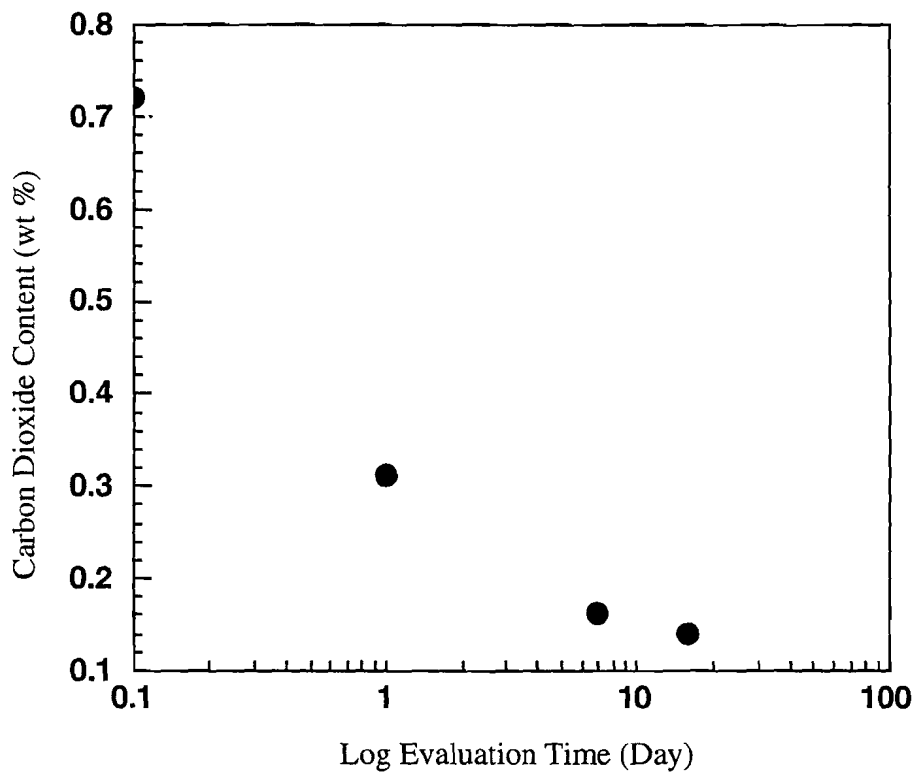


Figure 6. Carbon dioxide content (from TGA data) in PET as a function of evaluation time. PET has been treated in carbon dioxide at 3,000 psi and 25°C for 1 hour.

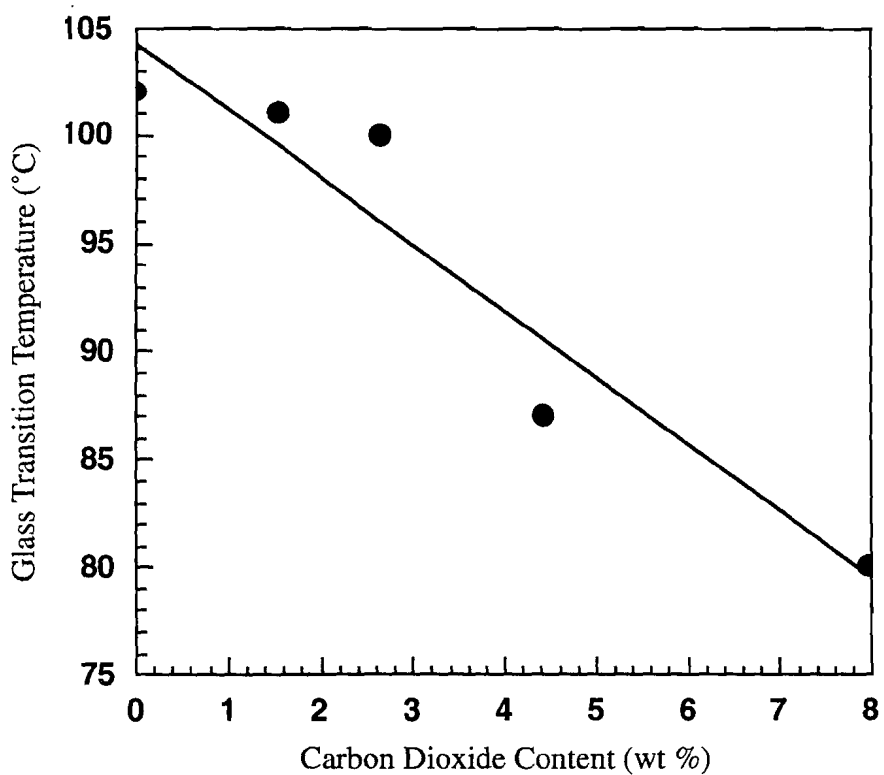


Figure 7. The glass transition temperature (from DSC) of PMMA as a function of carbon dioxide content (from TGA data) in PMMA. PMMA has been treated in carbon dioxide at 3,000 psi and 25°C for 1 hour.

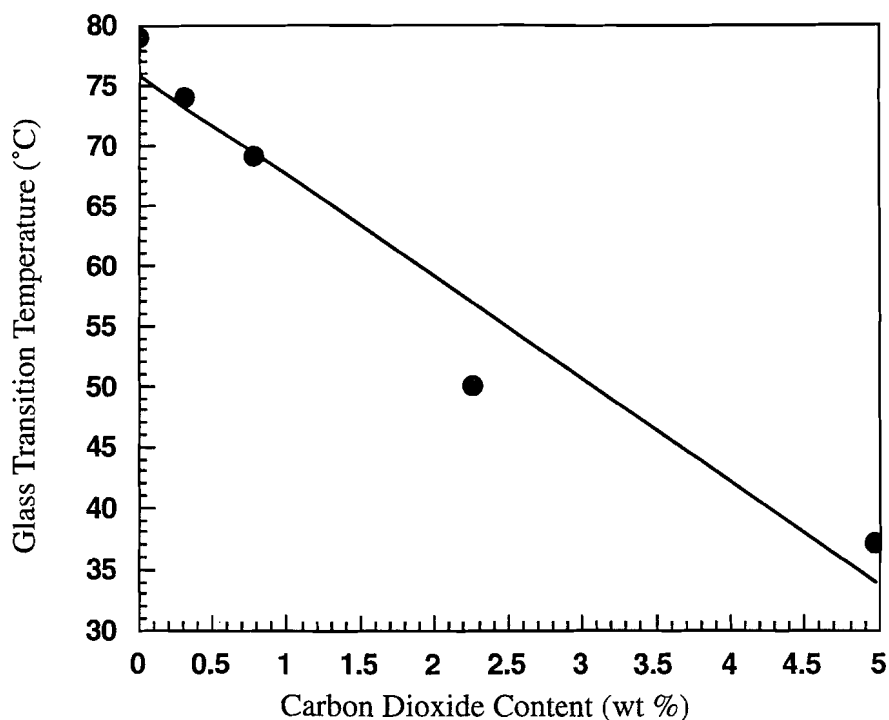


Figure 8. The glass transition temperature (from DSC) of PETG as a function of carbon dioxide content (from TGA data) in PETG. PETG has been treated in carbon dioxide at 3,000 psi and 25°C for 1 hour.

4.0 CONCLUSION

Carbon dioxide at high pressure can plasticize polymers and cause significant reductions in the glass transition temperature as well as induce crystallization and cause increases in the melting temperature and melting enthalpy of polymers. These phenomena may be quite important in certain applications, such as the formation of polymer foam, the impregnation of polymers with chemical additives, the extraction of low-molecular-weight species from polymers, and the separation of gas mixtures using polymer membranes. These applications are based on the fact that carbon dioxide can induce considerable swelling in glassy polymers at high pressures, thus enabling materials to easily diffuse into or out of the polymer matrix.

In addition, these data indicate when reasonable care needs to be exercised in using supercritical carbon dioxide for cleaning applications. Amorphous materials can show significant uptakes of carbon dioxide, depending on the treatment conditions employed. Secondly, even semicrystalline materials can show property changes that result from the absorption of carbon dioxide, whereby the percent crystallinity of the polymer may be increased by treatment with carbon dioxide.

III. Mechanical Properties

1.0 INTRODUCTION

Tensile properties are one of the most important indications of the strength of a material. Mechanical properties of polymeric materials are often measured using standard test sample configurations. In these tensile studies, a dumbbell-shaped test specimen that conformed to ASTM D638 was used for all measurements. Figure 1 shows the dimensions and configuration of such a sample.

Figure 2 shows a typical stress-strain plot of a plastic specimen. The plot provides five descriptive parameters: (1) tensile strength, that is, the maximum stress the material withstands at point of rupture; (2) yield strength, the stress at which nonelastic deformation begins; (3) ultimate elongation, the total amount of extension the sample undergoes; (4) modulus of elasticity, the slope of the initial steep portion of the curve, which represents the stress-strain ratio in the elastic region in which Hooke's law holds; and (5) toughness, or more precisely, the energy to break per unit volume, which is the integrated area under the curve and is a rough measure of a plastic's toughness.

Translating the data from such a diagram provides a terminology that is useful in describing various plastics. A hard plastic is one with a high modulus. A strong plastic would be represented by high tensile yield. A brittle plastic would generate a curve that terminates before reaching the yield point. A tough plastic is one with a high energy to break per unit volume; that is, a large area under the curve.

In this section of the report, we present the yield strength (tensile strength at yield), ultimate elongation (elongation at break), and modulus of elasticity for 12 different plastic materials and group these materials into 5 categories: (1) hard and tough; (2) soft and tough; (3) hard and brittle; (4) hard and strong; and (5) soft and weak. In addition, we report the effects of supercritical carbon dioxide on the above three mechanical properties of these plastic materials.

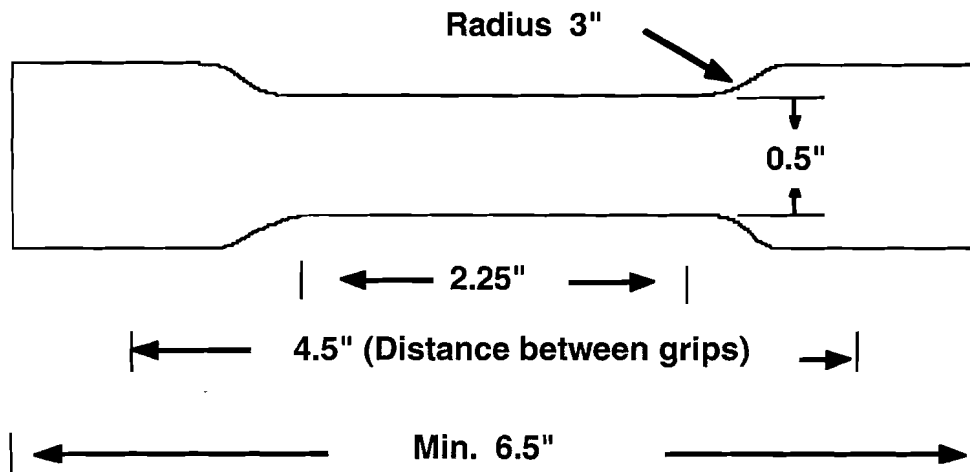


Figure 1. The dumbbell-shaped test specimen for the ASTM D638 tensile test method.

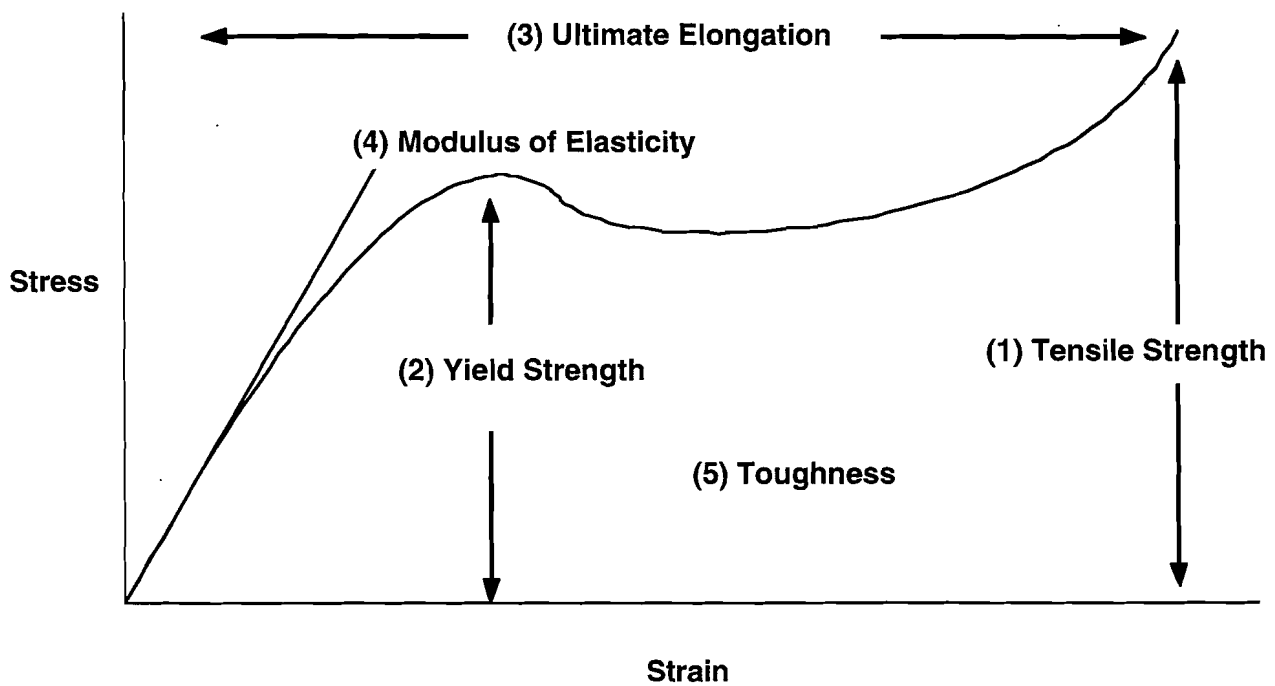


Figure 2. Typical stress-strain curve for plastics.

2.0 EXPERIMENTAL PROCEDURE

The dumbbell-shaped test specimens were prepared from plastic sheets by cutting them using a guide mold. The test specimens conformed to the dimensions of Type I in ASTM D638 (See Figure 1). An Instron Model 6025 universal testing machine was used for the stress-strain measurements. The testing machine had a fixed grip on the top and a movable grip on the bottom. The distance between the two grips was 4.5 inches. The rate of motion of the driven grip was controlled at 2 in. per min. The testing was performed at $23 \pm 2^\circ\text{C}$. Five specimens were used for each sample in the testing. Samples treated with supercritical carbon dioxide were evaluated 30 days after treatment. Yield strength, ultimate elongation, and modulus at elasticity were obtained from calculations performed by the computer connected to the testing machine; these calculations were based on the stress-strain curves.

3.0 RESULTS AND DISCUSSION

Table 1 shows the yield strength, ultimate elongation, and modulus for 12 different plastics materials before treatment in supercritical carbon dioxide. Yield strength can be noted to vary in a broad range from 1,547 psi for low-density polyethylene (LDPE) to 10,690 for polyoxymethylene (POM). LDPE is a material of high flexibility and low degree of crystallinity. When a stress is applied to an LDPE specimen, LDPE polymer chains readily disentangle or slip. As a result, LDPE shows high ultimate elongation and low modulus (See Table 1). On the other hand, POM has a very high degree of crystallinity, which can restrict disentanglement or slippage among polymer chains when a stress is applied on the specimen. Therefore, a high degree of crystallinity in polymers can lead to high yield strength and modulus but low elongation as seen in Table 1 for POM. PMMA and PVC are not crystalline materials, but they show high values in yield strength and modulus and a low value in elongation. Interestingly, the bulky and polar side group $-\text{COOCH}_3$ and the high dipole C-Cl bond somewhat simulate the effects of crystallinity to restrict disentanglement or slippage among polymer chains during stress-strain measurements.

In brief, crystallinity, chain flexibility, bulkiness of side group/main chain, and polarity (including dipole forces and hydrogen bonding) determine the mechanical property values and can be used to explain how the specific values can be compared for the materials shown in Table 1.

Plastic samples were subjected to carbon dioxide at three subcritical and four supercritical conditions in order to evaluate the effect of these treatments on the mechanical properties of the polymers. In this data summary, we compare the results from treatments at two extreme conditions: (1) a pressure of 3,000 psi at 70°C with a treatment time of 1 hour and a pressure-release time of 1 hour (which is summarized as 3,000 psi, 70°C , 1 hr, 1 hr) and (2) 3,000 psi, 70°C , 1 hr, 5 hr, where the decompression time is 5 hours rather than 1 hour as in the comparison experiment.

Data for two other conditions under which mechanical properties have been evaluated are provided in Table 3 but are not discussed in this data summary. Our discussion of these two treatment conditions are illustrative of the interpretations that can be made for the other materials and will be addressed in a subsequent report.

Table 2 shows the yield strength, ultimate elongation, and modulus for 11 materials after treatment in supercritical carbon dioxide at two conditions; the Table also gives the data obtained for the control samples. The effects of supercritical carbon dioxide on the mechanical properties of each material listed in Table 2 are discussed below.

- PC** Light dissolution was seen on the samples after SCF CO₂ treatment at both conditions. The increase in the modulus was due to the increase in the degree of crystallinity after treatment. The material became brittle with a concurrent decrease in ultimate elongation, which corroborates the proposed increase in the degree of crystallinity. This analysis is supported by Chiou and coworkers who have demonstrated that polymer crystallization could be induced by absorption of carbon dioxide gas [3]. On the other hand, the decrease in the yield strength resulted from the plasticization caused by the absorption of carbon dioxide in the amorphous regions after treatment. Longer decompression times appear to favor increased plasticization of the material.
- PP** The color of the material was noted to change from white translucent to light yellow translucent after treatment with carbon dioxide. The SCF carbon dioxide plasticized the material as suggested by the decreases in yield strength and modulus. It is not certain whether carbon dioxide had induced further crystallization in the samples since the ultimate elongation remained high and no increase in modulus after treatment at either condition was noted.
- CAB** This material, which is completely amorphous, showed extensive foam formation after treatment at both conditions presented in Table 2. This suggested the occurrence of high diffusivity, which led to high uptake of carbon dioxide in the material. Apparently, both the -OOCCH₃ and OOC(CH₂)₂CH₃ groups led to increased CO₂ absorption. The dimensions of the foam resulting from the 1-hour decompression were larger than those resulting from the 5-hour decompression.
- PMMA** Like CAB, PMMA had extensive foam formation after treatments at both conditions. The dimensions of the foam resulting from the 1-hour decompression were larger than those resulting from the 5-hour decompression. PMMA is an amorphous material and has a side-chain ester group. Weight change data (See "I. Absorption, Swelling, and Dissolution of Carbon Dioxide in Polymers at Elevated Pressure") for PMMA indicated a tremendous amount of CO₂ uptake, which led to extensive foam formation

during decompression. The large decrease in T_g (See "II. Thermal Properties") also suggested the occurrence of a large amount of CO_2 uptake. The COOCH_3 group must have played a special role in the high amount of carbon dioxide uptake.

- PVC** The as-received PVC was dark gray in color. PVC test specimens became lightly distorted after treatments at both conditions. Yield strength and modulus significantly decreased after treatments at both conditions, which indicated the occurrence of a high extent of plasticization.
- POM** POM had high values in yield strength and modulus and a low value in ultimate elongation because of the high degree of crystallinity in the material. SCF treatments caused a decrease in modulus, which suggested the occurrence of plasticization; but the extent of plasticization was not significant since the yield strength and ultimate elongation were almost identical to the control sample. As is apparent in many of the samples, a crystalline material shows a low uptake of carbon dioxide.
- ABS** Like CAB and PMMA, ABS showed extensive foam formation after treatments at both conditions. Significant dissolution of the carbon dioxide in this terpolymer allows for the generation of foam, which is exacerbated by the rubbery nature of the material due to the butadiene moieties.
- Nylon 66** The increases in yield strength and modulus and the decrease in ultimate elongation suggested that the degree of crystallinity of nylon 66 had been increased during the treatments at both conditions. No significant differences, in terms of the three mechanical properties, between the two treatment conditions were found.
- Teflon** Although Teflon has excellent chemical resistance properties, plasticization by CO_2 occurred readily at high pressures. Bubbles were found inside the material after treatment at condition C6, which led to the observed decrease in modulus. Longer (5-hour) decompression times demonstrated a higher residual modulus than shorter (1-hour) decompression times.
- LDPE** Slight decreases in ultimate elongation, modulus, and yield strength were found for condition C7—as compared with C6—because of significant plasticization under condition C7. Apparently, large bubbles (inclusions) were partially responsible for the observed changes in the mechanical properties.
- HDPE** Decreases in modulus at both condition C6 and C7 suggested the occurrence of plasticization although not to a significant extent. Compared with condition C6, condition C7 provided relatively significant plasticization.

Table 1. Yield strength, ultimate elongation, and modulus of elasticity of 12 plastics before treatment in supercritical carbon dioxide.

Plastic	Thickness (mm)	Yield Strength (psi)	Ultimate Elongation (%)	Modulus of Elasticity (psi)	Remarks
PC	3.00	9,825	69	281,800	hard, tough
PP	2.25	5,243	>300	198,700	soft, tough
CAB	2.40	5,534	59	209,200	soft, tough
PMMA	3.00	9,260	3	384,100	hard, brittle
PVC	2.24	8,839	9	435,900	hard, brittle
POM	1.50	10,690	11	376,300	hard, brittle
ABS	2.40	6,070	8	278,500	hard, brittle
Nylon 66	3.20	9,927	48	290,500	hard, strong
Teflon	1.70	1,982	101	142,950	soft, weak
LDPE	2.20	1,547	238	61,000	soft, weak
HDPE	2.25	3,822	92	161,900	soft, weak
HIPS	3.00	4,782	20	255,400	soft, weak

Table 2. Yield strength, ultimate elongation, and modulus of elasticity for various plastics after treatment in supercritical carbon dioxide.*

Plastic	Condition	Yield Strength (psi)	Ultimate Elongation (%)	Modulus of Elasticity (psi)	Remarks
PC	C	9,825	69	281,800	transparent
PC	C6	9,263	8	298,300	light dissolution on surface
PC	C7	9,225	35	287,600	light dissolution on surface
PP	C	5,243	>300	198,700	white translucent
PP	C6	5,072	>300	181,100	light yellow translucent
PP	C7	5,003	178	170,300	light yellow translucent
CAB	C	5,534	59	209,200	transparent
CAB	C6				extensive foam formation
CAB	C7				extensive foam formation
PMMA	C	9,260	3	384,100	transparent
PMMA	C6				extensive foam formation
PMMA	C7				extensive foam formation
PVC	C	8,839	9	435,900	dark gray
PVC	C6	7,189	12	320,600	bent
PVC	C7	7,141	13	367,100	bent
POM	C	10,690	11	376,300	white
POM	C6	10,685	9	355,900	white
POM	C7	10,570	10	346,800	white
ABS	C	6,070	8	278,500	black
ABS	C6				extensive foam formation
ABS	C7				extensive foam formation
Nylon 66	C	9,927	48	290,500	yellow opaque
Nylon 66	C6	10,738	25	299,200	yellow opaque
Nylon 66	C7	10,838	22	316,900	yellow opaque
Teflon	C	1,982	101	142,950	milky
Teflon	C6	1,916	105	98,980	a couple of bubbles
Teflon	C7	1,869	108	111,970	milky
LDPE	C	1,547	238	61,000	white transparent
LDPE	C6	1,537	75	49,500	some big bubbles
LDPE	C7	1,480	223	57,600	white translucent
HDPE	C	3,822	92	161,900	white translucent
HDPE	C6	3,887	97	155,700	white translucent
HDPE	C7	3,811	161	150,400	white translucent

*C: control; C6: 3,000 psi, 70°C, 1 hr, 1 hr; and C7: 3,000 psi, 70°C, 1 hr, 5 hr.

Table 3. Yield strength, ultimate elongation, and modulus of elasticity for various plastics after treatment in supercritical carbon dioxide.*

Plastic	Condition	Yield Strength (psi)	Ultimate Elongation (%)	Modulus of Elasticity (psi)	Remarks
PC	C	9,825	69	281,800	transparent
PC	C1	9,672	57	281,600	transparent
PC	C3	9,409	9	312,300	transparent
PP	C	5,243	>300	198,700	white translucent
PP	C1	5,297	>300	204,200	white translucent
PP	C3	5,144	>300	188,200	white translucent
CAB	C	5,534	59	209,200	transparent
CAB	C1	5,959	44	218,300	light dissolution on surface
CAB	C3				foam formation
PMMA	C	9,260	3	384,100	transparent
PMMA	C1	8,011	3	351,800	light dissolution on surface
PMMA	C3	9,745	5	314,500	dissolution and bubbles were seen
PVC	C	8,839	9	435,900	dark gray
PVC	C1	8,809	12	407,600	dark gray
PVC	C3	8,595	10	405,000	light dissolution on edges
POM	C	10,690	11	376,300	white
POM	C1	10,680	10	361,000	white
POM	C3	10,665	11	361,500	white
ABS	C	6,070	8	278,500	black
ABS	C1	5,953	4	243,200	light dissolution on edges
ABS	C3	6,259	6	266,400	bent
Nylon 66	C	9,927	48	290,500	yellow opaque
Nylon 66	C1	10,475	30	299,200	yellow opaque
Nylon 66	C3	10,625	24	298,100	yellow opaque
Teflon	C	1,982	101	143,000	milky
Teflon	C1	1,953	102	126,800	milky
Teflon	C3	1,902	100	101,500	milky
LDPE	C	1,547	238	61,000	white transparent
LDPE	C1	1,623	270	55,600	white transparent
LDPE	C3	1,580	224	54,800	white transparent
HDPE	C	3,822	92	161,900	white translucent
HDPE	C1	3,906	87	160,700	white translucent
HDPE	C3	3,853	92	154,400	white translucent

*C: control; C1: 1,000 psi, 25°C, 1 hr, 1 hr; and C3: 2,000 psi, 40°C, 1 hr, 1 hr.

4.0 CONCLUSION

Supercritical or high-pressure carbon dioxide can induce polymer crystallization and can plasticize polymers. Through the examination, analysis, and comparison of the yield strength, ultimate elongation and modulus both before and after treatments in supercritical carbon dioxide at 3,000 psi and 70°C, we found that two main factors, i.e., degree of crystallinity and polar side groups (e.g., esters), determine the degree of plasticization and the extent of foam formation. Materials belonging to this category include PC, CAB, PMMA, POM, and ABS.

On the other hand, other minor factors such as the flexibility, regularity, and bulkiness of side group/main chain of polymers determine the tendency of crystallization and, to a lesser extent, plasticization during treatment in high-pressure carbon dioxide. Polymers in this category include PC, PP, Nylon 66, Teflon, LDPE and HDPE.

Weight change data is not much related to plasticization since polymers such as Teflon, HDPE, LDPE, and PP show almost no change in their weight after treatment; however, these polymers do show the occurrence of plasticization based on decreases in their modulus of elasticity and yield strength. At present, there is no evidence that high-pressure carbon dioxide can destroy the crystallites within these polymers.

BIBLIOGRAPHY

- G. J. V. Amerongen, "Influence of Structure of Elastomers on Their Permeability to Gases," *J. Polym. Sci.* **V** (3), 307–332 (1950).
- E. J. Beckman et al., "Description of the Phase Behavior of Polymer-Supercritical Gas Mixtures using a Mean Field Lattice-Gas Model," *ACS Polym. Prep.* **31** (1), 683 (1990).
- A. R. Berens, "Gravimetric and Volumetric Study of the Sorption of Gases and Vapors in Poly(Vinyl Chloride) Powders," *Polym. Eng. & Sci.* **20** (1), 95–101 (1980).
- A. R. Berens et al., "Application of Compressed CO₂ in the Incorporation of Additives into Polymers," *J. Appl. Polym. Sci.* **46**, 231–242 (1992).
- A. R. Berens and G. S. Huvar, "Interaction of Polymers with Near-Critical Carbon Dioxide," *ACS Symp. Ser.* **406**, 207 (1989).
- A. R. Berens, "Sorption of Organic Liquids and Vapors by Rigid PVC," *J. Appl. Polym. Sci.* **37**, 901–913 (1989).
- A. R. Berens, "Solubility and Diffusion of Small Molecules in PVC," *J. Vinyl Tech* **11** (4), 171–175 (1989).
- E. Bok et al., "Supercritical Fluids for Single Wafer Cleaning," *Solid State Tech.* (June), 117 (1992).
- L. Boock et al., "Reactions in Supercritical Fluids," *Chemtech* (December), 719–723 (1992).
- J. S. Chiou et al., "Polymer Crystallization Induced by Sorption of CO₂ Gas," *J. Appl. Polym. Sci.* **30**, 3911–3924 (1985).
- J. S. Chiou et al., "Plasticization of Glassy Polymers by CO₂," *J. Appl. Polym. Sci.* **30**, 2633 (1985).
- E. J. Colman et al., "Solid-Fluid and Liquid-Gas Equilibria of Linear Polyethylene with Supercritical Propane," *ACS Polym. Prep.* **31** (1), 675 (1990).
- D. K. Dandge et al., "Structure Solubility Correlations: Organic Compounds and Dense CO₂ Binary Systems," *Ind. Eng. Chem. Prod. Res. Dev.* **24**, 162–166 (1985).
- J. M. Desimone et al., "Synthesis of Fluoropolymers in Supercritical Carbon Dioxide," *Science* **257**, 945–947 (1992).
- P. Doty and H. S. Zable, "Determination of Polymer-Liquid Interaction by Swelling Measurements," *J. Polym. Sci.* **1** (2), 90–101 (1946).

- C. A. Eckert et al., "Supercritical Fluid Processing," *Environ. Sci. Tech.* **20** (4), 319–325 (1986).
- C. S. Elsbernd et al., "The Application of Supercritical Fluids in the Fractionation and Characterization of Siloxane Oligomers and Graft Copolymers," *ACS Polym. Prep.* **31** (1), 673 (1990).
- G. K. Fleming and W. J. Koros, "Dilation of Polymers by Sorption of Carbon Dioxide Elevated Pressures. 1. Silicone Rubber and Unconditioned Polycarbonate," *Macromolecules* **19**, 2285–2291 (1986).
- P. M. Gallagher et al., "Supercritical Fluid Processing of Polymers," *ACS Polym. Prep.* **31** (1), 668 (1990).
- Z. Guan et al., "Homogeneous Free Radical Polymerizations in Supercritical Carbon Dioxide: 2. Thermal Decomposition of AIBN," *Macromolecules* **26**, 2663 (1993).
- C. W. Haschets and A. D. Shine, "Phase Behavior of Polymer-Supercritical Chlorodifluoromethane Solutions," *Macromolecules* **26**, 5052–60 (1993).
- T. Hirose et al., "Dilation of Polyethylene by Sorption of CO₂," *J. Polym. Sci.:Phy.Ed.* **24**, 2107 (1986).
- K. L. Hoy and M. D. Donobue, "Supercritical Fluid Spray Technology An Emission Control Technology for the Future," *ACS Polym. Prep.* **31** (1), 679 (1990).
- K. Johnston, "Supercritical Fluids," *Encyclo. Chem. Tech.*, 3rd Ed., Suppl. Vol., 872–893 (1984).
- S. Kamat et al., "Biocatalytic Synthesis of Acrylates in Organic Solvents and Supercritical Fluids," *Biotech. Bioeng.* **40**, 158–166 (1992).
- Y. Kamiya et al., "Gravimetric Study of High-Pressure Sorption of Gases in Polymers," *J. Polym. Sci.:Phy.Ed.* **24**, 1525 (1986).
- Y. Kamiya et al., "Gas Sorption in Poly(vinyl benzoate)," *J. Polym. Sci.:Phy.Ed.* **24**, 535 (1986).
- W. J. Koros et al., "Energetics of Gas Sorption in Glassy Polymers," *Polymer* **20**, 956–960 (1979).
- W. J. Koros et al., "High-Pressure Sorption of CO₂ in Solvent-Cast PMMA and PET Films," *J. Appl. Polym. Sci.* **26**, 159–170 (1981).
- S. K. Kumar and U. W. Suter, "Precipitation Polymerization of Styrene in Supercritical Ethane," *ACS Polym. Prep.* **28** (2), 286 (1987).

- S. K. Kumar et al., "Solubility of Polystyrene in Supercritical Fluids," *Macromolecules* **20**, 2550 (1987).
- A. K. Lale and A. D. Shine, "Dissolution and Precipitation of Polymers Using A Supercritical Solvent," *ACS Polym. Prep.* **31** (1), 677 (1990).
- A. K. Lele and A. D. Shine, "Morphology of Polymers Precipitated from a Supercritical Solvent," *AIChE J.* **38** (5), 742–752 (1992).
- M. A. McHugh et al., "Supercritical Fluids," *Encyclo. Polym. Sci. and Eng.* **16**, 2nd Ed., 368–399 (1989).
- M. A. Meilchen et al., "Supercritical Fluid Fractionation Extraction Studies of Polypropylene," *ACS Polym. Prep.* **31** (1), 671 (1990).
- R. W. Pekala and W. Schaefer, "Structure of Organic Aerogels. 1. Morphology and Scaling," *Macromolecules* **26**, 5487–93 (1993).
- V. P. Saraf and E. Kiran, "Free Radical Polymerization of Styrene in Supercritical Fluids," *ACS Polym. Prep.* **31** (1), 687 (1990).
- K. M. Scholsky, "Supercritical Polymerization Reactions," *ACS Polym. Prep.* **31** (1), 685 (1990).
- K. M. Scholsky, "Process Polymers with Supercritical Fluids," *Chemtech* (December), 750–757 (1987).
- R. W. Shaw et al., "Supercritical Water," *C&EN* **23** (December), 26–39 (1991).
- J. J. Shim and K. P. Johnston, "Molecular Thermodynamics of Sorption of Solutes into Polymers under Supercritical Fluid Conditions," *ACS Polym. Prep.* **31** (1), 681 (1990).
- G. Srinivasan and J. R. Elliott, "Microcellular Materials via Polymerization in Supercritical Fluids," *Ind. Eng. Chem. Res.* **31**, 1414 (1992).
- S. A. Stern and A. H. Meringo, "Solubility of Carbon Dioxide in Cellulose Acetate at Elevated Pressures," *J. Polym. Sci.: Phy. Ed* **16**, 735 (1978).
- B. Subramanlam et al., "Reactions in Supercritical Fluids—A Review," *Ind. Eng. Chem, Pro. Des. Dev.* **25** (1), 1–12 (1986).
- J. Tehrani, "Successful Supercritical Fluid Extraction Strategies," *Amer. Lab.* **40HH-MM** (February), (1993).

J. W. Tom and P. G. Debenedetti, "Formation of Bioerodible Polymeric Microspheres and Microparticles by Rapid Expansion of Supercritical Solutions," *Biotechnol. Prog.* **7**, 403–411 (1991).

W. Wang et al., "Effects of High-Pressure CO₂ on the Glass Transition Temperature and Mechanical Properties of Polystyrene," *J. Polym. Sci.:Phy. Ed.* **20**, 1371 (1982).

R. G. Wissinger and M. E. Paulaitis, "Swelling and Sorption in Polymer-CO₂ Mixtures at Elevated Pressures," *J. Polym. Sci.:Phy.Ed.* **25**, 2497 (1987).

J. M. Wong and K. P. Johnston, "Solubilization of Biomolecules in Carbon Dioxide Based Supercritical Fluids," *Biotech. Prog.* **2** (1), 29–39 (1986).

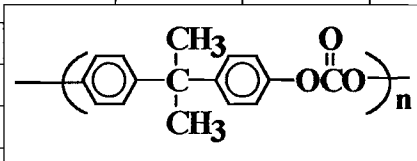
APPENDIX

DATA REFERENCE

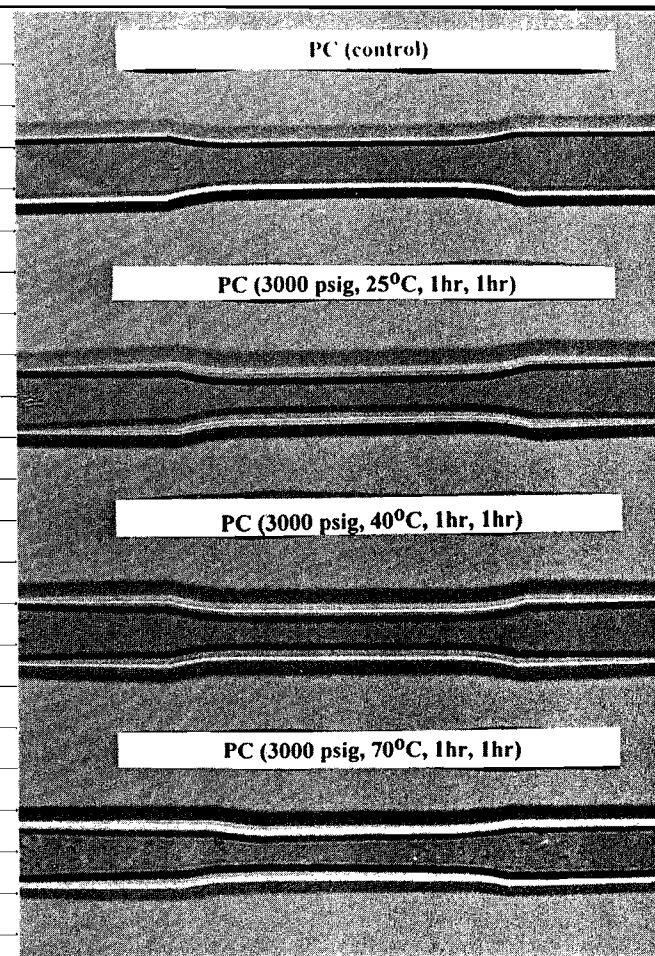
LIST OF APPENDIX DATA

Polycarbonate	65
Poly(methyl methacrylate)	69
Poly(vinyl chloride)	73
Tetraflouroethylene	77
Low Density Polyethylene	81
High Density Polyethylene	85
Polypropylene	89
Polyamide	93
Polyoxymethylene	97
High Impact Polystyrene (B:10%; S:90%)	101
High Impact Polystyrene	105
Poly(ethylene terephthalate) glycol modified	108
Cellulose Acetate Butyrate	112
Acrylonitrile Butadiene Styrene (A:20%; B:8%; S:72%)	116
High Molecular Weight Polyethylene	120
Poly(2,6-dimethylphenylene oxide)	123
Polyetherimide	126
Polyvinylidene fluoride	129
Polysulfone	132
Polyurethane	135
Poly(ethylene terphthalate)	138

Polycarbonate



Polymer I.D.	PC			
Trade name	Lexan			
Manufacturer	GE			
Control				
Appearance	transparent sheet with 3 mm in thickness for dumbbell samples			
Glass transition temperature, C				
Tensile strength, psi	9,825			
Elongation, %	69.2			
Tensile elastic modulus, psi	281,820			
Dispersion component, mJ/m²	23.07			
Polar component, mJ/m²	27.39			
Surface free energy, mJ/m²	50.46			
1000psi-25 C-1hr-1hr				
Appearance (dumbbell)	no change			
Weight change (coupon)				
Weight change (dumbbell)	0.44+%(0d)	0.09+%(4d)	0.02+%(10d)	
Glass transition temperature, C				
Tensile strength, psi	9,673			
Elongation, %	57.2			
Tensile elastic modulus, psi	281,600			
Dispersion component, mJ/m²	24.59			

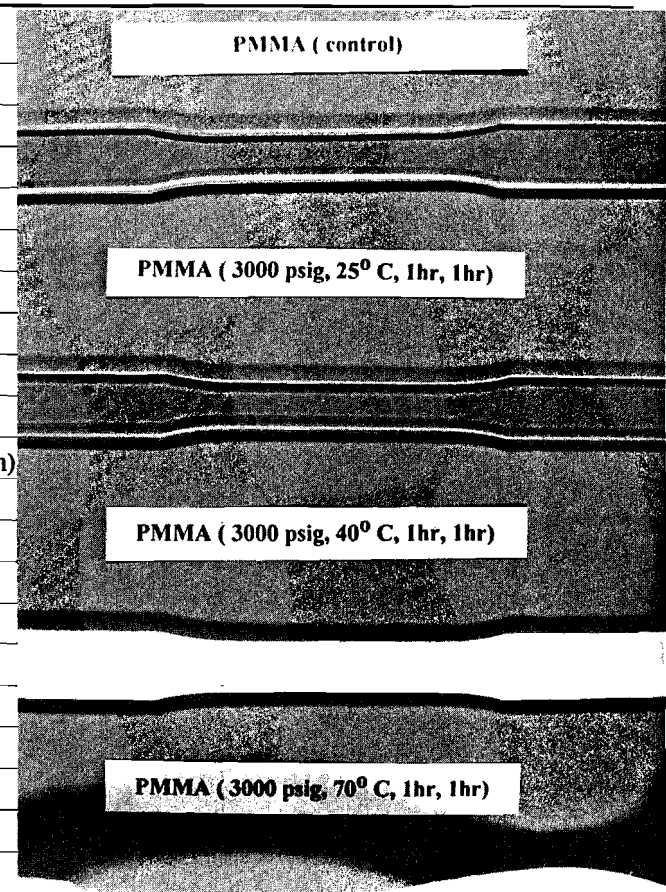


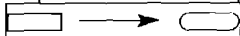
Polar component, mJ/m²	7.89						
Surface free energy, mJ/m²	32.49						
1000psi-40 C-1hr-1hr							
Appearance (dumbbell)	no change						
Glass transition temperature, C							
Weight change (coupon)							
Weight change (dumbbell)	0.87+%(0d)	0.37+%(1d)	0.12+%(6d)	0.08+%(12d)	0.05+%(22d)	0.04+%(60d)	
Tensile strength, psi							
Elongation, %							
Tensile elastic modulus, psi							
Dispersion component, mJ/m²							
Polar component, mJ/m²							
Surface free energy, mJ/m²							
2000psi-40 C-1hr-1hr							
Appearance (dumbbell)	no change						
Glass transition temperature, C							
Weight change (coupon)							
Weight change (dumbbell)	0.93+%(0d)	0.2+%(6d)	0.09+%(12d)				
Tensile strength, psi	9,409						
Elongation, %	9						
Tensile elastic modulus, psi	312,300						
Dispersion component, mJ/m²	23.98						
Polar component, mJ/m²	8.84						
Surface free energy, mJ/m²	32.81						
2300psi-70 C-15min-5min							
Appearance (dumbbell)	very fine bubbles on the sample surface						

Glass transition temperature, C							
Weight change (coupon)							
Weight change (dumbbell)	0.98+%(0d)	0.3+%(5d)					
Tensile strength, psi	9,360						
Elongation, %	17.5						
Tensile elastic modulus, psi	288,500						
Dispersion component, mJ/m2	30.22						
Polar component, mJ/m2	5.41						
Surface free energy, mJ/m2	35.63						
3000psi-25 C-1hr-1hr							
Appearance (dumbbell)	no change						
Glass transition temperature, C							
Weight change (coupon)							
Weight change (dumbbell)	1.16+%(0d)	0.53+%(1d)	0.21+%(6d)	0.10+%(12d)	0.08+%(22d)	0.02+%(60d)	
Tensile strength, psi							
Elongation, %							
Tensile elastic modulus, psi							
Dispersion component, mJ/m2							
Polar component, mJ/m2							
Surface free energy, mJ/m2							
3000psi-40 C-1hr-1hr							
Appearance (dumbbell)	no change						
Glass transition temperature, C							
Weight change (coupon)							
Weight change (dumbbell)	1.88+%(0d)	0.97+%(1d)	0.30+%(6d)	0.12+%(12d)	0.03+%(22d)	0.009+%(60d)	
Tensile strength, psi							
Elongation, %							

Tensile elastic modulus, psi					<p>PC (control)</p> <p>PC (1000 psig, 40°C, 1hr, 1hr)</p> <p>PC (2000 psig, 40°C, 1hr, 1hr)</p> <p>PC (3000 psig, 40°C, 1hr, 1hr)</p>
Dispersion component, mJ/m²					
Polar component, mJ/m²					
Surface free energy, mJ/m²					
3000psi-70 C-1hr-1hr					
Appearance (dumbbell)	still transparent; dissolution seen on the sample surface				
Glass transition temperature, C					
Weight change (coupon)					
Weight change (dumbbell)	1.23+%(4d)	0.51+%(11d)	0.33+%(17d)		
Tensile strength, psi	9,263				
Elongation, %	8.2				
Tensile elastic modulus, psi	298,300				
Dispersion component, mJ/m²	22.82				
Polar component, mJ/m²	45.63				
Surface free energy, mJ/m²	68.45				
3000psi-70 C-1hr-5hr					
Appearance (dumbbell)	still transparent; dissolution seen on the sample surface				
Glass transition temperature, C					
Weight change (coupon)					
Weight change (dumbbell)	3.53+%(0d)	1.5+%(4d)			
Tensile strength, psi	9,225				
Elongation, %	34.5				
Tensile elastic modulus, psi	287,575				
Dispersion component, mJ/m²	23.26				
Polar component, mJ/m²	39.69				
Surface free energy, mJ/m²	62.95				

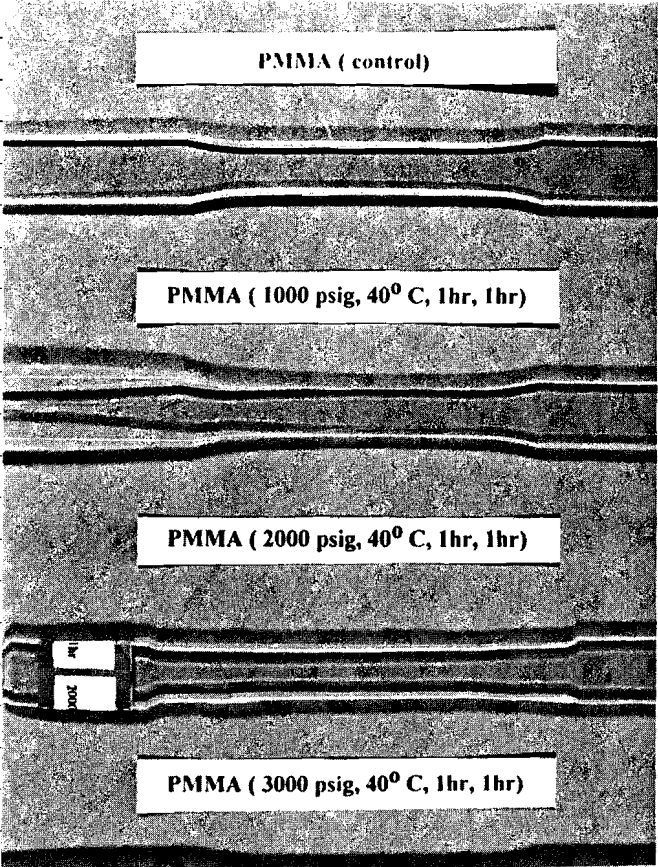
Poly(methyl methacrylate)									
$\left(\text{CH}_2 - \underset{\text{COOCH}_3}{\overset{\text{CH}_3}{\text{C}}} \right)_n$									
Polymer I.D.	PMMA								
Trade name	Plexiglas								
Manufacturer	Rohm&Haas								
Control									
Appearance	transparent sheet with thickness 3mm (dumbbell) and 1.5 mm (coupon)								
Glass transition temperature, C	102 C								
TGA Heating	1.03-%								
Tensile strength, psi	9,260								
Elongation, %	2.9								
Tensile elastic modulus, psi	384,100								
Dispersion component, mJ/m2	32.08								
Polar component, mJ/m2	5.6								
Surface free energy, mJ/m2	37.68								
1000psi-25 C-1hr-1hr									
Appearance (dumbbell)	a very light dissolution seen on the surface								
Glass transition temperature, C									
Weight change (coupon)	5.52+%(0d)	2.29+%(4d)	1.40+%(10d)	0.78-%(8m)					
Weight change (dumbbell)	3.7+%(0d)	1.43+%(4d)	0.85+%(10d)						
Tensile strength, psi	8,011								
Elongation, %	2.6								
Tensile elastic modulus, psi	351,800								
Dispersion component, mJ/m2	30.00								



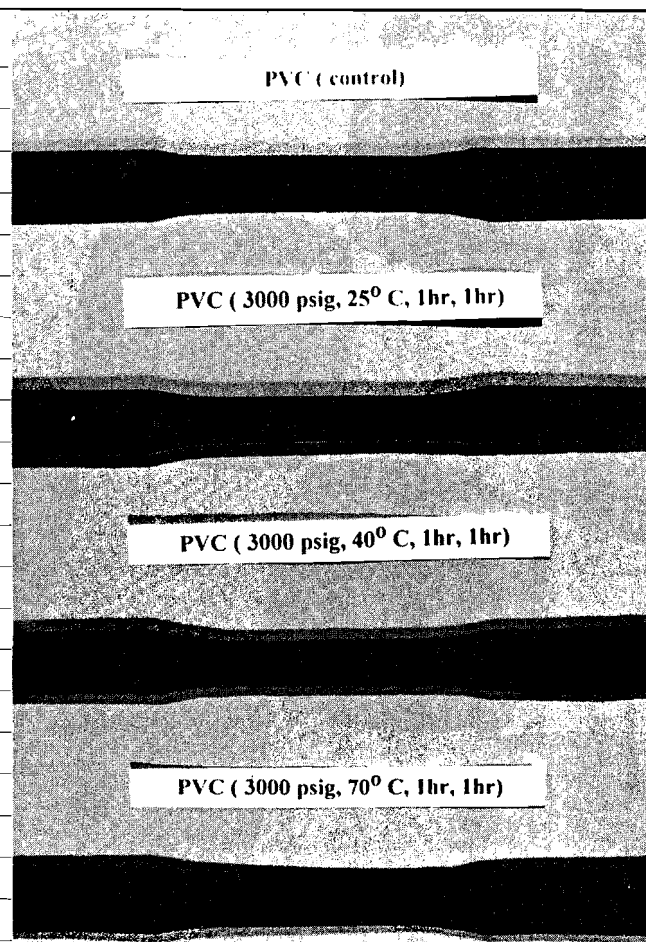
Polar component, mJ/m²	6.06					
Surface free energy, mJ/m²	36.06					
1000psi-40 C-1hr-1hr						
Appearance (dumbbell)	very light dissolution on the surface					
Glass transition temperature, C						
Weight change (coupon)	5.85+%(0d)	3.35+%(1d)	1.46+%(6d)	1.00+%(12d)	0.79+%(22d)	
Weight change (dumbbell)	4.05+%(0d)	2.45+%(1d)	1.24+%(6d)	0.97+%(12d)	0.79+%(22d)	
Tensile strength, psi						
Elongation, %						
Tensile elastic modulus, psi						
Dispersion component, mJ/m²						
Polar component, mJ/m²						
Surface free energy, mJ/m²						
2000psi-40 C-1hr-1hr						
Appearance (dumbbell)	dissolution on the surface; bubbles on the edges					
Glass transition temperature, C						
Weight change (coupon)	8.45+%(0d)	3.03+%(6d)	2.06+%(12d)	0.87+%(8m)		
Weight change (dumbbell)	7.86+%(0d)	3.57+%(6d)	2.66+%(12d)			
Tensile strength, psi	9,745					
Elongation, %	4.6					
Tensile elastic modulus, psi	324,500					
Dispersion component, mJ/m²	27.94					
Polar component, mJ/m²	5.32					
Surface free energy, mJ/m²	33.26					
2300psi-70 C-15min-5min						
Appearance (dumbbell)	dissolution seen on the surface 					

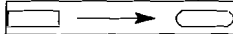
Glass transition temperature, C						
Weight change (coupon)	8.23+%(0d)	3.12+%(5d)				
Weight change (dumbbell)	5.89+%(0d)	2.57+%(5d)				
Tensile strength, psi	8,540					
Elongation, %	3.3					
Tensile elastic modulus, psi	337,075					
Dispersion component, mJ/m2	33.02					
Polar component, mJ/m2	3.54					
Surface free energy, mJ/m2	36.56					
3000psi-25 C-1hr-1hr						
Appearance (dumbbell)	light dissolution seen on the surface					
Glass transition temperature, C	80 C(0d)	87 C(1d)	100 C(7d)	101 C(16d)		
TGA Heating	8.99-% (0d)	5.46-%(1d)	3.69-%(7d)	2.57-%(16d)		
Weight change (coupon)	11.3+%(0d)	6.10+%(1d)	2.96+%(6d)	1.75+%(12d)	0.65+%(22d)	
Weight change (dumbbell)	9.51+%(0d)	5.87+%(1d)	3.78+%(6d)	2.72+%(12d)	2.10+%(22d)	
Tensile strength, psi						
Elongation, %						
Tensile elastic modulus, psi						
Dispersion component, mJ/m2						
Polar component, mJ/m2						
Surface free energy, mJ/m2						
3000psi-40 C-1hr-1hr						
Appearance (dumbbell)	white opaque foam; lots of tiny bubbles;					
Glass transition temperature, C						
Weight change (coupon)	12.9+%(0d)	6.33+%(1d)	2.91+%(6d)	1.64+%(12d)	0.83+%(22d)	0.49+%(60d)
Weight change (dumbbell)	11.3+%(0d)	7.64+%(1d)	4.17+%(6d)	2.72+%(12d)	1.93+%(22d)	1.15+%(60d)
Tensile strength, psi						

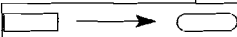
Elongation, %									
Tensile elastic modulus, psi									
Dispersion component, mJ/m ²									
Polar component, mJ/m ²									
Surface free energy, mJ/m ²									
3000psi-70 C-1hr-1hr									
Appearance (dumbbell)		same as described above but with bigger dimension of the foam							
Glass transition temperature, C									
Weight change (coupon)		7.7+%(1d)	3.61+%(4d)	1.95+%(8d)	0.88+%(17d)				
Weight change (dumbbell)									
Tensile strength, psi									
Elongation, %									
Tensile elastic modulus, psi									
Dispersion component, mJ/m ²		32.66							
Polar component, mJ/m ²		4.28							
Surface free energy, mJ/m ²		36.94							
3000psi-70 C-1hr-5hr									
Appearance (dumbbell)		white opaque foam; some parts of the foam are separate							
Glass transition temperature, C									
Weight change (coupon)		9.31+%(0d)	3.6+%(4d)	1.19+%(8m)					
Weight change (dumbbell)		4.4+%(0d)	0.74+%(4d)						
Tensile strength, psi									
Elongation, %									
Tensile elastic modulus, psi									
Dispersion component, mJ/m ²		29.55							
Polar component, mJ/m ²		5.68							
Surface free energy, mJ/m ²		35.23							



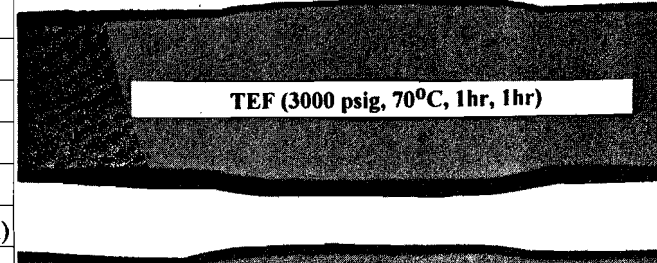
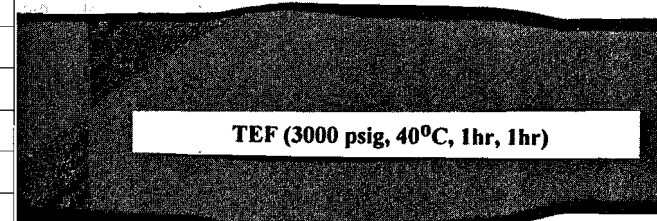
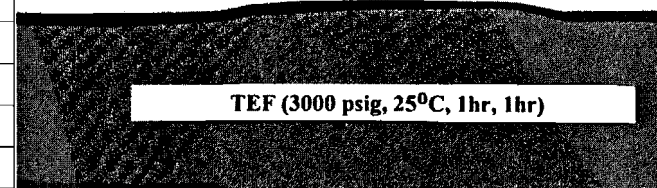
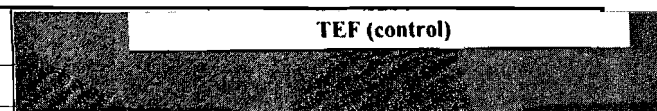
Poly(vinyl chloride)				
$\left(\text{CH}_2 - \underset{\text{Cl}}{\text{CH}} \right)_n$				
Polymer I.D.	PVC			
Trade name				
Manufacturer	Huls America			
Control				
Appearance	dark grey sheet with 2.24 mm (dumbbell) in thickness			
Glass transition temperature, C				
Tensile strength, psi	8,839			
Elongation, %	9			
Tensile elastic modulus, psi	435,900			
Dispersion component, mJ/m2	23.16			
Polar component, mJ/m2	5.11			
Surface free energy, mJ/m2	28.27			
1000psi-25 C-1hr-1hr				
Appearance (dumbbell)	no change			
Glass transition temperature, C				
Weight change (coupon)				
Weight change (dumbbell)	0.17+%(0d)	0.03-%(4d)	~0 %(10d)	
Tensile strength, psi	8,809			
Elongation, %	12			
Tensile elastic modulus, psi	407,550			
Dispersion component, mJ/m2	18.46			
Polar component, mJ/m2	5.61			



Surface free energy, mJ/m ²	28.28						
1000psi-40 C-1hr-1hr							
Appearance (dumbbell)	no change						
Glass transition temperature, C							
Weight change (coupon)							
Weight change (dumbbell)	0.52+%(0d)	0.18+%(1d)	0.02+%(6d)	0.008+%(12d)	0.03+%(22d)		
Tensile strength, psi							
Elongation, %							
Tensile elastic modulus, psi							PVC (control)
Dispersion component, mJ/m ²							
Polar component, mJ/m ²							
Surface free energy, mJ/m ²							
2000psi-40 C-1hr-1hr							
Appearance (dumbbell)							
Glass transition temperature, C							
Weight change (coupon)							
Weight change (dumbbell)	0.83+%(0d)	0.23+%(6d)	0.13+%(12d)				
Tensile strength, psi	8,595						
Elongation, %	9.5						
Tensile elastic modulus, psi	404,950						
Dispersion component, mJ/m ²	24.48						
Polar component, mJ/m ²	4.02						
Surface free energy, mJ/m ²	28.50						
2300psi-70 C-15min-5min							
Appearance (dumbbell)	no change						
Glass transition temperature, C							

Weight change (coupon)						
Weight change (dumbbell)	1.11+%(0d)	0.40+%(5d)				
Tensile strength, psi	8,382					
Elongation, %	11.5					
Tensile elastic modulus, psi	418,480					
Dispersion component, mJ/m2	22.47					
Polar component, mJ/m2	8.72					
Surface free energy, mJ/m2	31.19					
3000psi-25 C-1hr-1hr						
Appearance (dumbbell)	no change					
Glass transition temperature, C						
Weight change (coupon)						
Weight change (dumbbell)	0.84+%(0d)	0.27+%(1d)	0.07+%(6d)	0.05+%(12d)	0.05+%(22d)	
Tensile strength, psi						
Elongation, %						
Tensile elastic modulus, psi						
Dispersion component, mJ/m2						
Polar component, mJ/m2						
Surface free energy, mJ/m2						
3000psi-40 C-1hr-1hr						
Appearance (dumbbell)						
Glass transition temperature, C						
Weight change (coupon)						
Weight change (dumbbell)	1.55+%(0d)	0.81+%(1d)	0.29+%(6d)	0.15+%(12d)	0.10+%(22d)	0.07+%(60d)
Tensile strength, psi						
Elongation, %						
Tensile elastic modulus, psi						

Tetrafluoroethylene					
$\left(\text{CF}_2 - \text{CF}_2 \right)_n$					
Polymer I.D.	Teflon				
Trade name	Teflon				
Manufacturer	Du Pont				
Control					
Appearance	milky sheet with thickness 1.7 mm (dumbbell) and 0.8 mm (coupon)				
Glass transition temperature, C					
Tensile strength, psi	1,982				
Elongation, %	101				
Tensile elastic modulus, psi	142,950				
Dispersion component, mJ/m ²	13.47				
Polar component, mJ/m ²	6.35				
Surface free energy, mJ/m ²	19.82				
1000psi-25 C-1hr-1hr					
Appearance (dumbbell)	no change				
Glass transition temperature, C					
Weight change (coupon)	0.04+%(0d)	~0 %(4d)	0.03-%(10d)	0%(8m)	
Weight change (dumbbell)	0.27+%(0d)	0.05-%(4d)	0.06-%(10d)		
Tensile strength, psi	1,953				
Elongation, %	102				
Tensile elastic modulus, psi	126,775				
Dispersion component, mJ/m ²	12.64				
Polar component, mJ/m ²	6.69				
Surface free energy, mJ/m ²	19.33				



1000psi-40 C-1hr-1hr									
Appearance (dumbbell)		no change							
Glass transition temperature, C									
Weight change (coupon)		0.11+%(0d)	0.004+%(1d)	0.008+%(6d)	0.004-%(12d)	0.004-%(22d)			
Weight change (dumbbell)		0.58+%(0d)	0.04+%(1d)	0.03+%(6d)	0.01+%(12d)	0.02+%(22d)			
Tensile strength, psi									
Elongation, %									
Tensile elastic modulus, psi									
Dispersion component, mJ/m²									
Polar component, mJ/m²									
Surface free energy, mJ/m²									
2000psi-40 C-1hr-1hr									
Appearance (dumbbell)		no change							
Glass transition temperature, C									
Weight change (coupon)		0.05+%(0d)	0.01+%(6d)	0.01+%(12d)	0.03-%(8m)				
Weight change (dumbbell)		0.03+%(0d)	0.1-%(6d)	0.11-%(12d)					
Tensile strength, psi		1,902							
Elongation, %		100							
Tensile elastic modulus, psi		101,480							
Dispersion component, mJ/m²		12.96							
Polar component, mJ/m²		6.94							
Surface free energy, mJ/m²		19.46							
2300psi-70 C-15min-5min									
Appearance (dumbbell)		no change							
Glass transition temperature, C									
Weight change (coupon)		0.01+%(0d)	~0%(5d)	0.05-%(8m)					

TEF (control)

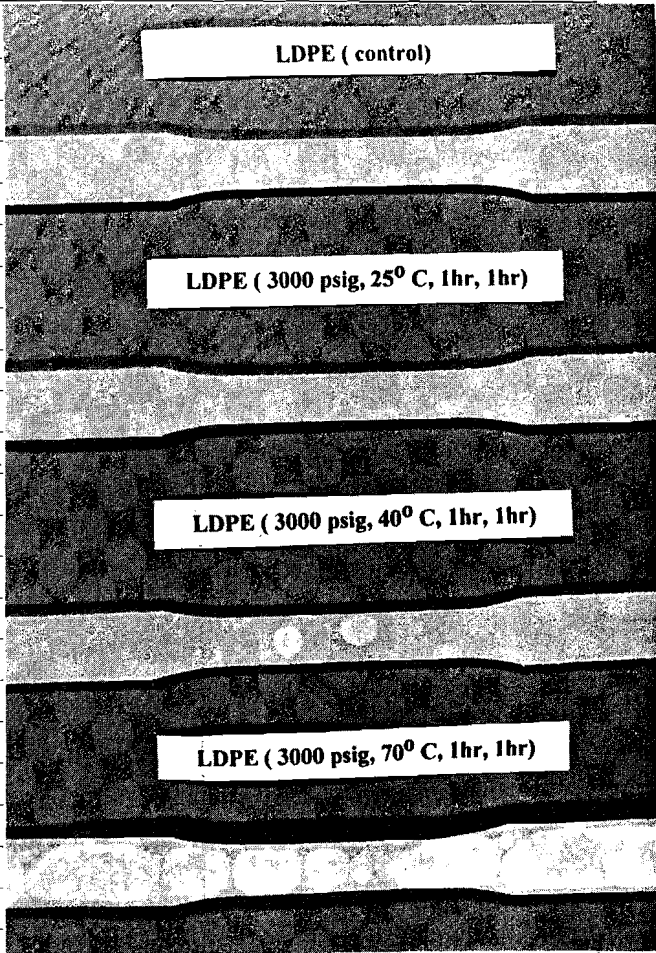
TEF (1000 psig, 40°C, 1hr, 1hr)

TEF (2000 psig, 40°C, 1hr, 1hr)

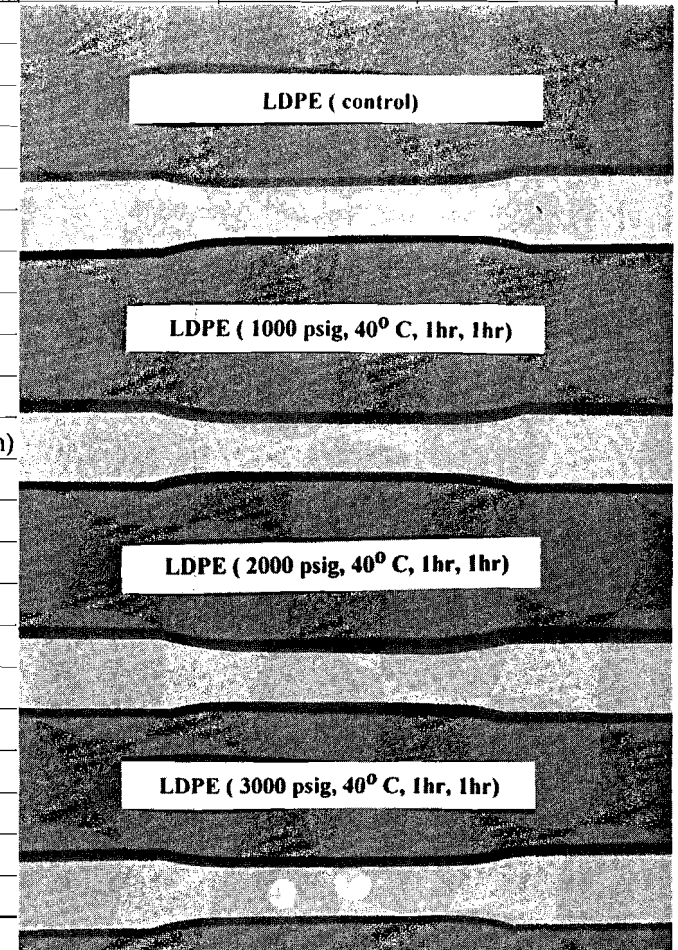
TEF (3000 psig, 40°C, 1hr, 1hr)

Weight change (dumbbell)	0.089+%(0d)	0.02+%(5d)				
Tensile strength, psi	1,972					
Elongation, %	105					
Tensile elastic modulus, psi	103,300					
Dispersion component, mJ/m2	13.29					
Polar component, mJ/m2	5.77					
Surface free energy, mJ/m2	19.06					
3000psi-25 C-1hr-1hr						
Appearance (dumbbell)	no change					
Glass transition temperature, C						
Weight change (coupon)	0.09+%(0d)	0.01+%(1d)	0.007+%(6d)	0.0005+%(12d)		
Weight change (dumbbell)	0.82+%(0d)	0.006+%(1d)	0.02+%(6d)	0.002+%(12d)	0.02+%(22d)	
Tensile strength, psi						
Elongation, %						
Tensile elastic modulus, psi						
Dispersion component, mJ/m2						
Polar component, mJ/m2						
Surface free energy, mJ/m2						
3000psi-40 C-1hr-1hr						
Appearance (dumbbell)	no change					
Glass transition temperature, C						
Weight change (coupon)	0.07+%(0d)	0.01+%(1d)	0.006+%(6d)	0.008+%(12d)	0.005+%(22d)	0.0004+%(60d)
Weight change (dumbbell)	0.51+%(0d)	0.13+%(1d)	0.18+%(6d)	0.18+%(12d)	1.59+%(22d)	1.59+%(60d)
Tensile strength, psi						
Elongation, %						
Tensile elastic modulus, psi						
Dispersion component, mJ/m2						

Low Density Polyethylene					
$\text{-(CH}_2\text{CH}_2\text{)(CH}_2\underset{\text{C}_n\text{H}_{2n+1}}{\text{CH}}\text{)-}_{n=2,4,6}$					
Polymer I.D.	LDPE				
Trade name					
Manufacturer	Poly-Hi/Menasha Corp.				
Control					
Appearance	translucent sheet with thickness 2.2mm (dumbbell) and 0.75 mm (coupon)				
Glass transition temperature, C					
Tensile strength, psi	1,547				
Elongation, %	238				
Tensile elastic modulus, psi	60,995				
Dispersion component, mJ/m ²	26.06				
Polar component, mJ/m ²	2.61				
Surface free energy, mJ/m ²	28.67				
1000psi-25 C-1hr-1hr					
Appearance (dumbbell)	no change				
Glass transition temperature, C					
Weight change (coupon)	0.04+%(0d)	~0 %(4d)	0.03-%(10d)	0%(8m)	
Weight change (dumbbell)	0.17+%(0d)	0.06-%(4d)	0.05-%(10d)		
Tensile strength, psi	1,623				
Elongation, %	270				
Tensile elastic modulus, psi	55,585				
Dispersion component, mJ/m ²	27.07				
Polar component, mJ/m ²	2.38				



Surface free energy, mJ/m ²	29.46							
1000psi-40 C-1hr-1hr								
Appearance (dumbbell)	no change							
Glass transition temperature, C								
Weight change (coupon)	0.31+%(0d)	0.29+%(1d)	0.27+%(6d)	0.23+%(12d)	0.23+%(22d)			
Weight change (dumbbell)	1.18+%(0d)	0.05+%(1d)	0.03+%(6d)	0.03+%(12d)	0.03+%(22d)			
Tensile strength, psi								
Elongation, %								
Tensile elastic modulus, psi								
Dispersion component, mJ/m ²								
Polar component, mJ/m ²								
Surface free energy, mJ/m ²								
2000psi-40 C-1hr-1hr								
Appearance (dumbbell)	a couple of big bubbles							
Glass transition temperature, C								
Weight change (coupon)	0.15+%(0d)	0.13+%(6d)	0.11+%(12d)	0.06+%(8m)				
Weight change (dumbbell)	0.23+%(0d)	0.03+%(6d)	0.04+%(12d)					
Tensile strength, psi	1,580							
Elongation, %	224							
Tensile elastic modulus, psi	54,748							
Dispersion component, mJ/m ²	24.3							
Polar component, mJ/m ²	3.35							
Surface free energy, mJ/m ²	27.65							
Surface free energy, mJ/m ²	29.27							
2300psi-70 C-15min-5min								
Appearance (dumbbell)	lots of big bubbles inside							



Glass transition temperature, C						
Weight change (coupon)	0.04 -%(0d)	~0 %(5d)	0.1-%(8m)			
Weight change (dumbbell)	0.04+%(0d)	~0 %(5d)				
Tensile strength, psi	1,492					
Elongation, %	55.6					
Tensile elastic modulus, psi	45,463					
Dispersion component, mJ/m2	24.42					
Polar component, mJ/m2	2.88					
Surface free energy, mJ/m2	27.3					
3000psi-25 C-1hr-1hr						
Appearance (dumbbell)	no change					
Glass transition temperature, C						
Weight change (coupon)	0.02-%(0d)	0.04-%(1d)	0.04-%(6d)	0.04-%(12d)	0.05-%(22d)	
Weight change (dumbbell)	1.39+%(0d)	0.02-%(1d)	0.04-%(6d)	0.05-%(12d)	0.05-%(22d)	
Tensile strength, psi						
Elongation, %						
Tensile elastic modulus, psi						
Dispersion component, mJ/m2						
Polar component, mJ/m2						
Surface free energy, mJ/m2						
3000psi-40 C-1hr-1hr						
Appearance (dumbbell)	some big bubbles inside					
Glass transition temperature, C						
Weight change (coupon)	0.14-%(0d)	0.10-%(1d)	0.09-%(6d)	0.08-%(12d)	0.10-%(22d)	0.11-%(60d)
Weight change (dumbbell)	1.36+%(0d)	0.003+%(1d)	0.08-%(6d)	0.10-%(12d)	0.10-%(22d)	0.10-%(60d)
Tensile strength, psi						
Elongation, %						

Tensile elastic modulus, psi							
Dispersion component, mJ/m²							
Polar component, mJ/m²							
Surface free energy, mJ/m²							
3000psi-70 C-1hr-1hr							
Appearance (coupon)	no change						
Glass transition temperature, C							
Weight change (coupon)	0.81+%(1d)	0.79+%(4d)	0.77+%(8d)	0.4+%(8m)			
Weight change (dumbbell)	0.15+%(4d)	0.15+%(11d)	0.13+%(17d)	0.69+%(12d)			
Appearance (dumbbell)	lots of big bubbles inside						
Tensile strength, psi	1,537						
Elongation, %	75.3						
Tensile elastic modulus, psi	49,523						
Dispersion component, mJ/m²	26.74						
Polar component, mJ/m²	2.53						
Surface free energy, mJ/m²	29.27						
3000psi-70 C-1hr-5hr							
Appearance (dumbbell)	no change						
Glass transition temperature, C							
Weight change (coupon)	1.24+%(0d)	1.02+%(4d)	0.73+%(8m)				
Weight change (dumbbell)	0.68+%(0d)	0.46+%(4d)					
Tensile strength, psi	1,480						
Elongation, %	223						
Tensile elastic modulus, psi	57,610						
Dispersion component, mJ/m²	26.04						
Polar component, mJ/m²	2.56						
Surface free energy, mJ/m²	28.6						

High Density Polyethylene			
$\left(\text{CH}_2 - \text{CH}_2 \right)_n$			
Polymer I.D.	HDPE		
Trade name			
Manufacturer	Poly-Hi/Menasha Corp.		
Control			
Appearance	white translucent sheet with thickness 2.25mm (dumbbell) and 0.8mm (coupon)		
Glass transition temperature			
Tensile strength, psi	3,822		
Elongation, %	92		
Tensile elastic modulus, psi	161,880		
Dispersion component, mJ/m ²	26.87		
Polar component, mJ/m ²	2.92		
Surface free energy, mJ/m ²	29.79		
1000psi-25 C-1hr-1hr			
Appearance (dumbbell)	no change		
Glass transition temperature, C			
Weight change (coupon)	~0 %(0d)	0.06-%(4d)	0.07-%(8m)
Weight change (dumbbell)	0.14+%(0d)	0.03-%(4d)	0.05-%(10d)
Tensile strength, psi	3,906		
Elongation, %	87		
Tensile elastic modulus, psi	160,680		
Dispersion component, mJ/m ²	26.46		
Polar component, mJ/m ²	2.45		
Surface free energy, mJ/m ²	28.91		

HDPE (control)

HDPE (3000 psig, 25°C, 1hr, 1hr)

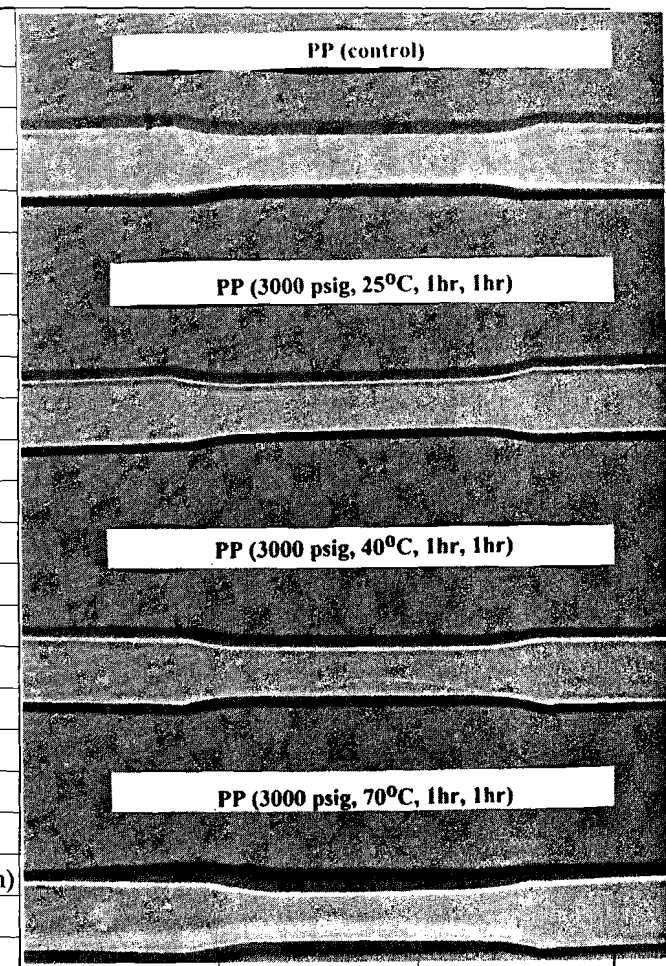
HDPE (3000 psig, 40°C, 1hr, 1hr)

HDPE (3000 psig, 70°C, 1hr, 1hr)

1000psi-40 C-1hr-1hr							
Appearance (dumbbell)	no change						
Glass transition temperature, C							
Weight change (coupon)	0.21+%(0d)	0.06+%(1d)	0.03+%(6d)	0.05+%(12d)	0.06+%(22d)		
Weight change (dumbbell)	0.57+%(0d)	0.05+%(1d)	0%(6d)	0%(12d)	0%(22d)		
Tensile strength, psi							
Elongation, %							
Tensile elastic modulus, psi							HDPE (control)
Dispersion component, mJ/m ²							
Polar component, mJ/m ²							
Surface free energy, mJ/m ²							
2000psi-40 C-1hr-1hr							HDPE (1000 psig, 40°C, 1hr, 1hr)
Appearance (dumbbell)	no change						
Glass transition temperature, C							
Weight change (coupon)	0.1+%(0d)	0.1+%(6d)	0.1+%(12d)	0.03+%(8m)			
Weight change (dumbbell)	0.38+%(0d)	0.02+%(6d)	0.02+%(12d)				
Tensile strength, psi	3,853						
Elongation, %	92						HDPE (2000 psig, 40°C, 1hr, 1hr)
Tensile elastic modulus, psi	155,425						
Dispersion component, mJ/m ²	27.57						
Polar component, mJ/m ²	2.40						
Surface free energy, mJ/m ²	29.97						
2300psi-70 C-15min-5min							HDPE (3000 psig, 40°C, 1hr, 1hr)
Appearance (dumbbell)	no change						
Glass transition temperature, C							
Weight change (coupon)	0.03+%(0d)	~0%(5d)	0.05+%(8m)				
Weight change (dumbbell)	0.48+%(0d)	0.02+%(5d)					

Tensile strength, psi	3,879					
Elongation, %	117					
Tensile elastic modulus, psi	155,820					
Dispersion component, mJ/m ²	26.79					
Polar component, mJ/m ²	2.38					
Surface free energy, mJ/m ²	29.17					
3000psi-25 C-1hr-1hr						
Appearance (dumbbell)	no change					
Glass transition temperature, C						
Weight change (coupon)	0.28+%(0d)	0.03+%(1d)	0.01+%(6d)	0.005-%(12d)	0.01+%(22d)	
Weight change (dumbbell)	0.65+%(0d)	0.08+%(1d)	0.007+%(6d)	0.004-%(12d)	0.02-%(22d)	
Tensile strength, psi						
Elongation, %						
Tensile elastic modulus, psi						
Dispersion component, mJ/m ²						
Polar component, mJ/m ²						
Surface free energy, mJ/m ²						
3000psi-40 C-1hr-1hr						
Appearance (dumbbell)	no change					
Glass transition temperature, C						
Weight change (coupon)	0.12+%(0d)	0.0001+%(1d)	0.03+%(6d)	0.04+%(12d)	0.03+%(22d)	0.06+%(60d)
Weight change (dumbbell)	1.22+%(0d)	0.18+%(1d)	0.003+%(6d)	0.01-%(12d)	0.02-%(22d)	0.03-%(60d)
Tensile strength, psi						
Elongation, %						
Tensile elastic modulus, psi						
Dispersion component, mJ/m ²						
Polar component, mJ/m ²						

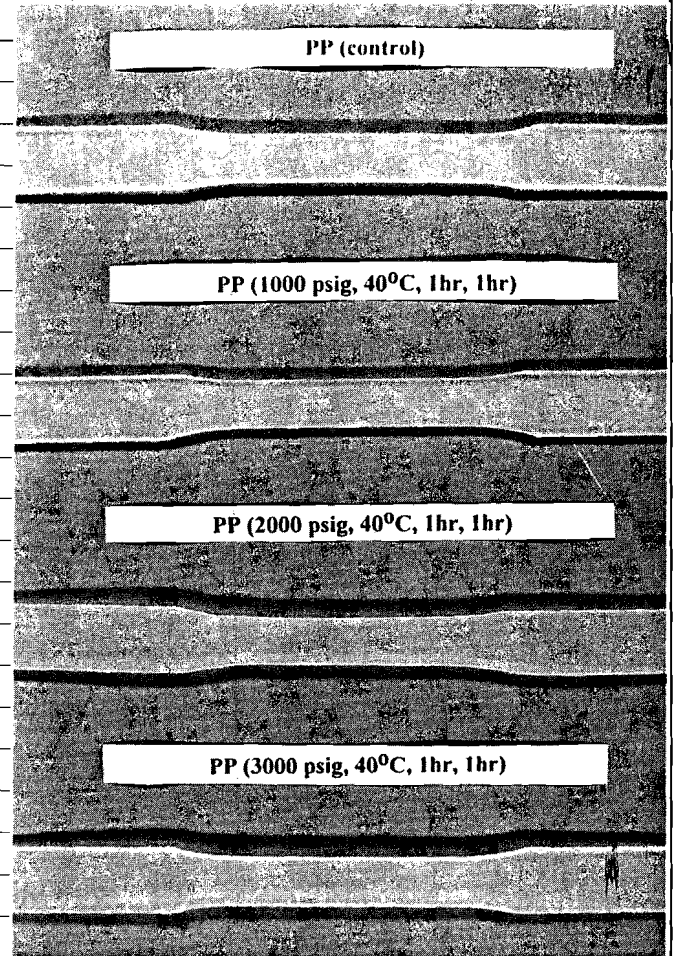
Polypropylene				
$\left(\text{CH}_2 - \underset{\text{CH}_3}{\text{CH}} \right)_n$				
Polymer I.D.	PP			
Trade name				
Manufacturer	Huls America			
Control				
Appearance	white translucent sheet with thickness 2.25mm (dumbbell) and 0.7mm (coupon)			
Tensile strength, psi	5,243			
Elongation, %	> 300			
Tensile elastic modulus, psi	198,725			
Dispersion component, mJ/m ²	21.11			
Polar component, mJ/m ²	3.73			
Surface free energy, mJ/m ²	24.85			
1000psi-25 C-1hr-1hr				
Appearance (dumbbell)	no change			
Weight change (coupon)	0.05+%(0d)	0.04 -(4d)	0.12-%(10d)	0.09-%(8m)
Weight change (dumbbell)	0.39+%(0d)	0.14 -(4d)	0.14 -(10d)	
Tensile strength, psi	5,297			
Elongation, %	> 300			
Tensile elastic modulus, psi	204,250			
Dispersion component, mJ/m ²	21.37			
Polar component, mJ/m ²	3.67			
Surface free energy, mJ/m ²	25.03			



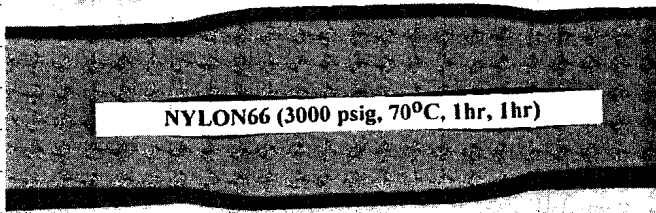
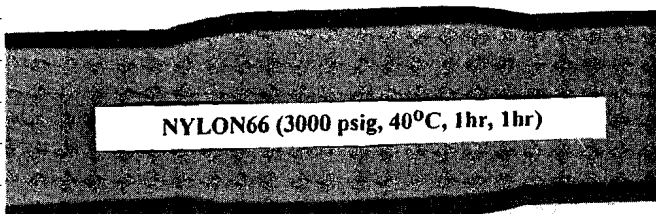
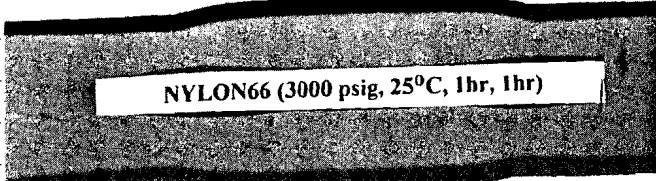
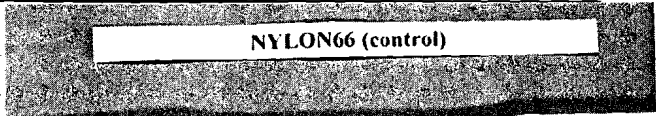
1000psi-40 C-1hr-1hr							
Appearance (dumbbell)	no change						
Weight change (coupon)	0.42+%(0d)	0.22+%(1d)	0.22+%(6d)	0.22+%(12d)	0.21+%(22d)		
Weight change (dumbbell)	1.56+%(0d)	0.21+%(1d)	0.03+%(6d)	0.04+%(12d)	0.02+%(22d)		
Tensile strength, psi							
Elongation, %							
Tensile elastic modulus, psi							
Dispersion component, mJ/m²							
Polar component, mJ/m²							
Surface free energy, mJ/m²							
2000psi-40 C-1hr-1hr							
Appearance (dumbbell)	no change						
Weight change (coupon)	~0 %(0d)	~0 %(6d)	~0 %(12d)	0.15-%(8m)			
Weight change (dumbbell)	0.69+%(0d)	0.14 -%(6d)	0.1-%(12d)				
Tensile strength, psi	5,144						
Elongation, %	> 300						
Tensile elastic modulus, psi	188,150						
Dispersion component, mJ/m²	22.28						
Polar component, mJ/m²	3.29						
Surface free energy, mJ/m²	25.58						
2300psi-70 C-15min-5min							
Appearance (dumbbell)	no change						
Weight change (coupon)	0.31-%(0d)	0.18-%(5d)	0.32-%(8m)				
Weight change (dumbbell)	0.89+%(0d)	0.05-%(5d)					
Tensile strength, psi	5,245						
Elongation, %	> 300						
Tensile elastic modulus, psi	191,530						

Dispersion component, mJ/m ²	20.52						
Polar component, mJ/m ²	3.62						
Surface free energy, mJ/m ²	24.14						
3000psi-25 C-1hr-1hr							
Appearance (dumbbell)	no change						
Glass transition temperature, C							
Weight change (coupon)	0.28+%(0d)	0.10-%(1d)	0.10-%(6d)	0.10-%(12d)	0.10-%(22d)		
Weight change (dumbbell)	1.83+%(0d)	0.25+%(1d)	0.04-%(6d)	0.05-%(12d)	0.03-%(22d)		
Tensile strength, psi							
Elongation, %							
Tensile elastic modulus, psi							
Dispersion component, mJ/m ²							
Polar component, mJ/m ²							
Surface free energy, mJ/m ²							
3000psi-40 C-1hr-1hr							
Appearance (dumbbell)	no change						
Glass transition temperature, C							
Weight change (coupon)	0.11-%(0d)	0.21-%(1d)	0.21-%(6d)	0.20-%(12d)	0.25-%(22d)	0.24-%(60d)	
Weight change (dumbbell)	1.98+%(0d)	0.28-%(1d)	0.09-%(6d)	0.11-%(6d)	0.12-%(12d)	0.12-%(60d)	
Tensile strength, psi							
Elongation, %							
Tensile elastic modulus, psi							
Dispersion component, mJ/m ²							
Polar component, mJ/m ²							
Surface free energy, mJ/m ²							
3000psi-70 C-1hr-1hr							

Appearance (dumbbell)	light yellow translucent sheet							
Glass transition temperature, C								
Weight change (coupon)	0.19+%(1d)	0.18+%(4d)	0.18+%(8d)	0.18+%(17d)	0.12+%(8m)			
Weight change (dumbbell)	0.12+%(4d)	0.04 -%(8d)	0.08-%(11d)	0.08+%(17d)				
Tensile strength, psi	5,072							
Elongation, %	> 300							
Tensile elastic modulus, psi	181,125							
Dispersion component, mJ/m2	20.69							
Polar component, mJ/m2	3.51							
Surface free energy, mJ/m2	24.2							
3000psi-70 C-1hr-5hr								
Appearance (dumbbell)	light yellow translucent sheet							
Glass transition temperature, C								
Weight change (coupon)	0.56+%(0d)	0.47+%(4d)	0.45+%(8m)					
Weight change (dumbbell)	0.72+%(0d)	0.14+%(4d)						
Tensile strength, psi	5,003							
Elongation, %	178							
Tensile elastic modulus, psi	170,250							
Dispersion component, mJ/m2	21.79							
Polar component, mJ/m2	3.29							
Surface free energy, mJ/m2	25.08							

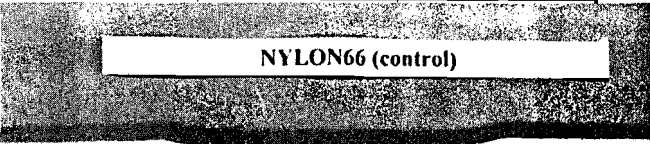
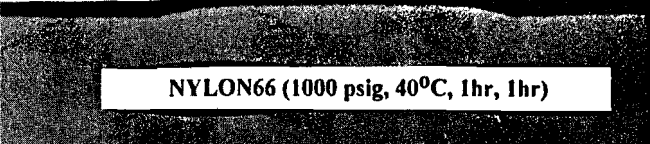
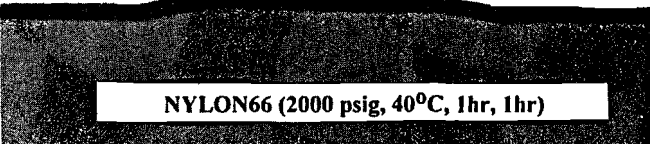
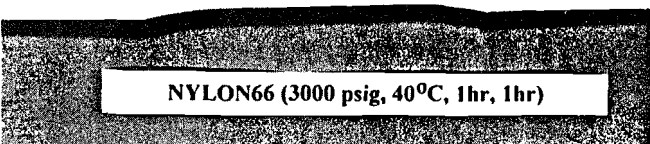

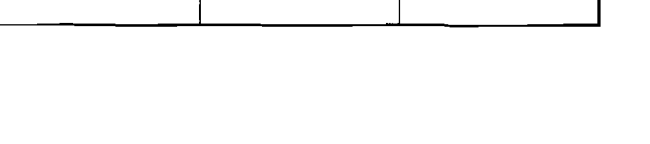


Polyamide					
$\text{---} \left(\text{CH}_2 \right)_6 \text{N} \begin{array}{c} \text{H} \\ \\ \text{C} \\ \\ \text{O} \end{array} \text{---} \left(\text{CH}_2 \right)_4 \text{C} \begin{array}{c} \text{O} \\ \\ \text{C} \\ \\ \text{H} \end{array} \text{---} \text{N} \text{---}$					
Polymer I.D.	Nylon 66				
Trade name	Nylon 66				
Manufacturer	Du Pont				
Control					
Appearance	yellow, opaque sheet with thickness 3.2mm (dumbbell) and 0.8 mm (coupon)				
Glass transition temperature, C					
Tensile strength, psi	9,927				
Elongation, %	47.6				
Tensile elastic modulus, psi	290,500				
Dispersion component, mJ/m2	29.45				
Polar component, mJ/m2	16.04				
Surface free energy, mJ/m2	45.49				
1000psi-25 C-1hr-1hr					
Appearance (dumbbell)	no change				
Glass transition temperature, C					
Weight change (coupon)	~0 %(0d)	0.11-%(4d)	0.1+-%(10d)	1.76-%(8m)	
Weight change (dumbbell)	~0 %(0d)	0.03+-%(4d)	0.11+-%(10d)		
Tensile strength, psi	10,475				
Elongation, %	30.3				
Tensile elastic modulus, psi	299,180				
Dispersion component, mJ/m2	28.97				
Polar component, mJ/m2	9.73				



Surface free energy, mJ/m²	38.70						
1000psi-40 C-1hr-1hr							
Appearance (dumbbell)	no change						
Glass transition temperature, C							
Weight change (coupon)	0.10-%(0d)	0.21-%(1d)	0.27-%(6d)	0.28-%(12d)	0.06+%(22d)		
Weight change (dumbbell)	0.05+%(0d)	0.01+%(1d)	0.008+%(6d)	0.03+%(12d)	0.15+%(22d)		
Tensile strength, psi							
Elongation, %							
Tensile elastic modulus, psi							
Dispersion component, mJ/m²							
Polar component, mJ/m²							
Surface free energy, mJ/m²							
2000psi-40 C-1hr-1hr							
Appearance (dumbbell)	no change						
Glass transition temperature, C							
Weight change (coupon)	0.04 -%(0d)	0.23-%(6d)	0.03-%(12d)	1.88-%(8m)			
Weight change (dumbbell)	0.04 -%(0d)	0.03+%(6d)	0.12+%(12d)				
Tensile strength, psi	10,625						
Elongation, %	24.2						
Tensile elastic modulus, psi	298,110						
Dispersion component, mJ/m²	35.02						
Polar component, mJ/m²	3.45						
Surface free energy, mJ/m²	38.47						
2300psi-70 C-15min-5min							
Appearance (dumbbell)	no change						
Glass transition temperature, C							

Weight change (coupon)	0.12+%(0d)	0.06-%(5d)	1.90-%(8m)			
Weight change (dumbbell)	0.04+%(0d)	0.04+%(5d)				
Tensile strength, psi	10,533					
Elongation, %	30.3					
Tensile elastic modulus, psi	315,030					
Dispersion component, mJ/m2	29.85					
Polar component, mJ/m2	7.18					
Surface free energy, mJ/m2	37.03					
3000psi-25 C-1hr-1hr						
Appearance (dumbbell)	no change					
Glass transition temperature, C						
Weight change (coupon)	0.29-%(0d)	0.46-%(1d)	0.13-%(6d)	0.04-%(12d)	0.18-%(22d)	
Weight change (dumbbell)	0.006+%(0d)	0.07-%(1d)	0.06-%(6d)	0.04-%(12d)	0.004%(22d)	
Tensile strength, psi						
Elongation, %						
Tensile elastic modulus, psi						
Dispersion component, mJ/m2						
Polar component, mJ/m2						
Surface free energy, mJ/m2						
3000psi-40 C-1hr-1hr						
Appearance (dumbbell)	no change					
Glass transition temperature, C						
Weight change (coupon)	1.14-%(0d)	1.15-%(1d)	0.98-%(6d)	0.74-%(12d)	0.17-%(22d)	0.17-%(60d)
Weight change (dumbbell)	0 %(0d)	0.08-%(1d)	0.09-%(6d)	0.02-%(12d)	0.13+%(22d)	0.36+%(60d)
Tensile strength, psi						
Elongation, %						
Tensile elastic modulus, psi						

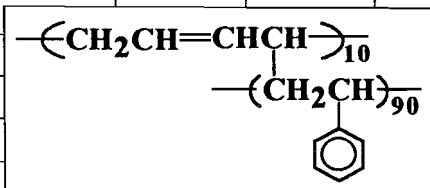
Dispersion component, mJ/m ²					
Polar component, mJ/m ²					
Surface free energy, mJ/m ²					
3000psi-70 C-1hr-1hr					
Appearance (dumbbell)	no change				
Glass transition temperature, C					
Weight change (coupon)	0.47-%(1d)	0.29-%(4d)	0.02-%(8d)	1.73-%(8m)	
Weight change (dumbbell)	0.09-%(4d)	0.03-%(11d)	0.06-%(17d)	0.35+%(17d)	
Tensile strength, psi	10,738				
Elongation, %	24.9				
Tensile elastic modulus, psi	299,240				
Dispersion component, mJ/m ²	33.39				
Polar component, mJ/m ²	2.86				
Surface free energy, mJ/m ²	36.25				
3000psi-70 C-1hr-5hr					
Appearance (dumbbell)	no change				
Glass transition temperature, C					
Weight change (coupon)	0.73-%(0d)	0.67-%(4d)	1.79-%(8m)		
Weight change (dumbbell)	0.29-%(0d)	0.23-%(4d)			
Tensile strength, psi	10,838				
Elongation, %	22.2				
Tensile elastic modulus, psi	316,930				
Dispersion component, mJ/m ²	30.35				
Polar component, mJ/m ²	5.38				
Surface free energy, mJ/m ²	35.72				

Polyoxymethylene					[Redacted]
$\left(\text{CH}_2 - \text{O} \right)_n$					
Polymer I.D.	POM				[Redacted]
Trade name	Delrin				[Redacted]
Manufacturer	Du Pont				[Redacted]
Control					[Redacted]
Appearance	white, opaque sheet with thickness 1.5mm (dumbbell) and 0.8mm (coupon)				[Redacted]
Glass transition temperature, C					[Redacted]
Tensile strength, psi	10,685				[Redacted]
Elongation, %	11				[Redacted]
Tensile elastic modulus, psi	376,300				[Redacted]
Dispersion component, mJ/m ²	31.16				[Redacted]
Polar component, mJ/m ²	6.82				[Redacted]
Surface free energy, mJ/m ²	37.98				[Redacted]
1000psi-25 C-1hr-1hr					[Redacted]
Appearance (dumbbell)	no change				[Redacted]
Weight change (coupon)	0.81+%(0d)	0.02+%(4d)	0.1+%(10d)	0.14-%(8m)	[Redacted]
Weight change (dumbbell)	0.35+%(0d)	0.04+%(4d)	0.1-%(10d)		[Redacted]
Tensile strength, psi	10,680				[Redacted]
Elongation, %	10.2				[Redacted]
Tensile elastic modulus, psi	361,030				[Redacted]
Dispersion component, mJ/m ²	28.89				[Redacted]
Polar component, mJ/m ²	4.25				[Redacted]
Surface free energy, mJ/m ²	33.15				[Redacted]

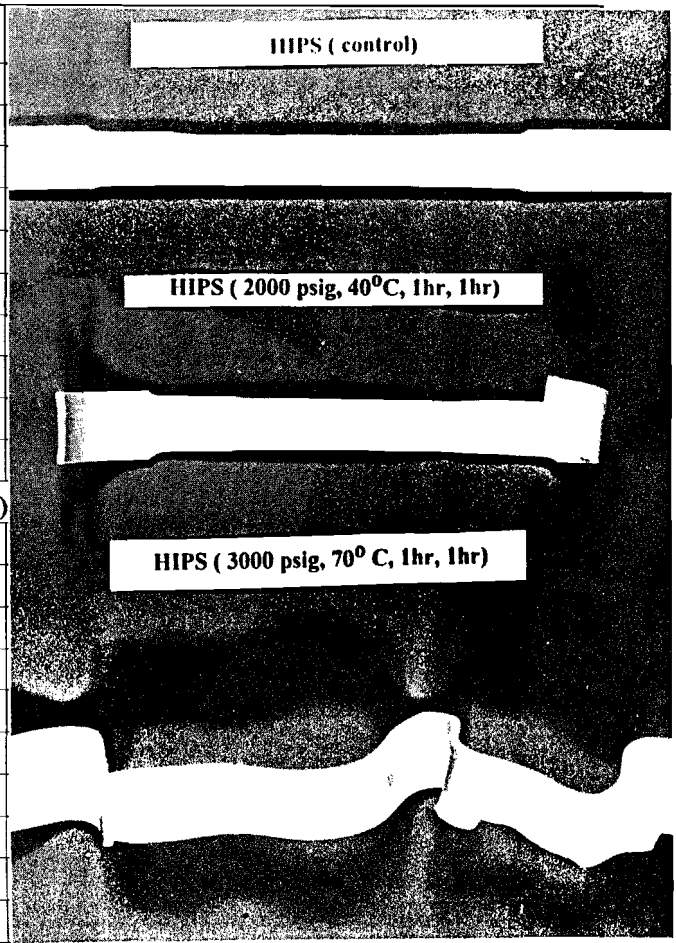
1000psi-40 C-1hr-1hr							
Appearance (dumbbell)	no change						
Weight change (coupon)	1.38+%(0d)	0.26+%(1d)	0.04-%(6d)	0.01-%(12d)	0.05+%(22d)		
Weight change (dumbbell)	0.94+%(0d)	0.37+%(1d)	0.37-%(6d)	0.04-%(12d)	0.003+%(22d)		
Tensile strength, psi						POM (control)	
Elongation, %							
Tensile elastic modulus, psi							
Dispersion component, mJ/m2							
Polar component, mJ/m2							
Surface free energy, mJ/m2							
2000psi-40 C-1hr-1hr						POM (1000 psig, 40°C, 1hr, 1hr)	
Appearance (dumbbell)	no change						
Weight change (coupon)	1.06+%(0d)	0.06+%(6d)	0.06+%(12d)	0.20-%(8m)			
Weight change (dumbbell)	1.17+%(0d)	0.04+%(6d)	0.04-%(12d)				
Tensile strength, psi	10,665					POM (2000 psig, 40°C, 1hr, 1hr)	
Elongation, %	11						
Tensile elastic modulus, psi	361,530						
Dispersion component, mJ/m2	32.56						
Polar component, mJ/m2	2.47						
Surface free energy, mJ/m2	35.02						
2300psi-70 C-15min-5min						POM (3000 psig, 40°C, 1hr, 1hr)	
Appearance (dumbbell)	no change						
Weight change (coupon)	1.04+%(0d)	~0%(5d)	0.22-%(8m)				
Weight change (dumbbell)	1.17+%(0d)	0.13+%(5d)					
Tensile strength, psi	10,673						
Elongation, %	11.1						
Tensile elastic modulus, psi	355,350						

Dispersion component, mJ/m2	33.46						
Polar component, mJ/m2	2.91						
Surface free energy, mJ/m2	36.37						
3000psi-25 C-1hr-1hr							
Appearance (dumbbell)	no change						
Weight change (coupon)	1.79+%(0d)	0.36+%(1d)	0.03+%(6d)	0.03-%(12d)	0.04-%(22d)		
Weight change (dumbbell)	1.68+%(0d)	0.52+%(1d)	0.10+%(6d)	0.01-%(12d)	0.03-%(22d)		
Tensile strength, psi							
Elongation, %							
Tensile elastic modulus, psi							
Dispersion component, mJ/m2							
Polar component, mJ/m2							
Surface free energy, mJ/m2							
3000psi-40 C-1hr-1hr							
Appearance (dumbbell)	no change						
Weight change (coupon)	1.54+%(0d)	0.31+%(1d)	0.08-%(6d)	0.06-%(12d)	0.02-%(22d)	0 %(60d)	
Weight change (dumbbell)	2.07+%(0d)	0.81+%(1d)	0.80+%(6d)	0.01-%(12d)	0.003+%(22d)	0 %(60d)	
Tensile strength, psi							
Elongation, %							
Tensile elastic modulus, psi							
Dispersion component, mJ/m2							
Polar component, mJ/m2							
Surface free energy, mJ/m2							
3000psi-70 C-1hr-1hr							
Appearance (dumbbell)	little bent						
Weight change (coupon)	0.29+%(1d)	0.05+%(4d)	0.06+%(8d)	0.21-%(8m)			

High Impact Polystyrene (B:10 %; S:90 %)



Polymer I.D.	HIPS			
Trade name				
Manufacturer	Farber			
Control				
Appearance	white, opaque sheet with thickness 1.5mm (dumbbell) and 1 mm (coupon)			
Glass transition temperature, C				
Tensile strength, psi	3,585			
Elongation, %	8.7			
Tensile elastic modulus, psi	230,320			
Dispersion component, mJ/m2	34.18			
Polar component, mJ/m2	1.91			
Surface free energy, mJ/m2	36.09			
1000psi-25 C-1hr-1hr				
Appearance (dumbbell)	no change			
Glass transition temperature, C				
Weight change (coupon)	0.76+%(0d)	0.05+%(4d)	~0 %(10d)	0%(8m)
Weight change (dumbbell)	0.44+%(0d)	0.05-%(4d)	0.07-%(10d)	
Tensile strength, psi	3,502			
Elongation, %	16.6			
Tensile elastic modulus, psi	225,100			
Dispersion component, mJ/m2	32.82			

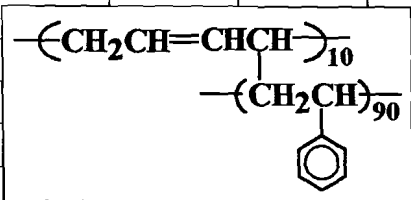


Polar component, mJ/m²	1.66					
Surface free energy, mJ/m²	34.48					
1000psi-40 C-1hr-1hr						
Appearance (dumbbell)	no change					
Glass transition temperature, C						
Weight change (coupon)	1.83+%(0d)	0.23+%(1d)	0.11+%(6d)	0.09+%(12d)	0.10+%(22d)	
Weight change (dumbbell)						
Tensile strength, psi						
Elongation, %						
Tensile elastic modulus, psi						
Dispersion component, mJ/m²						
Polar component, mJ/m²						
Surface free energy, mJ/m²						
2000psi-40 C-1hr-1hr						
Appearance (dumbbell)	tremendous bent					
Glass transition temperature, C						
Weight change (coupon)	1.09+%(0d)	0.16+%(6d)	0.15+%(12d)	0.04+%(8m)		
Weight change (dumbbell)	1.77+%(0d)	0.04+%(6d)	~0 %(12d)			
Tensile strength, psi						
Elongation, %						
Tensile elastic modulus, psi						
Dispersion component, mJ/m²	32.77					
Polar component, mJ/m²	3.59					
Surface free energy, mJ/m²	36.37					
2300psi-70 C-15min-5min						
Appearance (dumbbell)	tremendous bent					

Glass transition temperature, C						
Weight change (coupon)	0.82+%(0d)	~0 %(5d)	0.13-%(8m)			
Weight change (dumbbell)	1.15+%(0d)	0.03+%(5d)				
Tensile strength, psi						
Elongation, %						
Tensile elastic modulus, psi						
Dispersion component, mJ/m2	27.17					
Polar component, mJ/m2	3.07					
Surface free energy, mJ/m2	30.23					
3000psi-25 C-1hr-1hr						
Appearance (dumbbell)	bent					
Glass transition temperature, C						
Weight change (coupon)	1.91+%(0d)	0.22+%(1d)	0.01+%(6d)	0.006-%(12d)		
Weight change (dumbbell)						
Tensile strength, psi						
Elongation, %						
Tensile elastic modulus, psi						
Dispersion component, mJ/m2						
Polar component, mJ/m2						
Surface free energy, mJ/m2						
3000psi-40 C-1hr-1hr						
Appearance (dumbbell)						
Glass transition temperature, C						
Weight change (coupon)	2.17+%(0d)	0.13+%(1d)	0.01+%(6d)	0.0043+%(12d)	0.01-%(22d)	0.01-%(60d)
Weight change (dumbbell)						
Tensile strength, psi						
Elongation, %						

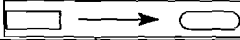
Tensile elastic modulus, psi						
Dispersion component, mJ/m2						
Polar component, mJ/m2						
Surface free energy, mJ/m2						
3000psi-70 C-1hr-1hr						
Appearance (dumbbell)	1. tremendous bent and big swelling (like foam) with very fine bubbles					
	2. more significant changes than those from 3000psi x 70c x 1hr x 5hr					
Glass transition temperature, C						
Weight change (coupon)	0.08+%(1d)	0.09+%(4d)	0.07+%(8d)	0.09+%(8m)		
Weight change (dumbbell)	0.11+%(4d)	0.08+%(11d)	0.06+%(17d)	0.08+%(17d)		
Tensile strength, psi						
Elongation, %						
Tensile elastic modulus, psi						
Dispersion component, mJ/m2	32.66					
Polar component, mJ/m2	4.28					
Surface free energy, mJ/m2	36.94					
3000psi-70 C-1hr-5hr						
Appearance (dumbbell)	tremendous bent and big swelling (like foam) with very fine bubbles					
Glass transition temperature, C						
Weight change (coupon)	0.68+%(0d)	0.19+%(4d)	0.16+%(8m)			
Weight change (dumbbell)	0.26+%(0d)	0.09+%(4d)				
Tensile strength, psi						
Elongation, %						
Tensile elastic modulus, psi						
Dispersion component, mJ/m2	28.63					
Polar component, mJ/m2	4.73					
Surface free energy, mJ/m2	33.36					

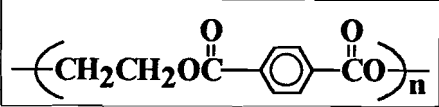
High Impact Polystyrene

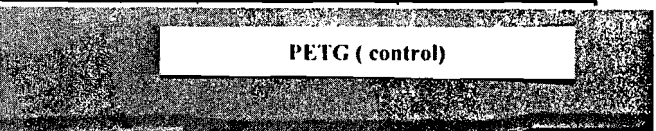


polymer I.D.	HIPS		
Trade name	Polysar 3350		
Manufacturer	Polysar		
Control			
Appearance	yellow, opaque sheet with 3.0 mm (dumbbell) in thickness		
Glass transition temperature, C			
Tensile strength, psi	4,782		
Elongation, %	19.5		
Tensile elastic modulus, psi	255,400		
1000psi-25 C-1hr-1hr			
Appearance (dumbbell)	no change		
Glass transition temperature, C			
Weight change (coupon)			
Weight change (dumbbell)	0.72+%(0d)	0.02-%(4d)	0.06-%(10d)
Tensile strength, psi	4,849		
Elongation, %	6.2		
Tensile elastic modulus, psi	250,800		
1000psi-40 C-1hr-1hr			
Appearance (dumbbell)	no change		
Glass transition temperature, C			

Weight change (coupon)							
Weight change (dumbbell)	1.99+%(0d)	0.47+%(1d)	0.03+%(6d)	0.02+%(12d)	0.02+%(22d)		
Tensile strength, psi							
Elongation, %							
Tensile elastic modulus, psi							
2000psi-40 C-1hr-1hr							
Appearance (dumbbell)	no change						
Glass transition temperature, C							
Weight change (coupon)							
Weight change (dumbbell)	2.04+%(0d)	0.08+%(6d)	0.03+%(12d)				
Tensile strength, psi	4,713						
Elongation, %	14.9						
Tensile elastic modulus, psi	248,750						
2300psi-70 C-15min-5min							
Appearance (dumbbell)	no change						
Glass transition temperature, C							
Weight change (coupon)							
Weight change (dumbbell)	2.06+%(0d)	0.11+%(5d)					
Tensile strength, psi	4,319						
Elongation, %	4.4						
Tensile elastic modulus, psi	238,630						
3000psi-25 C-1hr-1hr							
Appearance (dumbbell)	no change						
Glass transition temperature, C							
Weight change (coupon)							
Weight change (dumbbell)	3.51+%(0d)	0.66+%(1d)	0.04+%(6d)	0.003+%(12d)	0.01+%(22d)		

Tensile strength, psi						
Elongation, %						
Tensile elastic modulus, psi						
3000psi-40 C-1hr-1hr						
Appearance (dumbbell)	dissolution seen on edges					
Glass transition temperature, C						
Weight change (coupon)						
Weight change (dumbbell)	4.48+%(0d)	1.66+%(1d)	0.15+%(6d)	0.02+%(12d)	0.01+%(22d)	0.01+%(60d)
Tensile strength, psi						
Elongation, %						
Tensile elastic modulus, psi						
3000psi-70 C-1hr-1hr						
Appearance (dumbbell)						
Weight change (coupon)						
Weight change (dumbbell)						
Tensile strength, psi						
Elongation, %						
Tensile elastic modulus, psi						
3000psi-70 C-1hr-5hr						
Appearance (dumbbell)	tremendous bent and big swelling (like foam)					
Glass transition temperature, C						
Weight change (coupon)						
Weight change (dumbbell)	1.91+%(0d)	0.09+%(4d)				
Tensile strength, psi						
Elongation, %						
Tensile elastic modulus, psi						

Poly(ethylene terephthalate) glycol modified					
		The glycol segment is modified by cyclohexanedimethanol			
Polymer I.D.	PETG				
Trade name	Vivak				
Manufacturer	Lustro Plastics Corp.				
Control					
Appearance	transparent sheet with thickness 2.4mm (dumbbell) and 1mm (coupon)				
Glass transition temperature	79 C				
TGA Heating	0.45-%				
Tensile strength, psi					
Elongation, %					
Tensile elastic modulus, psi					
Dispersion component, mJ/m ²	33.46				
Polar component, mJ/m ²	3.52				
Surface free energy, mJ/m ²	38.97				
1000psi-25 C-1hr-1hr					
Appearance (dumbbell)	a coupon dissolution seen on the surface				
Glass transition temperature, C					
Weight change (coupon)	1.91+%(0d)	0.72+%(4d)	0.39+%(10d)	0.19-%(8m)	
Weight change (dumbbell)	0.77+%(0d)	0.28+%(4d)	0.16+%(10d)		
Tensile strength, psi	8,466				
Elongation, %	17				
Tensile elastic modulus, psi	250,025				
Dispersion component, mJ/m ²	34.51				
Polar component, mJ/m ²	2.65				



PETG (control)



PETG (3000 psig, 25⁰ C, 1hr, 1hr)

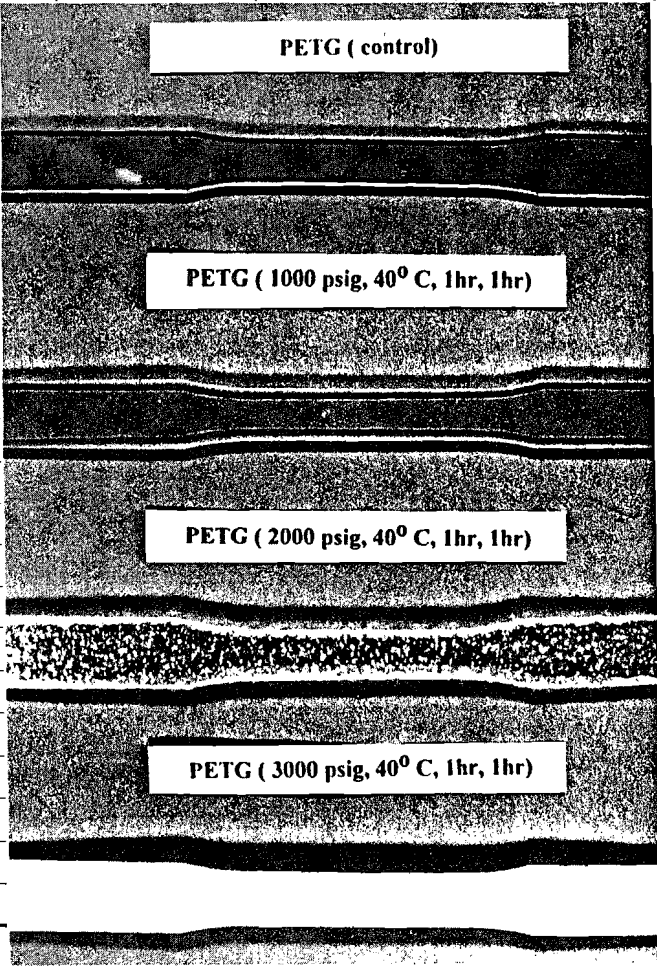


PETG (3000 psig, 40⁰ C, 1hr, 1hr)



PETG (3000 psig, 70⁰ C, 1hr, 1hr)

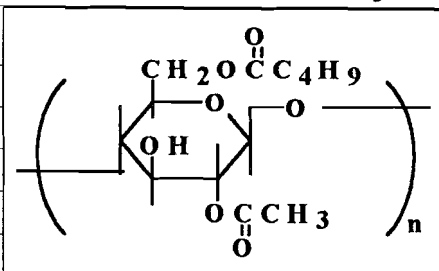
Surface free energy, mJ/m ²	37.17					
1000psi-40 C-1hr-1hr						
Appearance (dumbbell)	some small bubbles; light dissolution on the surface					
Glass transition temperature, C						
Weight change (coupon)	2.98+%(0d)	1.89+%(1d)	0.85+%(6d)	0.60+%(12d)	0.45+%(22d)	
Weight change (dumbbell)	1.47+%(0d)	0.87+%(1d)	0.42+%(6d)	0.33+%(12d)	0.28+%(22d)	
Tensile strength, psi						
Elongation, %						
Tensile elastic modulus, psi						
Dispersion component, mJ/m ²						
Polar component, mJ/m ²						
Surface free energy, mJ/m ²						
2000psi-40 C-1hr-1hr						
Appearance (dumbbell)	lots of bubbles					
Glass transition temperature, C						
Weight change (coupon)	5.22+%(0d)	1.99+%(6d)	1.32+%(12d)			
Weight change (dumbbell)	2.35+%(0d)	1.09+%(6d)	0.79+%(12d)			
Tensile strength, psi	7,910					
Elongation, %	13.1					
Tensile elastic modulus, psi	255,000					
Dispersion component, mJ/m ²	32.08					
Polar component, mJ/m ²	6.72					
Surface free energy, mJ/m ²	38.80					
2300psi-70 C-15min-5min						
Appearance (dumbbell)	lots of bubbles; dissolution seen on the surface					
Glass transition temperature, C						



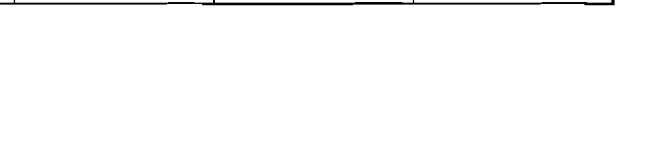
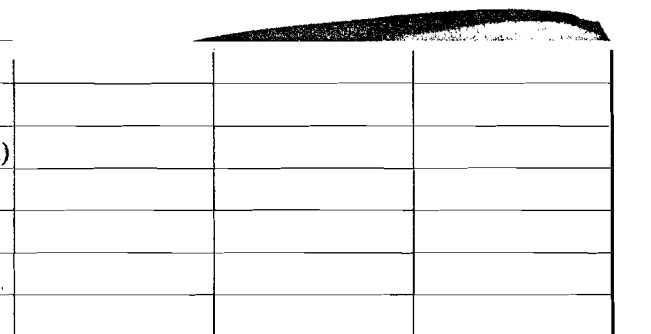
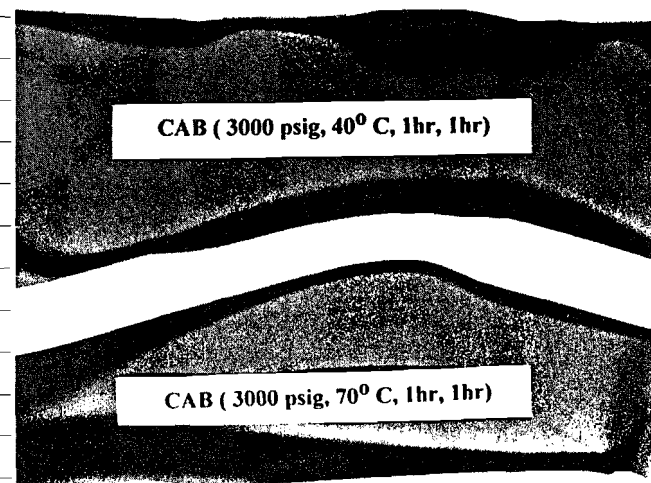
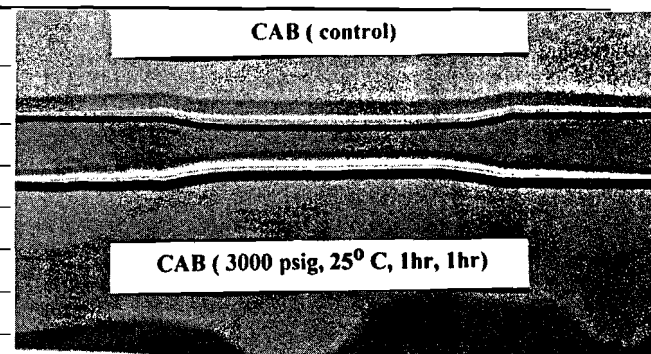
Weight change (coupon)	5.08+%(0d)	1.18+%(5d)				
Weight change (dumbbell)	2.69+%(0d)	1.12+%(5d)				
Tensile strength, psi	7,674					
Elongation, %	4.3					
Tensile elastic modulus, psi	245,400					
Dispersion component, mJ/m ²	40.55					
Polar component, mJ/m ²	2.42					
Surface free energy, mJ/m ²	42.96					
3000psi-25 C-1hr-1hr						
Appearance (dumbbell)	lots of bubbles					
Glass transition temperature, C	37 C(0d)	50 C(1d)	69 C(7d)	74 C(16d)		
TGA Heating	5.43-%(0d)	2.71-%(1d)	1.23-%(7d)	0.77-%(16d)		
Weight change (coupon)	5.36+%(0d)	3.33+%(1d)	1.51+%(6d)	0.81+%(12d)	0.49+%(22d)	
Weight change (dumbbell)	2.52+%(0d)	1.43+%(1d)	0.81+%(6d)	0.50+%(12d)	0.40+%(22d)	
Tensile strength, psi						
Elongation, %						
Tensile elastic modulus, psi						
Dispersion component, mJ/m ²						
Polar component, mJ/m ²						
Surface free energy, mJ/m ²						
3000psi-40 C-1hr-1hr						
Appearance (dumbbell)	gray to white opaque foam; lots of tiny bubbles					
Glass transition temperature, C						
Weight change (coupon)	5.14+%(0d)	2.12+%(1d)	1.49+%(6d)	2.33+%(12d)	2.60+%(22d)	2.58+%(60d)
Weight change (dumbbell)	4.18+%(0d)	3.27+%(1d)	1.39+%(6d)	0.72+%(12d)	0.49+%(22d)	0.34+%(60d)
Tensile strength, psi						
Elongation, %						


Tensile elastic modulus, psi							
Dispersion component, mJ/m²							
Polar component, mJ/m²							
Surface free energy, mJ/m²							
3000psi-70 C-1hr-1hr							
Appearance (coupon)	big bubble						
Appearance (dumbbell)	white, opaque foam; more significant change than that from the above						
Glass transition temperature, C							
Weight change (coupon)	0.28+%(1d)	0.28+%(4d)	0.28+%(8d)	0.31+%(17d)			
Weight change (dumbbell)	4.23+%(1d)	3.95+%(4d)	3.34+%(11d)	2.91+%(17d)			
Tensile strength, psi							
Elongation, %							
Tensile elastic modulus, psi							
Dispersion component, mJ/m²	39.35						
Polar component, mJ/m²	2.12						
Surface free energy, mJ/m²	41.47						
3000psi-70 C-1hr-5hr							
Appearance (dumbbell)	grey to white foam						
Glass transition temperature, C							
Weight change (coupon)	0.82+%(0d)	0.25+%(4d)	0.04+%(8m)				
Weight change (dumbbell)	5.19+%(0d)	4.58+%(4d)					
Tensile strength, psi							
Elongation, %							
Tensile elastic modulus, psi							
Dispersion component, mJ/m²	37.81						
Polar component, mJ/m²	2.79						
Surface free energy, mJ/m²	40.6						

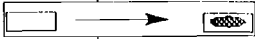
Cellulose Acetate Butyrate



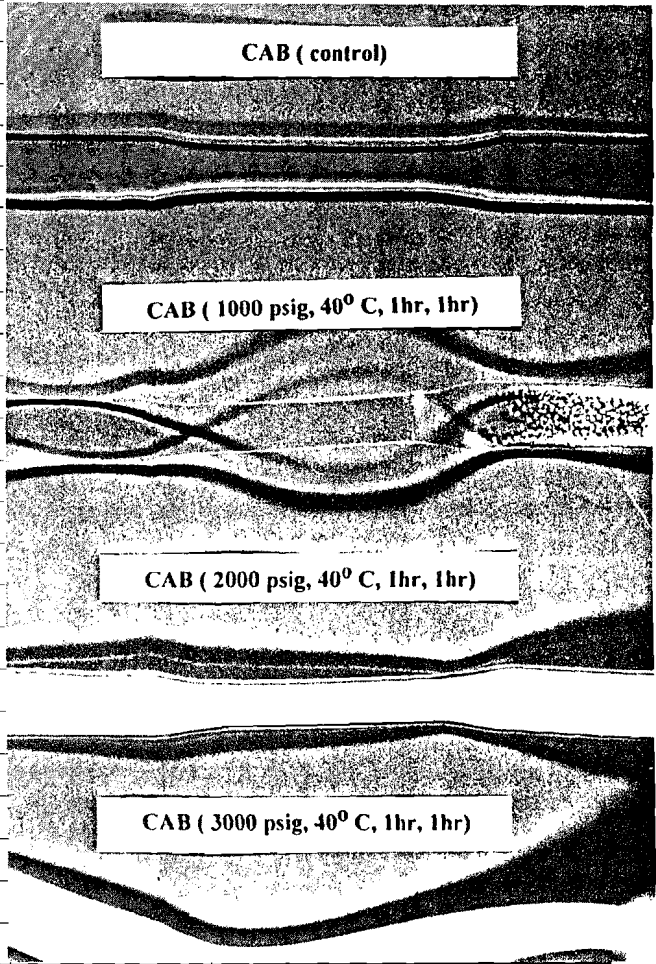
Polymer I.D.	CAB			
Trade name	UVEX			
Manufacturer	Eastman Kodak Corp.			
Control				
Appearance	transparent sheet with thickness 2.4mm (dumbbell) and 1.5mm (coupon)			
Glass transition temperature, C				
Tensile strength, psi	5,534			
Elongation, %	58.8			
Tensile elastic modulus, psi	209,160			
Dispersion component, mJ/m²	30.86			
Polar component, mJ/m²	4.06			
Surface free energy, mJ/m²	34.92			
1000psi-25 C-1hr-1hr				
Appearance (dumbbell)	bent shape and a light dissolution on the surface			
Glass transition temperature, C				
Weight change (coupon)	0.24 -%(0d)	1.41-%(4d)	1.33-%(10d)	2.11-%(8m)
Weight change (dumbbell)	1.9+%(0d)	1.46-%(4d)	1.34 -%(10d)	
Tensile strength, psi	5,959			
Elongation, %	44.2			
Tensile elastic modulus, psi	218,275			



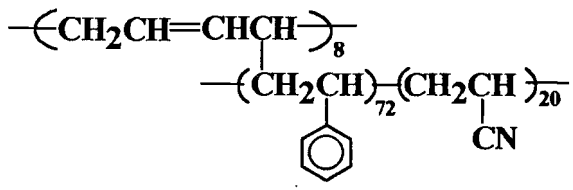
Dispersion component, mJ/m ²	27.91					
Polar component, mJ/m ²	5.17					
Surface free energy, mJ/m ²	33.08					
1000psi-40 C-1hr-1hr						
Appearance (dumbbell)	tremendous bent; bubbles on one end of the sample					
Glass transition temperature, C						
Weight change (coupon)	1.90+%(0d)	0.45-%(1d)	0.58-%(6d)	0.45-%(12d)	0.23-%(22d)	
Weight change (dumbbell)	6.61+%(0d)	0.03+%(1d)	0.45-%(6d)	0.38-%(12d)	0.23-%(22d)	
Tensile strength, psi						
Elongation, %						
Tensile elastic modulus, psi						
Dispersion component, mJ/m ²						
Polar component, mJ/m ²						
2000psi-40 C-1hr-1hr						
Appearance (dumbbell)	white foam inside: 					
Glass transition temperature, C						
Weight change (coupon)	2.1-%(0d)	3.22-%(6d)	3.12-%(12d)	3.90-%(8m)		
Weight change (dumbbell)	0.19+%(0d)	2.61-%(6d)	2.38-%(12d)			
Tensile strength, psi						
Elongation, %						
Tensile elastic modulus, psi						
Dispersion component, mJ/m ²	28.59					
Polar component, mJ/m ²	2.71					
Surface free energy, mJ/m ²	31.3					
2300psi-70 C-15min-5min						
Appearance (dumbbell)	foam with big bubbles					


Glass transition temperature, C						
Weight change (coupon)	1.07-%(0d)	2.51-%(5d)	3.21-%(8m)			
Weight change (dumbbell)	0.46-%(0d)	1.94 -%(5d)				
Tensile strength, psi						
Elongation, %						
Tensile elastic modulus, psi						
Dispersion component, mJ/m2	29.18					
Polar component, mJ/m2	2.82					
Surface free energy, mJ/m2	32.01					
3000psi-25 C-1hr-1hr						
Appearance (dumbbell)	tremendous bent; transparent colorless ---> opaque milky color					
Glass transition temperature, C						
Weight change (coupon)	4.4-%(0d)	4.18-%(1d)	4.04-%(6d)	4.24-%(12d)	4.21-%(22d)	
Weight change (dumbbell)	15.29+%(0d)	2.01-%(1d)	2.80-%(6d)	2.80-%(12d)	2.80-%(22d)	
Tensile strength, psi						
Elongation, %						
Tensile elastic modulus, psi						
Dispersion component, mJ/m2						
Polar component, mJ/m2						
Surface free energy, mJ/m2						
3000psi-40 C-1hr-1hr						
Appearance (dumbbell)	tremendous bent; transparent colorless --> opaque milky color 					
Glass transition temperature, C						
Weight change (coupon)	1.03-%(0d)	4.47-%(1d)	4.59-%(6d)	4.43-%(12d)	4.25-%(22d)	4.24-%(60d)
Weight change (dumbbell)	7.92+%(0d)	2.26-%(1d)	2.82-%(6d)	2.69-%(12d)	2.64-%(22d)	2.54-%(60d)
Tensile strength, psi						
Elongation, %						

Tensile elastic modulus, psi							
Dispersion component, mJ/m ²							
Polar component, mJ/m ²							
Surface free energy, mJ/m ²							
3000psi-70 C-1hr-1hr							
Appearance (dumbbell)	bent, milky foam; but its size is bigger than that from above conditions						
Glass transition temperature, C							
Weight change (coupon)	5.16-%(1d)	4.85-%(4d)	4.79-%(8d)	4.67-%(17d)			
Weight change (dumbbell)	4.71-%(1d)	4.53-%(4d)	4.09-%(11d)	4.01-%(17d)			
Tensile strength, psi							
Elongation, %							
Tensile elastic modulus, psi							
Dispersion component, mJ/m ²	31.88						
Polar component, mJ/m ²	3.89						
Surface free energy, mJ/m ²	35.78						
3000psi-70 C-1hr-5hr							
Appearance (dumbbell)	bent, milky foam; ink was not cleaned up						
Glass transition temperature, C							
Weight change (coupon)	3.43-%(0d)	4.95-%(4d)					
Weight change (dumbbell)	2.05-%(0d)	5-%(4d)					
Tensile strength, psi							
Elongation, %							
Tensile elastic modulus, psi							
Dispersion component, mJ/m ²	30.28						
Polar component, mJ/m ²	4.13						
Surface free energy, mJ/m ²	34.41						



Acrylonitrile Butadiene Styrene (A:20 %; B:8 %; S:72 %)



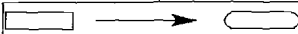
Polymer I.D.	ABS			
Trade name	Royalite			
Manufacturer	Polycast Tech. Corp.			
Control				
Appearance	black sheet with thickness 2.4 mm (dumbbell) and 1.6 mm (coupon)			
Glass transition temperature, C				
Tensile strength, psi	6,066			
Elongation, %	7.8			
Tensile elastic modulus, psi	278,540			
Dispersion component, mJ/m ²	35.04			
Polar component, mJ/m ²	1.1			
Surface free energy, mJ/m ²	36.14			
1000psi-25 C-1hr-1hr				
Appearance (dumbbell)	a very light dissolution on the surface; 			
Glass transition temperature, C				
Weight change (coupon)	2.34+%(0d)	0.3+%(4d)	0.16+%(10d)	0.14+%(8m)
Weight change (dumbbell)	1.46+%(0d)	0.18+%(4d)	0.01+%(10d)	
Tensile strength, psi	5,953			
Elongation, %	7.3			
Tensile elastic modulus, psi	243,230			
Dispersion component, mJ/m ²	26.91			

ABS (control)

ABS (3000 psig, 25^o C, 1hr, 1hr)

ABS (3000 psig, 40^o C, 1hr, 1hr)

ABS (3000 psig, 70^o C, 1hr, 1hr)

Polar component, mJ/m ²	2.22					
Surface free energy, mJ/m ²	29.13					
1000psi-40 C-1hr-1hr						
Appearance (dumbbell)	a very light dissolution on the surface					
Glass transition temperature, C						
Weight change (coupon)	4.32+%(0d)	1.40+%(1d)	0.24+%(6d)	0.19+%(12d)	0.27+%(22d)	
Weight change (dumbbell)	3.16+%(0d)	1.05+%(1d)	0.18+%(6d)	0.10+%(12d)	0.14+%(22d)	
Tensile strength, psi						
Elongation, %						ABS (control)
Tensile elastic modulus, psi						
Dispersion component, mJ/m ²						
Polar component, mJ/m ²						
Surface free energy, mJ/m ²						
2000psi-40 C-1hr-1hr						
Appearance (dumbbell)	bent					
Glass transition temperature, C						
Weight change (coupon)	4.87+%(0d)	0.53+%(6d)	0.37+%(12d)	0.08+%(8m)		
Weight change (dumbbell)	4.14+%(0d)	0.7+%(6d)	0.35+%(12d)			
Tensile strength, psi	6,259					
Elongation, %	5.5					
Tensile elastic modulus, psi	266,350					
Dispersion component, mJ/m ²	30.88					
Polar component, mJ/m ²	2.14					
Surface free energy, mJ/m ²	33.02					
2300psi-70 C-15min-5min						
Appearance (dumbbell)	a very light dissolution on the surface;					

ABS (1000 psig, 40^o C, 1hr, 1hr)

ABS (2000 psig, 40^o C, 1hr, 1hr)

ABS (3000 psig, 40^o C, 1hr, 1hr)

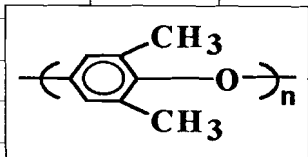
Glass transition temperature, C							
Weight change (coupon)	4.58+%(0d)	0.43+%(5d)	0.25+%(8m)				
Weight change (dumbbell)	3.65+%(0d)	0.61+%(5d)					
Tensile strength, psi	5,999						
Elongation, %	5.5						
Tensile elastic modulus, psi	266,350						
Dispersion component, mJ/m²	29.06						
Polar component, mJ/m²	1.75						
Surface free energy, mJ/m²	30.81						
3000psi-25 C-1hr-1hr							
Appearance (dumbbell)	very light dissolution on the surface						
Glass transition temperature, C							
Weight change (coupon)	6.49+%(0d)	2.05+%(1d)	0.39+%(6d)	0.18+%(12d)	0.65+%(22d)		
Weight change (dumbbell)	4.57+%(0d)	1.38+%(1d)	0.18+%(6d)	0.03+%(12d)	0.05+%(22d)		
Tensile strength, psi							
Elongation, %							
Tensile elastic modulus, psi							
Dispersion component, mJ/m²							
Polar component, mJ/m²							
Surface free energy, mJ/m²							
3000psi-40 C-1hr-1hr							
Appearance (dumbbell)	light dissolution on the surface;						
Glass transition temperature, C							
Weight change (coupon)	7.35+%(0d)	1.76+%(1d)	0.18+%(6d)	1.96+%(12d)	0.10+%(22d)	0.11+%(60d)	
Weight change (dumbbell)	7.24+%(0d)	2.58+%(1d)	0.34+%(6d)	0.06+%(12d)	0.10+%(22d)	0.12+%(60d)	
Tensile strength, psi							
Elongation, %							

Tensile elastic modulus, psi						
Dispersion component, mJ/m²						
Polar component, mJ/m²						
Surface free energy, mJ/m²						
3000psi-70 C-1hr-1hr						
Appearance (dumbbell)	foam with very fine bubbles					
Glass transition temperature, C						
Weight change (coupon)	0.08+%(1d)	0.1+%(4d)	0.13+%(8d)	0.18+%(17d)	0.07-%(8m)	
Weight change (dumbbell)	0.14 -%(4d)	0.03-%(8d)	0.02+%(11d)	0.05+%(17d)		
Tensile strength, psi						
Elongation, %						
Tensile elastic modulus, psi						
Dispersion component, mJ/m²	36.98					
Polar component, mJ/m²	1.32					
Surface free energy, mJ/m²	38.3					
3000psi-70 C-1hr-5hr						
Appearance (dumbbell)	foam, but its size is couponer than that from 3000psi x 70c x 1hr x 1hr					
Glass transition temperature, C						
Weight change (coupon)	5.8+%(0d)	0.12+%(4d)	0.10-%(8m)			
Weight change (dumbbell)	5.48+%(0d)	0.04+%(4d)				
Tensile strength, psi						
Elongation, %						
Tensile elastic modulus, psi						
Dispersion component, mJ/m²	36.5					
Polar component, mJ/m²	1.46					
Surface free energy, mJ/m²	37.97					

High Molecular Weight Polyethylene							
$\left(\text{CH}_2 - \text{CH}_2 \right)_n$							
Polymer I.D.	HMWPE						HMPE (control)
Trade name	Tivar						
Manufacturer	Poly-Hi/Menasha Corp.						
Control							HMPE (3000 psig, 25°C, 1hr, 1hr)
Appearance	white opaque sheet with 3.02mm in thickness						
Tensile strength, psi							
Elongation, %							
Tensile elastic modulus, psi							
1000psi-25 C-1hr-1hr							HMPE (3000 psig, 40°C, 1hr, 1hr)
Appearance (dumbbell)							
Weight change (coupon)							
Weight change (dumbbell)							
Tensile strength, psi							
Elongation, %							HMPE (3000 psig, 70°C, 1hr, 1hr)
Tensile elastic modulus, psi							
1000psi-40 C-1hr-1hr							
Appearance (dumbbell)	no change						
Weight change (coupon)	0.98+%(0d)	0.73+%(1d)	0.64+%(6d)	0.63+%(12d)	0.64+%(22d)	0.63+%(60d)	
Weight change (dumbbell)	0.14+%(0d)	0.11+%(1d)	0.05+%(6d)	0.06+%(12d)	0.05+%(22d)	0.04+%(60d)	
Tensile strength, psi							
Elongation, %							
Tensile elastic modulus, psi							

2000psi-40 C-1hr-1hr							
Appearance (dumbbell)	no change						
Weight change (coupon)	0.55+%(0d)	0.08+%(1d)	0.07-%(6d)	0.07-%(12d)	0.07-%(22d)	0.09-%(60d)	
Weight change (dumbbell)	0.67+%(0d)	0.19+%(1d)	0.09+%(6d)	0.05+%(12d)	0.05+%(22d)	0.04+%(60d)	
Tensile strength, psi							
Elongation, %							
Tensile elastic modulus, psi							
3000psi-25 C-1hr-1hr							
Appearance (dumbbell)	no change						
Weight change (coupon)	0.26+%(0d)	0.04+%(1d)	0.01-%(6d)	0.02-%(12d)	0.02-%(22d)		
Weight change (dumbbell)	0.30+%(0d)	0.06+%(1d)	0.006-%(6d)	0.003-%(12d)	0.003-%(22d)		
Tensile strength, psi							
Elongation, %							
Tensile elastic modulus, psi							
3000psi-40 C-1hr-1hr							
Appearance (dumbbell)	no change						
Weight change (coupon)	0.67+%(0d)	0.16+%(1d)	0.01-%(6d)	0.008-%(12d)	0.001-%(22d)	0.02-%(60d)	
Weight change (dumbbell)	0.35+%(0d)	0.07+%(1d)	0.09-%(6d)	0.09-%(12d)	0.11-%(22d)	0.11-%(60d)	
Tensile strength, psi							
Elongation, %							
Tensile elastic modulus, psi							
3000psi-70 C-1hr-1hr							
Appearance (dumbbell)	no change						
Weight change (coupon)	1.24+%(0d)	0.02-%(1d)	0.04-%(6d)	0.05-%(12d)	0.06-%(22d)	0.07-%(60d)	0.07-%(5m)
Weight change (dumbbell)	1.38+%(0d)	0.02-%(1d)	0.046-%(6d)	0.09+%(12d)	0.06-%(22d)	0.07-%(60d)	0.07-%(5m)
Tensile strength, psi							

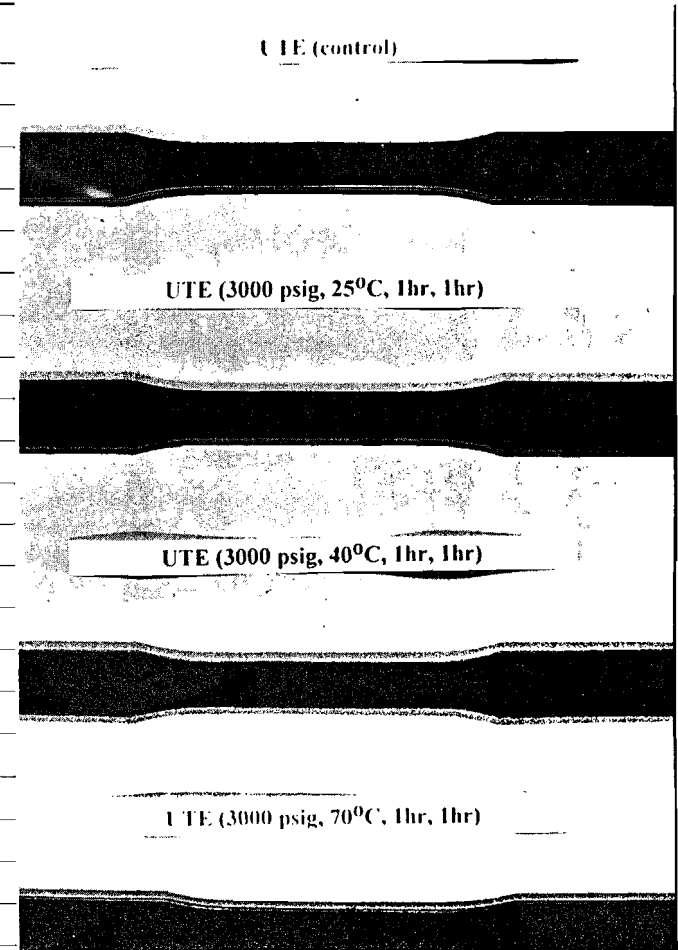
Poly(2,6-dimethylphenylene oxide)



				NOR (control)	
Polymer I.D.		PPO		NOR (3000 psig, 25°C, 1hr, 1hr)	
Trade name		Noryl			
Manufacturer		GE			
Control					
Appearance		black opaque sheet with 6.63mm in thickness		NOR (3000 psig, 40°C, 1hr, 1hr)	
Glass transition temperature, C					
Tensile strength, psi					
Elongation, %					
Tensile elastic modulus, psi					
1000psi-25 C-1hr-1hr				NOR (3000 psig, 70°C, 1hr, 1hr)	
Appearance (dumbbell)					
Glass transition temperature, C					
Weight change (coupon)					
Weight change (dumbbell)					
Tensile strength, psi					
Elongation, %					
Tensile elastic modulus, psi					
1000psi-40 C-1hr-1hr					
Appearance (dumbbell)		no change			
Glass transition temperature, C					

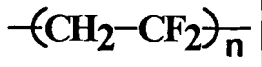
3000psi-70 C-1hr-1hr								
Appearance (dumbbell)		no change						
Weight change (coupon)		3.43+%(0d)	0.58+%(1d)	0.32+%(6d)	0.15+%(12d)	0.003-%(22d)	0.05+%(60d)	0.05+%(5m)
Weight change (dumbbell)		3.12+%(0d)	0.84+%(1d)	0.42+%(6d)	0.20+%(12d)	0.06-%(22d)	0.02+%(60d)	0.02+%(5m)
3000psi-70 C-1hr-5hr								
Appearance (dumbbell)							NOR (control)	
Weight change (coupon)								
Weight change (dumbbell)								
							NOR (1000 psig, 40°C, 1hr, 1hr)	
							NOR (2000 psig, 40°C, 1hr, 1hr)	
							NOR (3000 psig, 40°C, 1hr, 1hr)	

Polyetherimide						
Polymer I.D.	PEI					
Trade name	Ultem					
Manufacturer	GE					
Control						
Appearance	brown transparent sheet with 1.74mm in thickness					
Glass transition temperature, C						
Tensile strength, psi						
Elongation, %						
Tensile elastic modulus, psi						
1000psi-40 C-1hr-1hr						
Appearance (dumbbell)	no change					
Glass transition temperature, C						
Weight change (coupon)	0.45+%(0d)	0.22+%(1d)	0.12+%(6d)	0.12+%(12d)	0.14+%(22d)	0.17+%(60d)
Weight change (dumbbell)	0.56+%(0d)	0.29+%(1d)	0.18+%(6d)	0.15+%(12d)	0.19+%(22d)	0.27+%(60d)
Tensile strength, psi						
Elongation, %						
Tensile elastic modulus, psi						
2000psi-40 C-1hr-1hr						



Appearance (dumbbell)	no change						
Glass transition temperature, C							
Weight change (coupon)	0.88+%(0d)	0.43+%(1d)	0.18+%(6d)	0.13+%(12d)	0.11+%(22d)	0.03+%(60d)	
Weight change (dumbbell)	0.87+%(0d)	0.55+%(1d)	0.79+%(6d)	0.34+%(12d)	0.37+%(22d)	0.35+%(60d)	
Tensile strength, psi							
Elongation, %							
Tensile elastic modulus, psi							
3000psi-25 C-1hr-1hr							
Appearance (dumbbell)	no change						
Glass transition temperature, C							
Weight change (coupon)	0.52+%(0d)	0.22+%(1d)	0.003+%(6d)	0.04+%(12d)	0.01+%(22d)		
Weight change (dumbbell)	0.58+%(0d)	0.35+%(1d)	0.29+%(6d)	0.14+%(12d)	0.17+%(22d)		
Tensile strength, psi							
Elongation, %							
Tensile elastic modulus, psi							
3000psi-40 C-1hr-1hr							
Appearance (dumbbell)	no change						
Glass transition temperature, C							
Weight change (coupon)	1.04+%(0d)	0.62+%(4d)	0.37+%(6d)	0.33+%(12d)	0.35+%(22d)	0.34+%(60d)	
Weight change (dumbbell)	0.36+%(0d)	0.17+%(1d)	0.07+%(6d)	0.12+%(12d)	0.10+%(22d)	0.09+%(60d)	
Tensile strength, psi							
Elongation, %							
Tensile elastic modulus, psi							
3000psi-70 C-1hr-1hr							
Appearance (dumbbell)	no change						
Glass transition temperature, C							

Polyvinylidene fluoride



Polymer I.D.	PVDF							
Trade name	Kynar							
Manufacturer	Pennwalt Chemical Corp.							
Control								
Appearance	colorless translucent sheet with 1.5mm in thickness							
Glass transition temperature								
Tensile strength, psi								
Elongation, %								
Tensile elastic modulus, psi								
1000psi-25 C-1hr-1hr								
Appearance (dumbbell)								
Glass transition temperature, C								
Weight change (coupon)								
Weight change (dumbbell)								
Tensile strength, psi								
Elongation, %								
Tensile elastic modulus, psi								
1000psi-40 C-1hr-1hr								
Appearance (dumbbell)	no change							
Glass transition temperature, C								
Weight change (coupon)	1.00+%(0d)	0.65+%(1d)	0.33+%(6d)	0.19+%(12d)	0.03+%(22d)	0.01-%(60d)		
Weight change (dumbbell)	0.52+%(0d)	0.13+%(1d)	0.13-%(6d)	0.22-%(12d)	0.41-%(22d)	0.46-%(60d)		

K Y R (CONT'D)

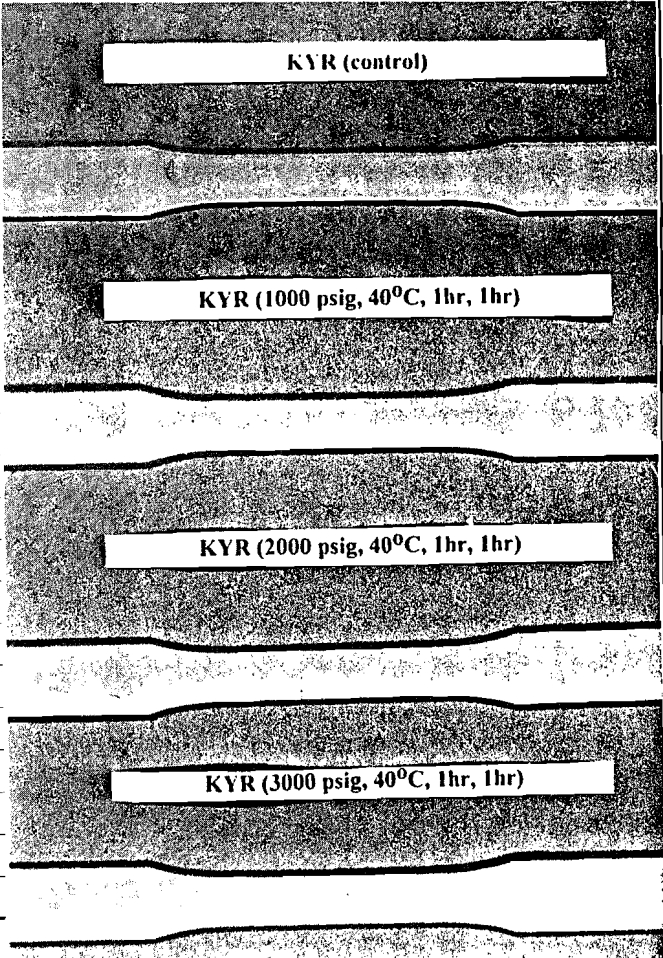
K Y R (3000 psig, 25°C, 1hr, 1hr)

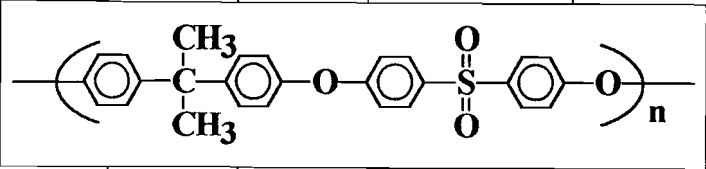
K Y R (3000 psig, 40°C, 1hr, 1hr)

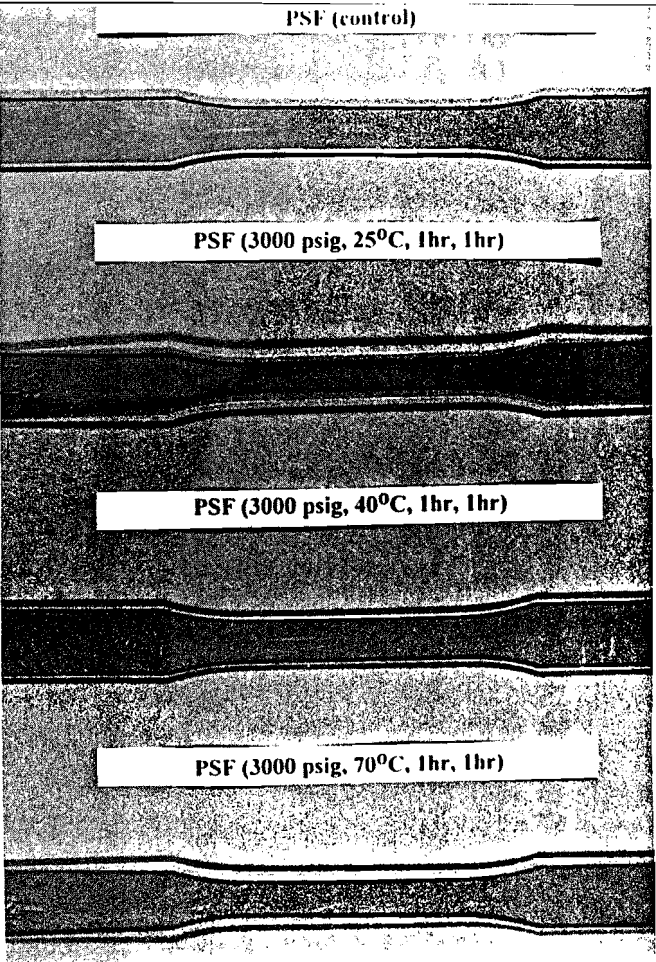
K Y R (3000 psig, 70°C, 1hr, 1hr)

Tensile strength, psi							
Elongation, %							
Tensile elastic modulus, psi							
2000psi-40 C-1hr-1hr							
Appearance (dumbbell)	no change						
Glass transition temperature, C							
Weight change (coupon)	2.73+%(0d)	1.38+%(1d)	0.55+%(6d)	0.26+%(12d)	0.006+%(22d)	0.06+%(60d)	
Weight change (dumbbell)	2.45+%(0d)	1.37+%(1d)	0.82+%(6d)	0.39+%(12d)	0.05+%(22d)	0.004+%(60d)	
Tensile strength, psi							
Elongation, %							
Tensile elastic modulus, psi							
3000psi-25 C-1hr-1hr							
Appearance (dumbbell)	no change						
Glass transition temperature, C							
Weight change (coupon)	1.15+%(0d)	20.42+%(1d)	0.21+%(6d)	0.11+%(12d)	0.04+%(22d)		
Weight change (dumbbell)	1.11+%(0d)	0.56+%(1d)	0.26+%(6d)	0.14+%(12d)	0.10+%(22d)		
Tensile strength, psi							
Elongation, %							
Tensile elastic modulus, psi							
3000psi-40 C-1hr-1hr							
Appearance (dumbbell)	no change						
Glass transition temperature, C							
Weight change (coupon)	3.02+%(0d)	1.62+%(1d)	0.68+%(6d)	0.03+%(12d)	0.03+%(22d)	0.002+%(60d)	
Weight change (dumbbell)	2.97+%(0d)	1.71+%(1d)	0.77+%(6d)	0.38+%(12d)	0.07+%(22d)	0.05+%(60d)	
Tensile strength, psi							
Elongation, %							

Tensile elastic modulus, psi								
3000psi-70 C-1hr-1hr								
Appearance (dumbbell)	no change							
Glass transition temperature, C								
Weight change (coupon)	3.59+%(0d)	0.82+%(1d)	0.53+%(6d)	0.28+%(12d)	0.03-%(22d)	0.02-%(60d)	0.02-%(5m)	
Weight change (dumbbell)	4.00+%(0d)	0.89+%(1d)	0.48+%(6d)	0.31+%(12d)	0.07-%(22d)	0.02-%(60d)	0.02-%(5m)	
Tensile strength, psi								
Elongation, %								
Tensile elastic modulus, psi								
3000psi-70 C-1hr-5hr								
Appearance (dumbbell)								
Glass transition temperature, C								
Weight change (coupon)								
Weight change (dumbbell)								
Tensile strength, psi								
Elongation, %								
Tensile elastic modulus, psi								

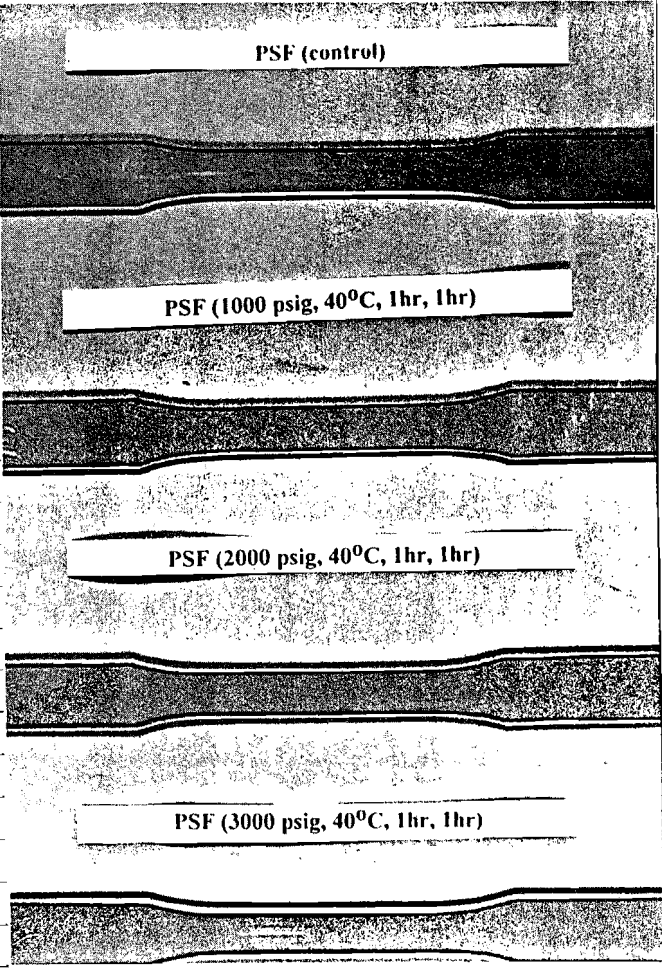


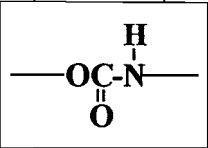
Polysulfone							
							
Polymer I.D.	PSF						
Trade name	Thermalux						
Manufacturer	Westlake Plastics Corp.						
Control							
Appearance	brown transparent sheet with 1.46mm in thickness						
Glass transition temperature, C							
Tensile strength, psi							
Elongation, %							
Tensile elastic modulus, psi							
1000psi-25 C-1hr-1hr							
Appearance (dumbbell)							
Glass transition temperature, C							
Weight change (coupon)							
Weight change (dumbbell)							
Tensile strength, psi							
Elongation, %							
Tensile elastic modulus, psi							
1000psi-40 C-1hr-1hr							
Appearance (dumbbell)	no change						
Glass transition temperature, C							

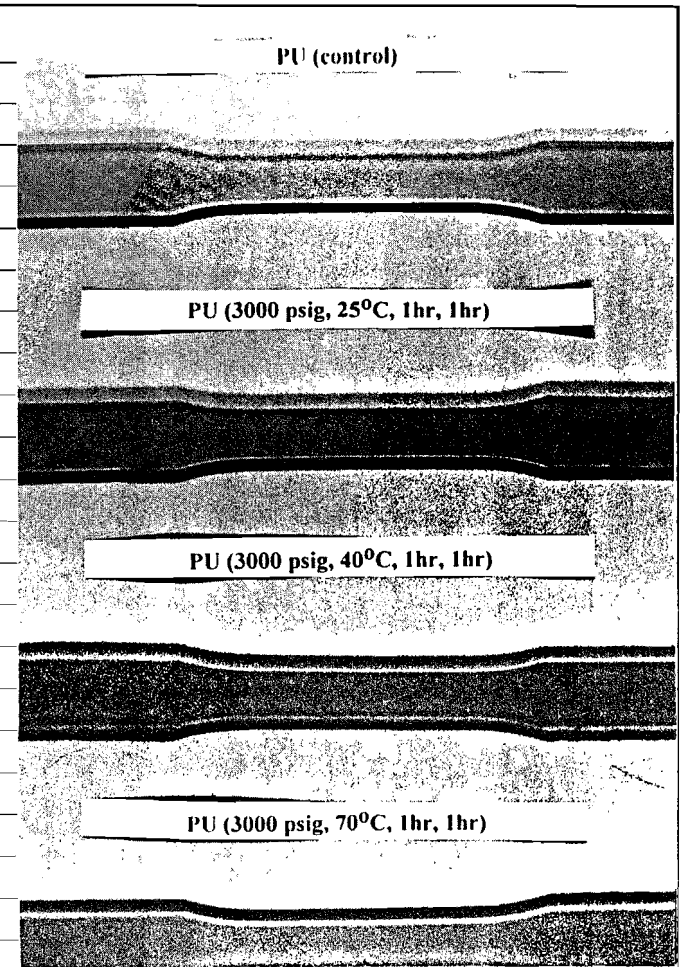


Weight change (coupon)	1.25+%(0d)	0.56+%(1d)	0.11+%(6d)	0.007+%(12d)	0.01+%(22d)	0.04+%(60d)
Weight change (dumbbell)	1.31+5(0d)	0.65+%(1d)	0.27+%(6d)	0.08+%(12d)	0.13+%(22d)	0.07+%(60d)
Tensile strength, psi						
Elongation, %						
Tensile elastic modulus, psi						
2000psi-40 C-1hr-1hr						
Appearance (dumbbell)	no change					
Glass transition temperature, C						
Weight change (coupon)	2.3+%(0d)	0.96+%(1d)	0.20+%(6d)	0.07+%(12d)	0.07+%(22d)	0.10+%(60d)
Weight change (dumbbell)	2.05+%(0d)	1.03+%(1d)	0.36+%(6d)	0.19+%(12d)	0.12+%(22d)	0.14+%(60d)
Tensile strength, psi						
Elongation, %						
Tensile elastic modulus, psi						
3000psi-25 C-1hr-1hr						
Appearance (dumbbell)	no change					
Glass transition temperature, C						
Weight change (coupon)	1.25+%(0d)	0.50+%(1d)	0.003+%(6d)	0.04+%(12d)	0.01+%(22d)	
Weight change (dumbbell)	1.30+%(0d)	0.57+%(1d)	0.12+%(6d)	0.04+%(12d)	0.04+%(22d)	
Tensile strength, psi						
Elongation, %						
Tensile elastic modulus, psi						
3000psi-40 C-1hr-1hr						
Appearance (dumbbell)	no change					
Glass transition temperature, C						
Weight change (coupon)	2.2+%(0d)	1.1+%(1d)	0.25+%(6d)	0.12+%(12d)	0.15+%(22d)	0.16+%(60d)
Weight change (dumbbell)	1.7+%(0d)	0.97+%(1d)	0.04+%(6d)	0.14+%(12d)	0.12+%(22d)	0.09+%(60d)

3000psi-70 C-1hr-1hr								
Appearance (dumbbell)		no change						
Glass transition temperature, C								
Weight change (coupon)		4.09+%(0d)	0.72+%(1d)	0.38+%(6d)	0.13+%(12d)	0.08+%(22d)	0.48+%(60d)	0.49+%(5m)
Weight change (dumbbell)		3.87+%(0d)	1.05+%(1d)	0.24+%(6d)	0.26+%(12d)	0.19+%(22d)	0.07+%(60d)	0.07+%(5m)
Tensile strength, psi								
Elongation, %								
Tensile elastic modulus, psi								
3000psi-70 C-1hr-5hr								
Appearance (dumbbell)								
Glass transition temperature, C								
Weight change (coupon)								
Weight change (dumbbell)								
Tensile strength, psi								
Elongation, %								
Tensile elastic modulus, psi								

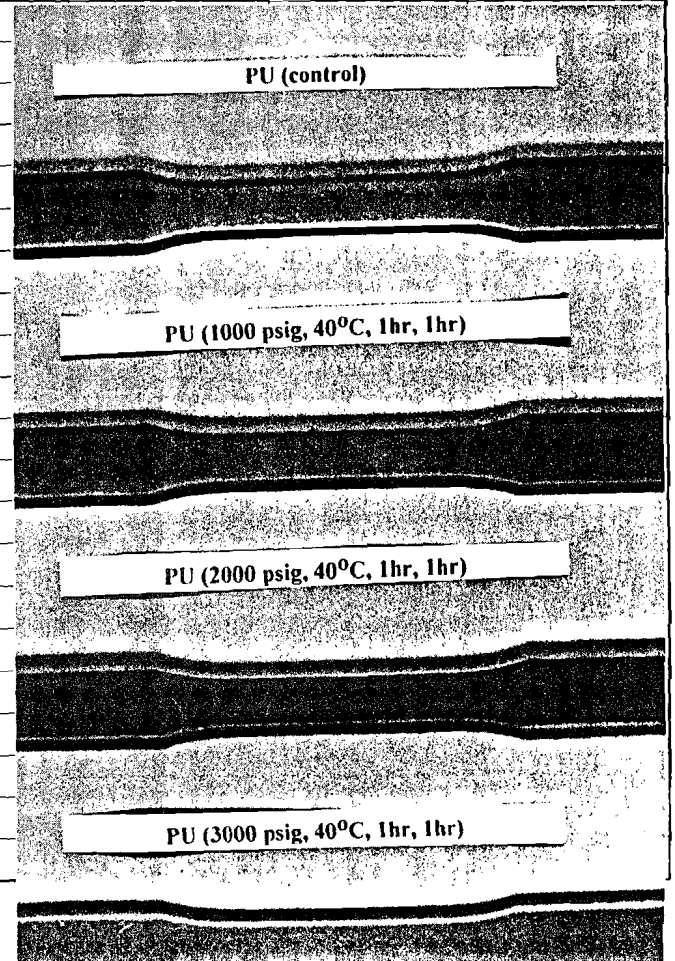


Polyurethane							
		(repeat unit)					
Polymer I.D.		PU					
Trade name							
Manufacturer		Harkness					
Control							
Appearance		orange, hard translucent sheet with 3.05mm in thickness					
Glass transition temperature, C							
Tensile strength, psi							
Elongation, %							
Tensile elastic modulus, psi							
1000psi-25 C-1hr-1hr							
Appearance (dumbbell)							
Glass transition temperature, C							
Weight change (coupon)							
Weight change (dumbbell)							
Tensile strength, psi							
Elongation, %							
Tensile elastic modulus, psi							
1000psi-40 C-1hr-1hr							
Appearance (dumbbell)		no change					
Glass transition temperature, C							
Weight change (coupon)		2.2+%(0d)	0.10+%(1d)	0.09+%(6d)	0.80+%(12d)	0.25+%(22d)	0.35+%(60d)

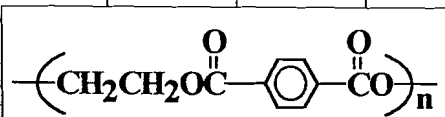


Weight change (dumbbell)	2.8+%(0d)	0.18+%(1d)	0.19+%(6d)	0.25+%(12d)	0.35+%(22d)	0.49+%(60d)	
Tensile strength, psi							
Elongation, %							
Tensile elastic modulus, psi							
2000psi-40 C-1hr-1hr							
Appearance (dumbbell)	no change						
Glass transition temperature, C							
Weight change (coupon)	4.4+%(0d)	0.14-%(1d)	0.09-%(6d)	0.04-%(12d)	4.99-%(22d)	0.19+%(60d)	
Weight change (dumbbell)	3.9+%(0d)	0.002-%(1d)	0.04-%(6d)	0.11+%(12d)	0.19+%(22d)	0.33+%(60d)	
Tensile strength, psi							
Elongation, %							
Tensile elastic modulus, psi							
3000psi-25 C-1hr-1hr							
Appearance (dumbbell)	no change						
Glass transition temperature, C							
Weight change (coupon)	2.48+%(0d)	0.29-%(1d)	0.38-%(6d)	0.35-%(12d)	0.18-%(22d)		
Weight change (dumbbell)	3.72+%(0d)	0.07+%(1d)	0.02+%(6d)	0.10+%(12d)	0.22+%(22d)		
Tensile strength, psi							
Elongation, %							
Tensile elastic modulus, psi							
3000psi-40 C-1hr-1hr							
Appearance (dumbbell)	no change						
Glass transition temperature, C							
Weight change (coupon)	3.5+%(0d)	0.35+%(1d)	0.13+%(6d)	0.19+%(12d)	0.42+%(22d)	0.44+%(60d)	
Weight change (dumbbell)	3.1+%(0d)	0.14+%(1d)	0.07+%(6d)	0.13+%(12d)	0.38+%(22d)	0.46+%(60d)	
Tensile strength, psi							

Elongation, %							
Tensile elastic modulus, psi							
3000psi-70 C-1hr-1hr							
Appearance (dumbbell)	no change						
Glass transition temperature, C							
Weight change (coupon)	2.78+%(0d)	0.24+%(1d)	0.32+%(6d)	0.24+%(12d)	0.12+%(22d)	0.61+%(60d)	0.16+%(5m)
Weight change (dumbbell)	3.48+%(0d)	0.15+%(1d)	0.23+%(6d)	0.24+%(12d)	0.10+%(22d)	0.51+%(60d)	0.51+%(5m)
Tensile strength, psi							
Elongation, %							
Tensile elastic modulus, psi							
3000psi-70 C-1hr-5hr							
Appearance (dumbbell)							
Glass transition temperature, C							
Weight change (coupon)							
Weight change (dumbbell)							
Tensile strength, psi							
Elongation, %							
Tensile elastic modulus, psi							



Poly(ethylene terephthalate)



Polymer I.D.	PET					
Trade name	Mylar					
Manufacturer	Du Pont					
Control						
Appearance	colorless transparent sheet with 0.26mm in thickness					
Glass transition temperature						
Melting Temperature, C	259 C					
TGA Heating	0.36-%					
Tensile strength, psi						
Elongation, %						
Tensile elastic modulus, psi						
1000psi-25 C-1hr-1hr						
Appearance (dumbbell)						
Glass transition temperature, C						
Weight change (coupon)						
Weight change (dumbbell)						
Tensile strength, psi						
Elongation, %						
Tensile elastic modulus, psi						
1000psi-40 C-1hr-1hr						
Appearance (dumbbell)	no change					

Glass transition temperature, C							
Weight change (coupon)	0.89+%(0d)	0.38+%(1d)	0.077+%(6d)	0.026+%(12d)	0.10+%(22d)	0.11+%(60d)	
Weight change (dumbbell)							
Tensile strength, psi							
Elongation, %							
Tensile elastic modulus, psi							
2000psi-40 C-1hr-1hr							
Appearance (dumbbell)	no change						
Glass transition temperature, C							
Weight change (coupon)	0.69+%(0d)	0.41+%(1d)	0.82+%(6d)	0.82+%(12d)	0.82+%(22d)	0.80+%(60d)	
Weight change (dumbbell)							
Tensile strength, psi							
Elongation, %							
Tensile elastic modulus, psi							
3000psi-25 C-1hr-1hr							
Appearance (dumbbell)	no change						
Glass transition temperature, C							
Melting Temperature, C			261 C(7d)	262 C(16d)			
TGA Heating	1.08+%(0d)	0.67+%(1d)	0.52+%(7d)	0.50+%(16d)			
Weight change (coupon)	0.79+%(0d)	0.21+%(1d)	0.02+%(6d)	0.06+%(12d)	0.08+%(22d)		
Weight change (dumbbell)							
Tensile strength, psi							
Elongation, %							
Tensile elastic modulus, psi							
3000psi-40 C-1hr-1hr							
Appearance (dumbbell)	no change						

Glass transition temperature, C							
Weight change (coupon)	1.81+%(0d)	0.67+%(1d)	0.13+%(6d)	0.69+%(12d)	0.24+%(22d)	0.23+%(60d)	
Weight change (dumbbell)							
Tensile strength, psi							
Elongation, %							
Tensile elastic modulus, psi							
3000psi-70 C-1hr-1hr							
Appearance (dumbbell)	no change						
Glass transition temperature, C							
Weight change (coupon)	2.05+%(0d)	0.26+%(1d)	0.17+%(6d)	0.15+%(12d)	0.11+%(22d)	0.54+%(60d)	0.54+%(5m)
Weight change (dumbbell)							
Tensile strength, psi							
Elongation, %							
Tensile elastic modulus, psi							
3000psi-70 C-1hr-5hr							
Appearance (dumbbell)							
Glass transition temperature, C							
Weight change (coupon)							
Weight change (dumbbell)							
Tensile strength, psi							
Elongation, %							
Tensile elastic modulus, psi							